CHAPTER IV

RESULTS AND DISCUSSION

1. PURIFICATION AND STRUCTURE ELUCIDATION OF THE SECONDARY PRODUCTS FROM *I. BALSAMINA* ROOT CULTURES

The dried cultured roots of *I. balsamina* were successively extracted with ethyl acetate and methanol. Each crude extract was fractionated using various column chromatographic techniques as described in the Experimental (Chapter 3). The ethyl acetate extract yielded 3 compounds (**ET-1** to **ET-3**) whereas the methanolic extract yielded 4 compounds (**ME-1** to **ME-4**). The structure elucidation of these compounds are described below.

1.1 Identification of ET-1

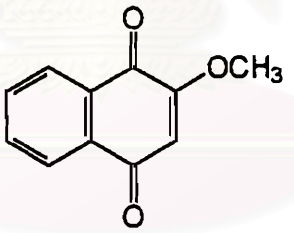

Fig. 7 Structure of **ET-1**

ET-1 was obtained as yellow needle (5.1 mg, 0.003% dry weight) crystallized from a mixture of ethanol and water. Examination of the spectroscopic data of **ET-1** clearly established this compound as 2-methoxy-1,4-naphthoquinone (Fig. 7). Its mass spectrum (Fig. 8) exhibited a molecular ion peak [M^+] at *m/z* 188 corresponding to a molecular formula of $C_{11}H_8O_3$. The fragment at *m/z* 173 is due to a facile loss of the methyl group, while the fragment at *m/z* 158 is due to a loss of the methoxy group (Fig. 9). The IR spectrum (Fig. 10) displayed absorption bands of C=O stretching at 1,680 and 1,645 cm^{-1}, C=C stretching of aromatic ring at 1,605 cm^{-1} and C-O stretching at 1,240 cm^{-1}. The UV spectrum showed the absorption maxima at 243, 248, 277 and 330 nm (Fig. 11).

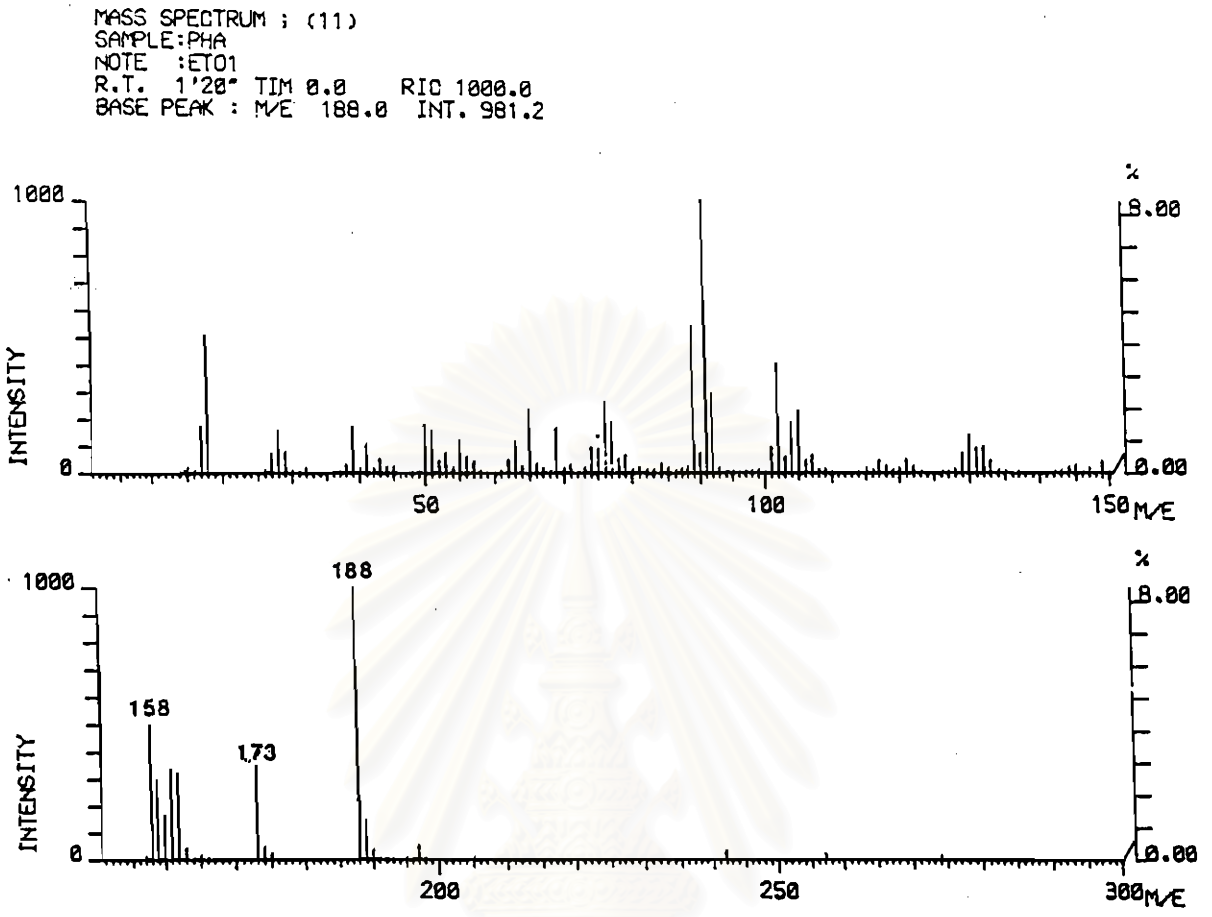

Fig. 8 Mass spectrum of **ET-1**

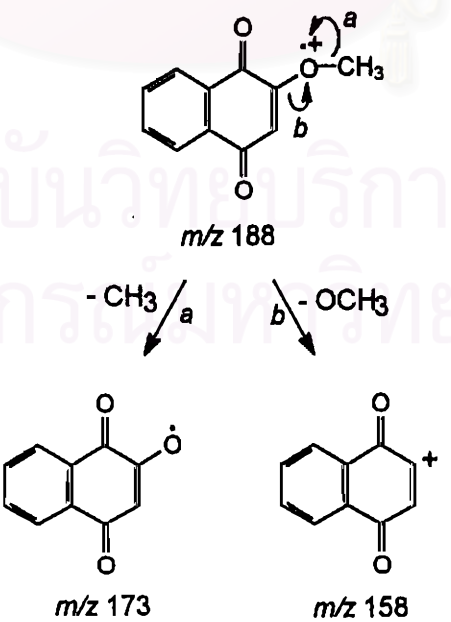

Fig. 9 Fragmentation of **ET-1**

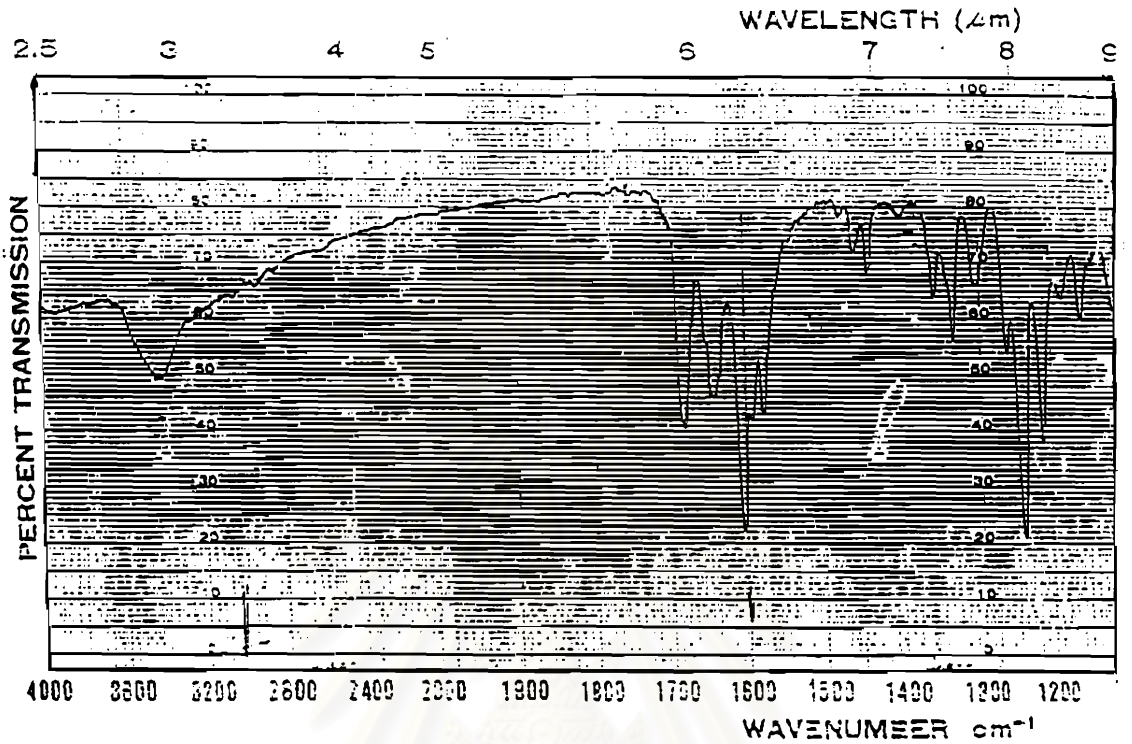

Fig. 10 IR spectrum of **ET-1** (KBr disc)

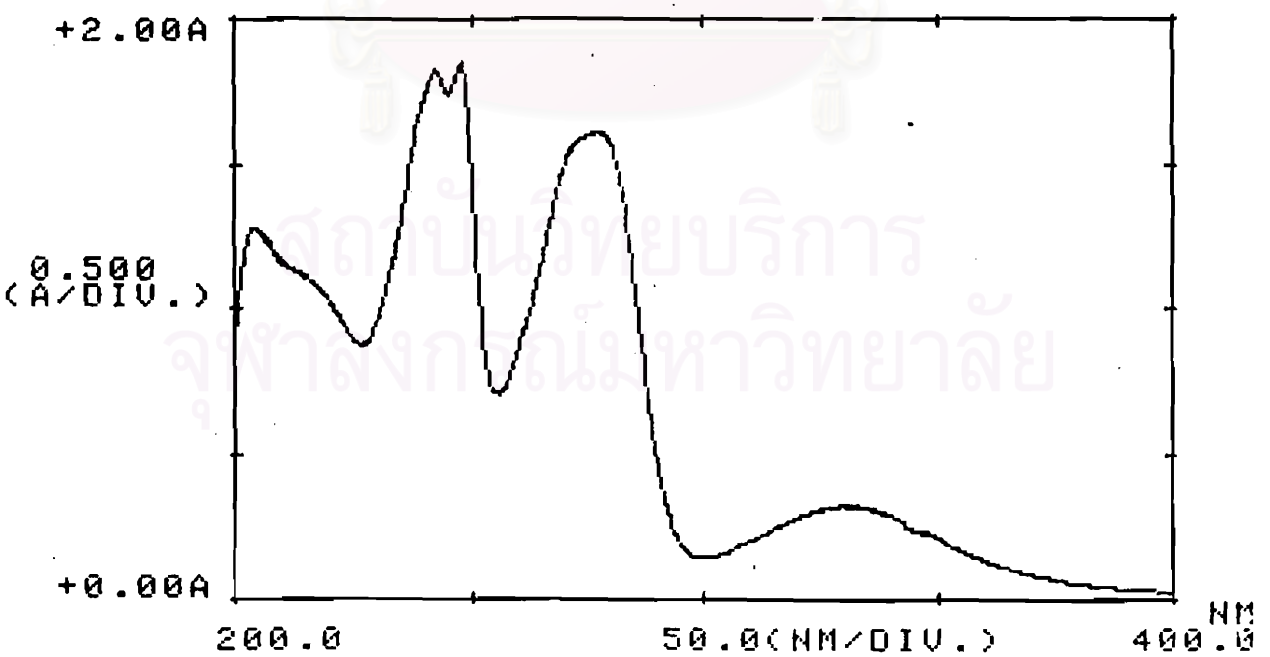

Fig. 11 UV spectrum of **ET-1** (in ethanol)

With regard to its NMR properties, the ^{1}H NMR data of 2-methoxy-1,4-naphthoquinone have been reported previously (Chapelle, 1974). Nevertheless, its structure assignment was not complete due to the simplicity of the ^{1}H NMR spectrum. Therefore, an attempt was made in this study to obtaine complete ^{1}H and ^{13}C NMR assignments using ^{1}H and ^{13}C NMR, HMQC and HMBC. Figure 12 shows the complete proton decoupled ^{13}C NMR spectrum which displayed eleven carbon signals. Among these, the methoxy signal is clear due to the presence of chemical shift value of 56.5 ppm. This assignment is supported by the three proton singlet signal in ^{1}H NMR (Fig. 13) which appeared at δ 3.91. The other ^{13}C NMR signas are all located between δ 100 and 200, while the ^{1}H NMR showed one olefinic singlet at δ 6.18 and two aromatic multiplets between δ 7.5 and 8.2.

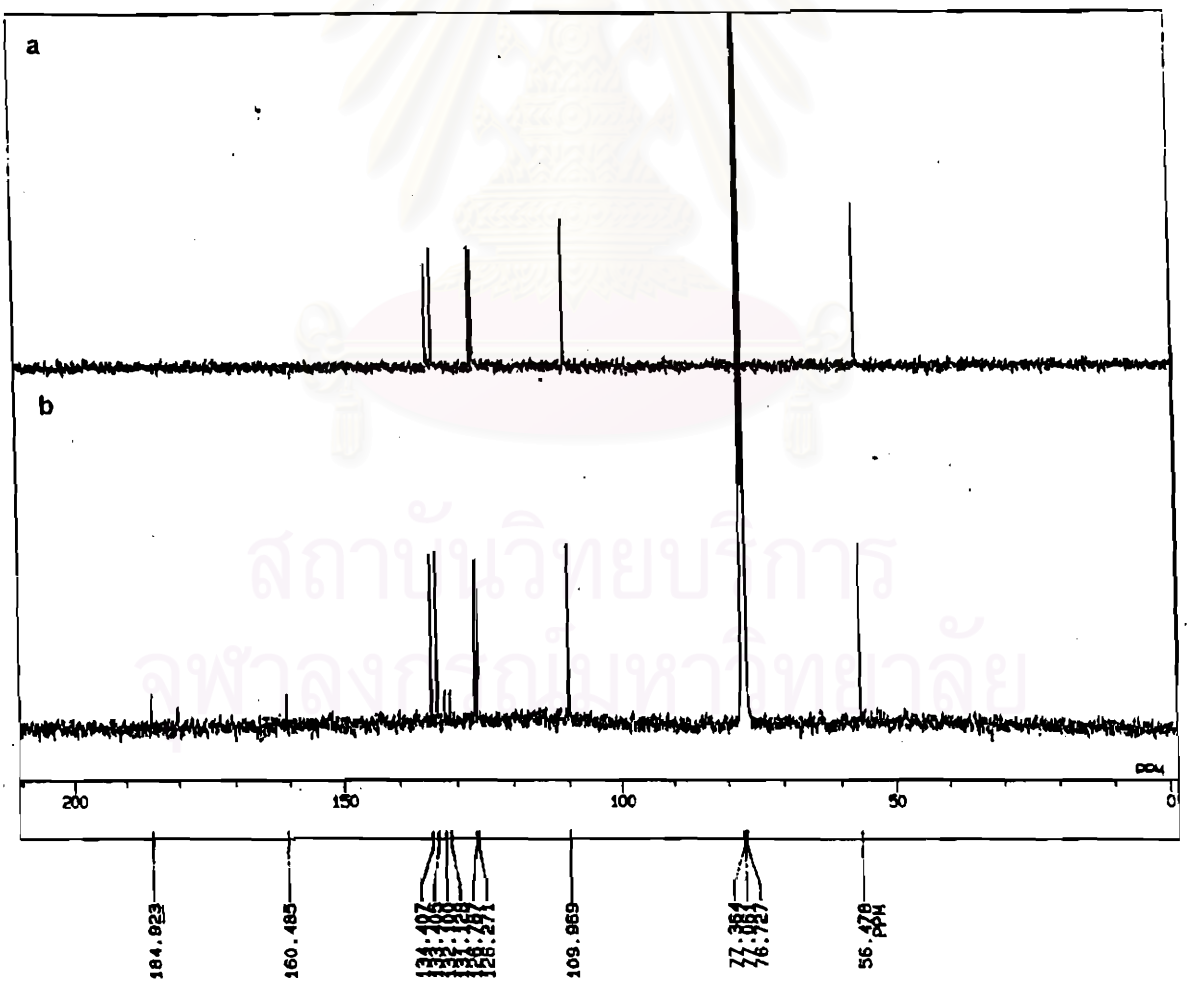

Fig. 12 DEPT 135° (a) and the proton decoupled (b) ^{13}C NMR (125 MHz) spectra of **ET-1** (in $CDCl_3$)

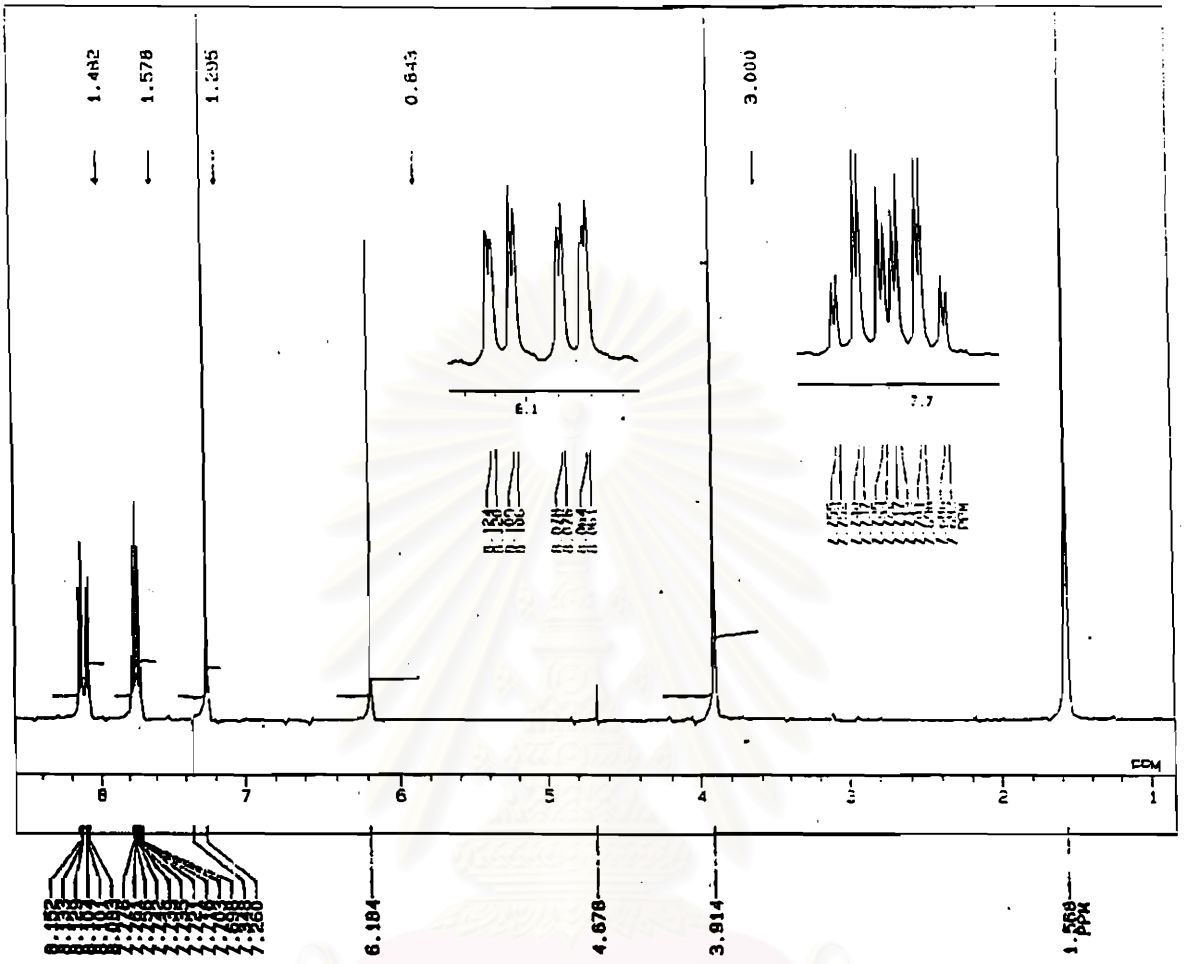

Fig. 13 ^{1}H NMR (500 MHz) spectrum of **ET-1** (in $CDCl_3$)

From its structure (Fig. 7), the proton resonance at δ 6.18 ppm should be assigned to H-3 (Table 5). The proton signals of H-6, H-7 and also H-5, H-8 seem to be almost identical, but they actually show small differences in the chemical shifts due to the methoxy group. For the proton signals of H-5 and H-8 each should have one *ortho* and one *meta* couplings, whereas for H-6 and H-7 each should have two *ortho* and one *meta* couplings. In ordinary *ortho* and *meta* couplings, the coupling constant values are approximately 7-8 Hz and 2-3 Hz, respectively. Therefore, the splitting patterns of these signals (Fig. 13) are interpreted as shown in Table 5, and the signals at δ 8.09 and 8.14 could be assigned to H-5 and H-8. Similarly, the protons with the chemical shift values of 7.72 and 7.76 ppm could be assigned to H-6 and H-7.

In order to obtain unambigerous assignments for these protons, heteronuclear chemical shift correlation (C-H COSY) and heteronuclear multiple bond coherence (HMBC) experiment (Fig. 14 and 15) were used. The results also helped unequivocally assign all carbon resonances.

Table 5 ^{1}H NMR data of **ET-1** (500 MHz, $CDCl_3$)

H	δ_H (ppm)	Splittig pattern and coupling constant
3	6.18	1H, s
5	8.09	1H, dd, *J* = 7.3, 1.2 Hz
6	7.76	1H, ddd, *J* = 7.3, 7.3, 1.2 Hz
7	7.72	1H, ddd, *J* = 7.3, 7.3, 1.8 Hz
8	8.14	1H, dd, *J* = 7.3, 1.8 Hz
2-OMe	3.91	3H, s

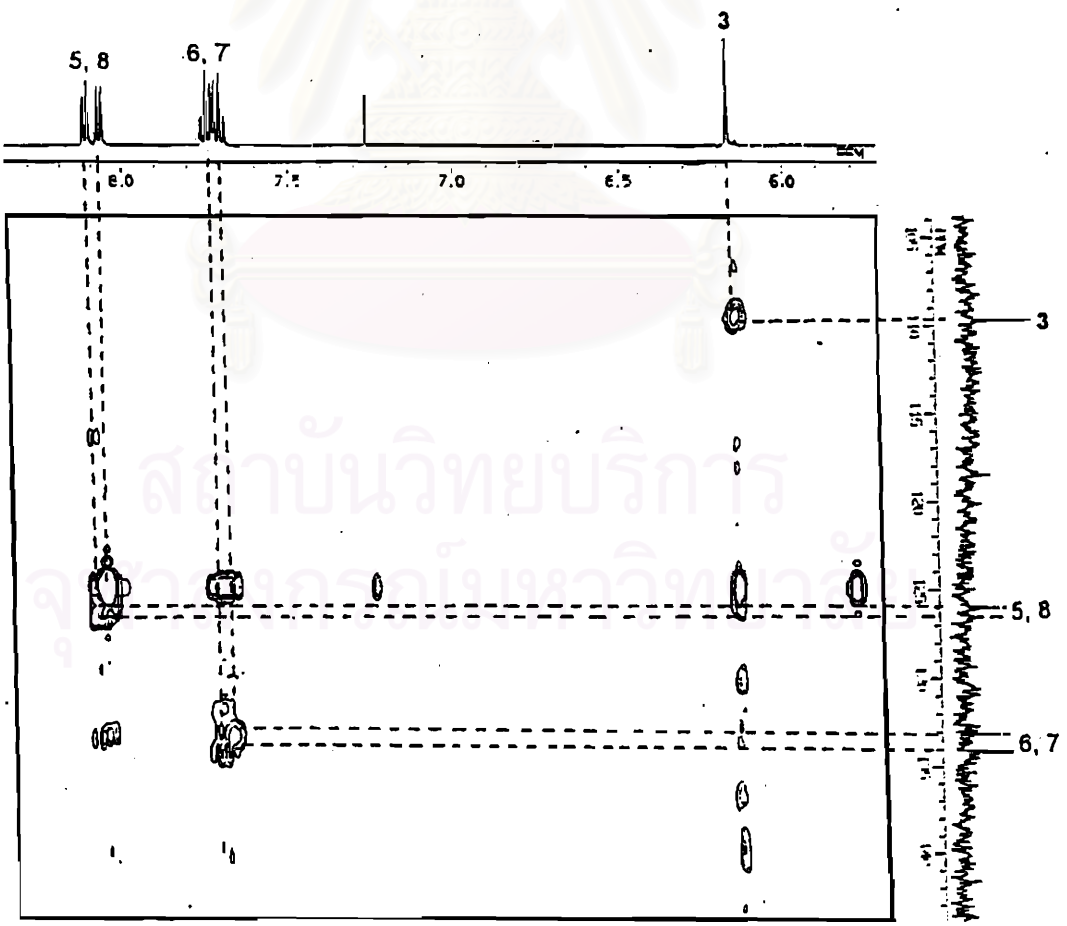

Fig. 14 CH hetero COSY spectrum (125 MHz) of **ET-1** (in $CDCl_3$)

As shown in figure 14, the carbons C-5, C-6, C-7 and C-8 can be correlated to signals at δ 8.09, 7.76, 7.72 and 8.14, respectively. The CH hetero COSY also confirmed the results of ^{1}H and ^{13}C spectra but give no futher information. Therefore, long range CH COSY observing proton nuclear (so call HMBC) was further established (Fig. 15). The results showed that the methoxy protons gave a correlation with the signal at δ 160.5. The signal at δ 160.5 was quite reasonable to be assigned as the quaternary sp^2 carbon bearing hetero atom. The proton signal at δ 6.18 gave the correlations to C-4a, C-2 and C-1. Except for the correlation to C-2, the other are three bond couplings. Thus, the carbon with the chemical shifts of 132.1 and 180.0 ppm should be assigned as C-4a and C-1, respectively (Table 6).

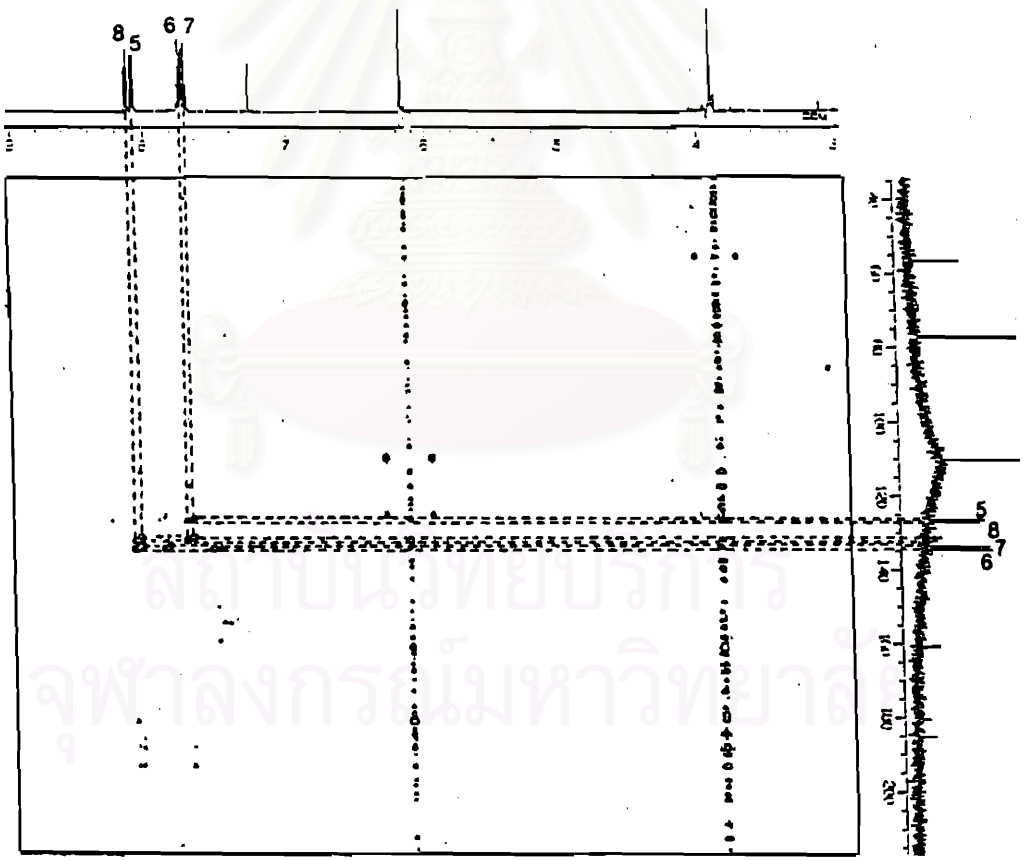

Fig. 15 The HMBC spectrum (125 MHz) of **ET-1** (in $CDCl_3$)

Table 6 ^{13}C NMR data of **ET-1** (125 MHz, $CDCl_3$)

C	δ_C (ppm)
1	180.0
2	160.5
3	110.0
4	184.9
4a	132.1
5	126.3
6	134.4
7	133.4
8	126.8
8a	131.1
2-OMe	56.5

The protons with chemical shift values of 8.09, 7.76, 7.72 and 8.4 ppm give the three bond correlation with C-7 and C-8a, C-8, C-5 and C-8a, and C-6, respectively (Fig. 16). Thus proton signal at δ 8.09, 7.76, 7.72 and 8.14 should be assigned as H-5, H-6, H-7 and H-8, respectively. Another quinone carbon, C-4 (δ 184.9) should show the correlation to H-5, but it could not be observed.

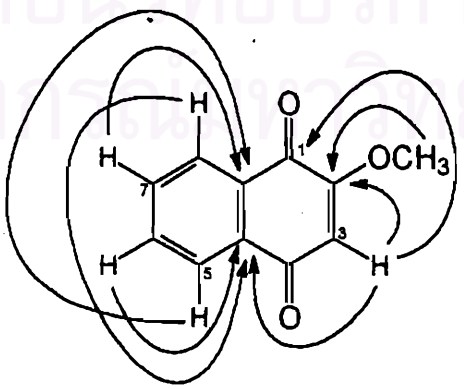

Fig. 16 Important ^{13}C-^{1}H long range correlations observed by heteronuclear COSY of **ET-1**

1.2 Identification of ET-2

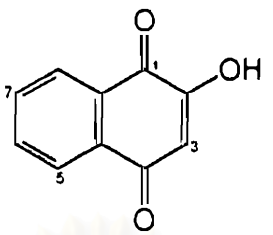

Fig. 17 Structure of ET-2

ET-2 was obtained as yellow crystals (3.4 mg, 0.002% dry weight) crystallized from a mixture of methanol and water. ET-2 was identified as lawsone (Fig. 17) by its melting point (192 °C) and by spectroscopic means including MS, IR and NMR. Its mass spectrum (Fig. 18) showed a molecular ion peak [M^+] at *m/z* 174, suggesting a molecular formula of $C_{10}H_6O_3$.

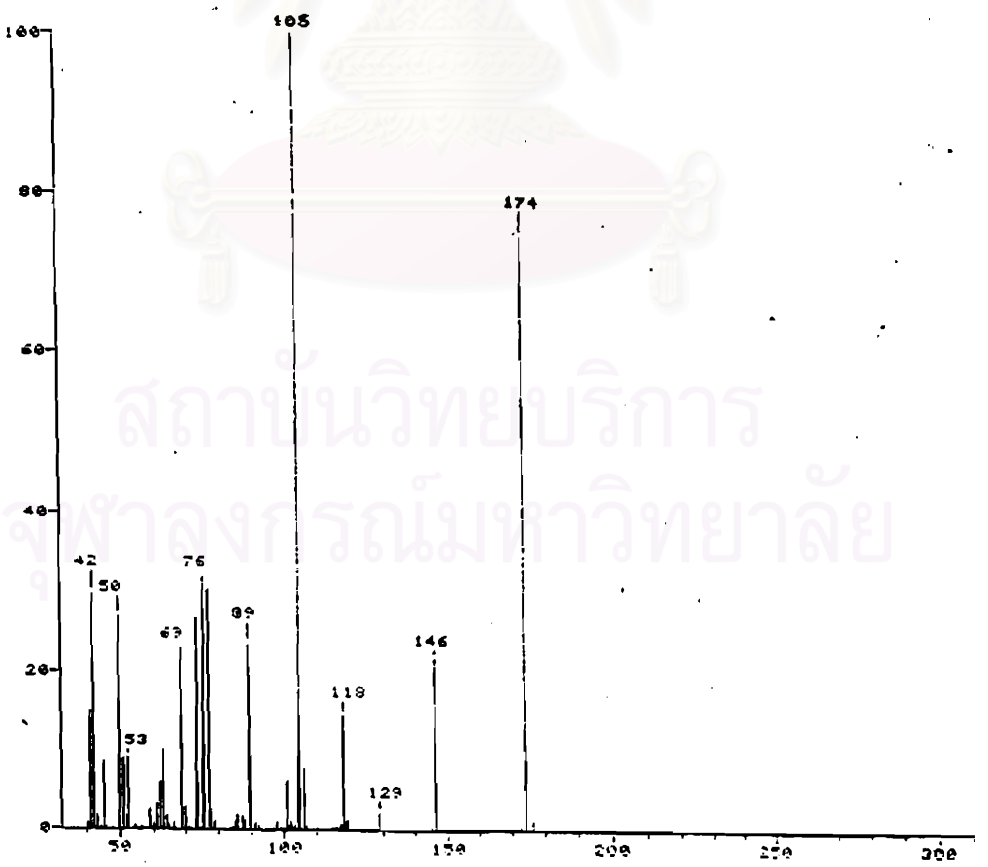

Fig. 18 Mass spectrum of ET-2

The fragment ions at *m/z* 146 and 118 were due to expulsion of -CO from the quinone carbonyl groups (Fig. 19). The fragment at *m/z* 105 was suggested as [C_6H_5CO]. The IR spectrum (Fig. 20) showed absorption bands of O-H stretching at 3,160 cm^{-1}, C=O stretching at 1,674 cm^{-1}, C=C stretching of aromatic ring at 1,630 cm^{-1} and C-O stretching at 1,220 cm^{-1}. The UV spectrum showed absorption maxima at 244, 250 and 273 nm (Fig. 21).

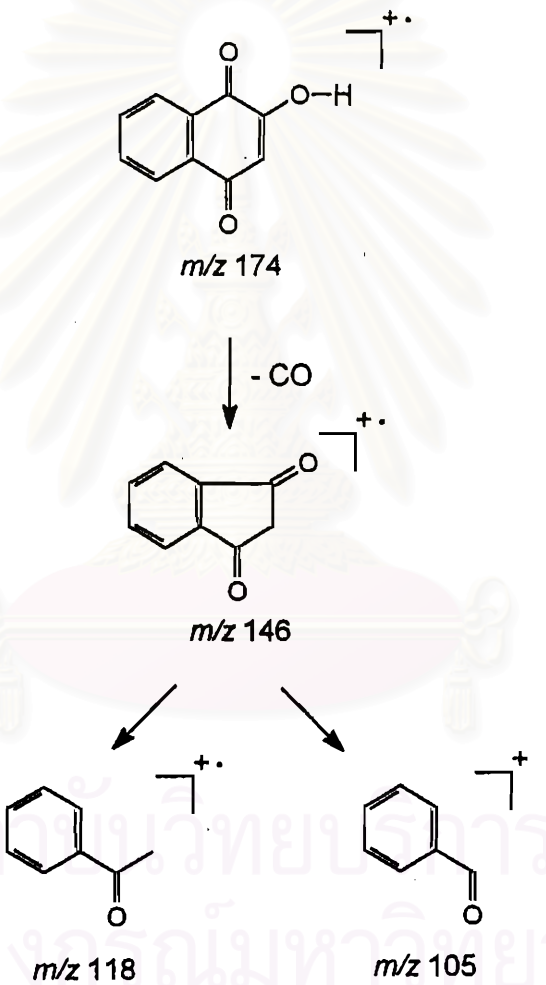

Fig. 19 Fragmentation of **ET-2**

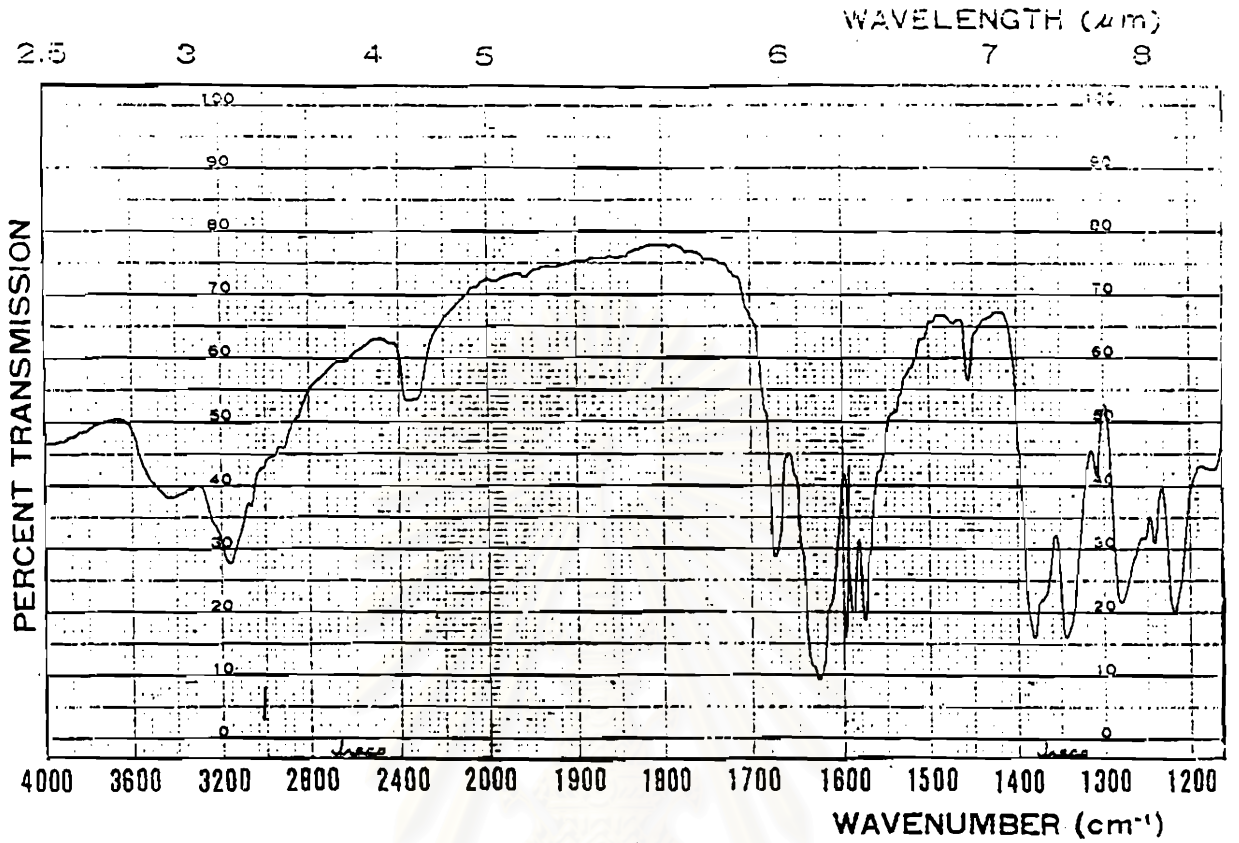

Fig. 20 IR spectrum of **ET-2** (KBr disc)

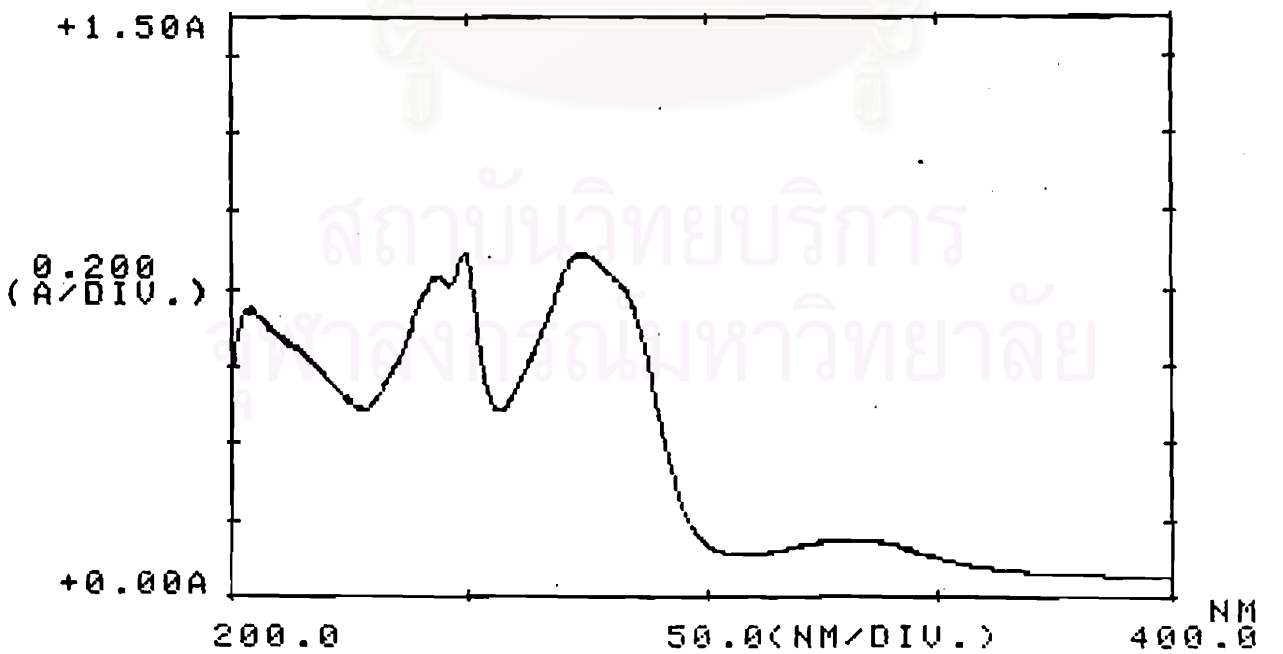

Fig. 21 UV spectrum of **ET-2** (in ethanol)

The ^{1}H (Fig. 22) and ^{13}C (Fig. 23) NMR spectra of **ET-2** were almost similar to those of 2-methoxy-1,4-naphthoquinone. The complete assignment of its structure is given in Tables 7 and 8. The difference between the ^{1}H NMR spectra of lawsone and 2-methoxy-1,4-naphthoquinone was the occurrence of a singlet signal at δ 9.81 of lawsone instead of the methoxy proton signal of 2-methoxy-1,4-naphthoquinone. This proton signal disappeared when D_2O was added into the NMR sample (Fig. 24). These results indicated that the signal at δ 9.81 should be an intramolecular hydrogen bonded proton of the hydroxyl group. In addition, no methoxy carbon signal at δ 56.5 was observed in the ^{13}C NMR spectrum of lawsone.

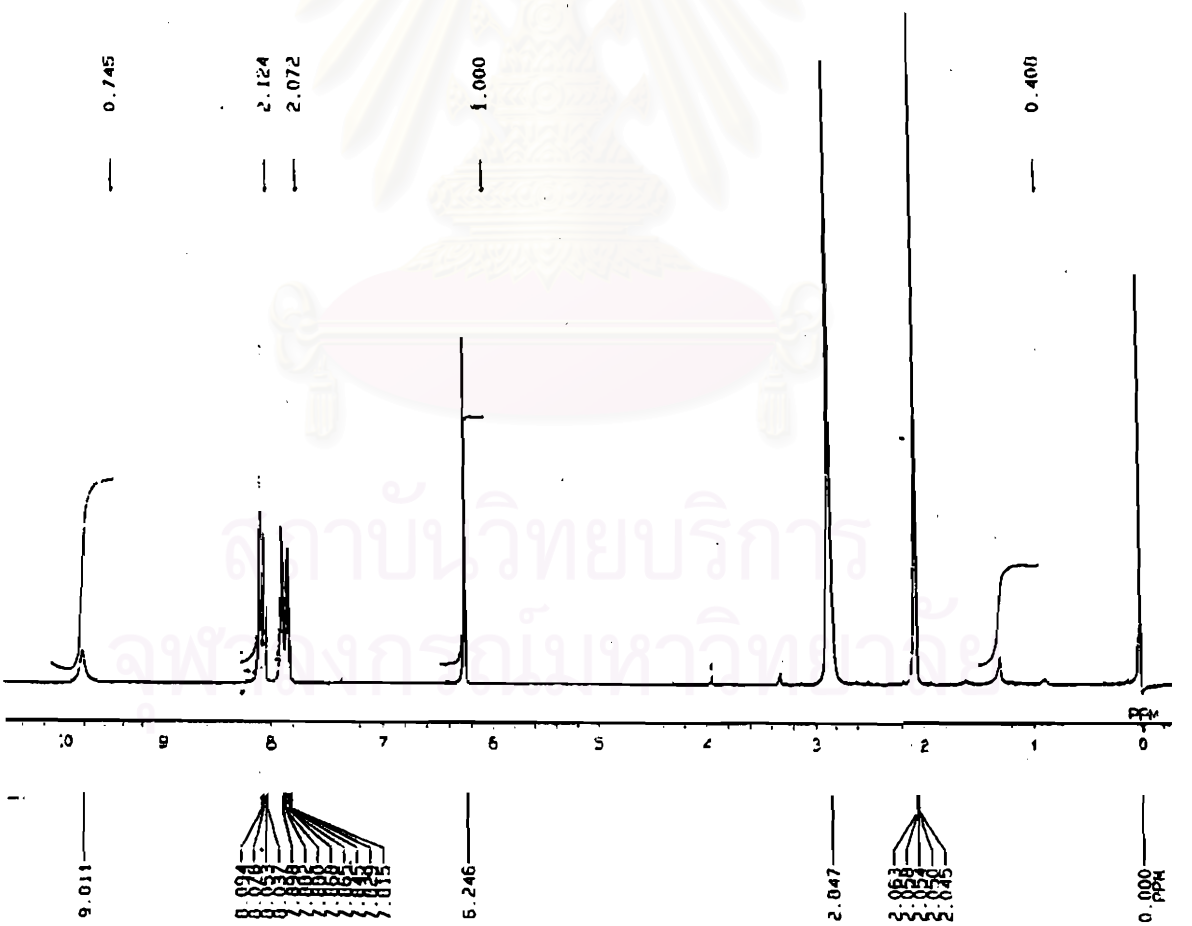

Fig. 22 ^{1}H NMR (500 MHz) spectrum of **ET-2** (in CD_3OD)

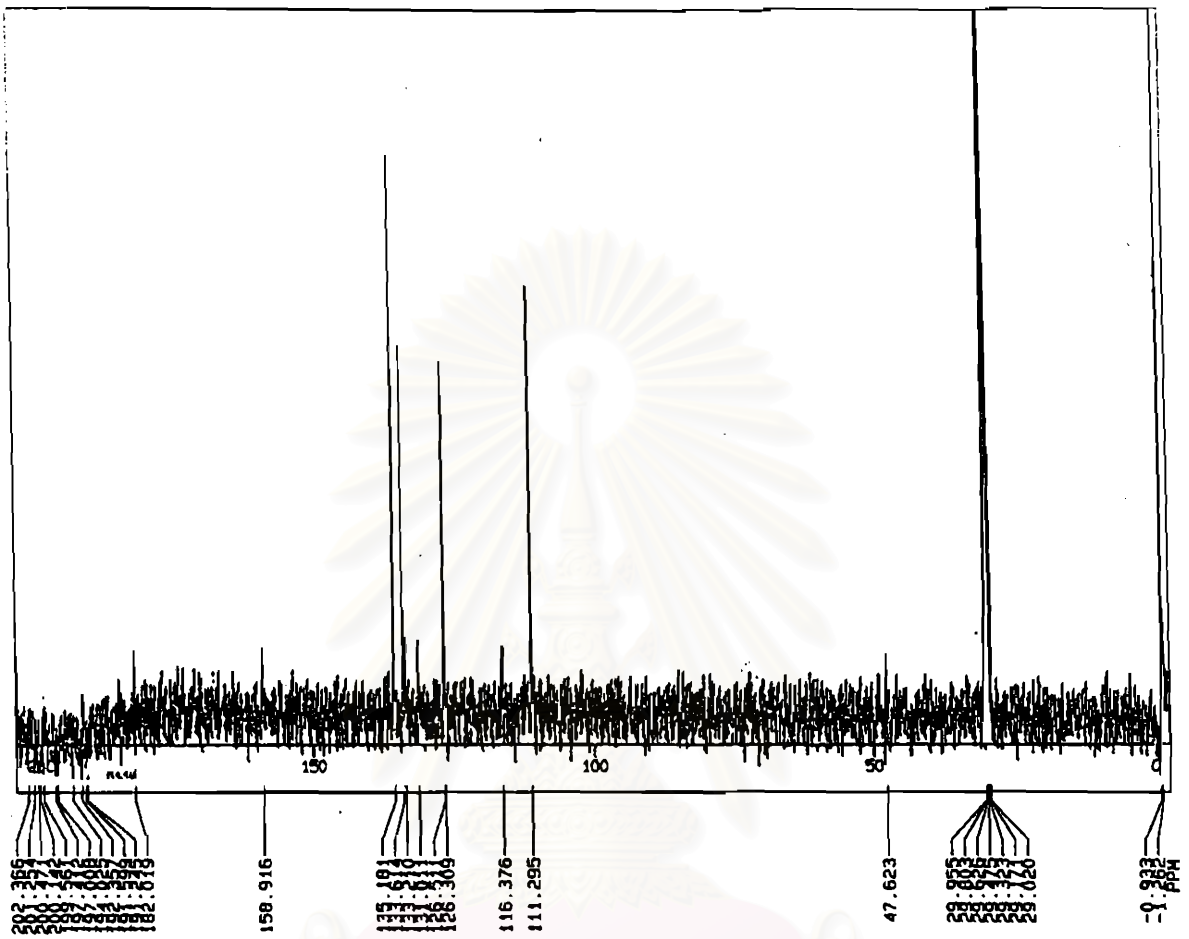

Fig. 23 ^{13}C NMR (125 MHz) spectrum of **ET-2** (in CD_3OD)

Table 7 ^{1}H NMR data of **ET-2** (500 MHz, CD_3OD)

H	δ_H (ppm)	Splittig pattern and coupling constant
3	6.25	1H, s
5	8.04	1H, d, J = 7.9 Hz
6	7.88	1H, ddd, J = 7.9, 7.3, 1.3 Hz
7	7.83	1H, ddd, J = 7.9, 7.3, 1.3 Hz
8	8.09	1H, d, J = 7.9 Hz
2-OH	3.91	1H, s

Table 8 ^{13}C NMR data of **ET-2** (125 MHz, CD_3OD)

C	δ_C (ppm)
1	182.9
2	158.9
3	111.3
4	185.0
4a	133.2
5	126.3
6	135.2
7	133.6
8	126.5
8a	131.0

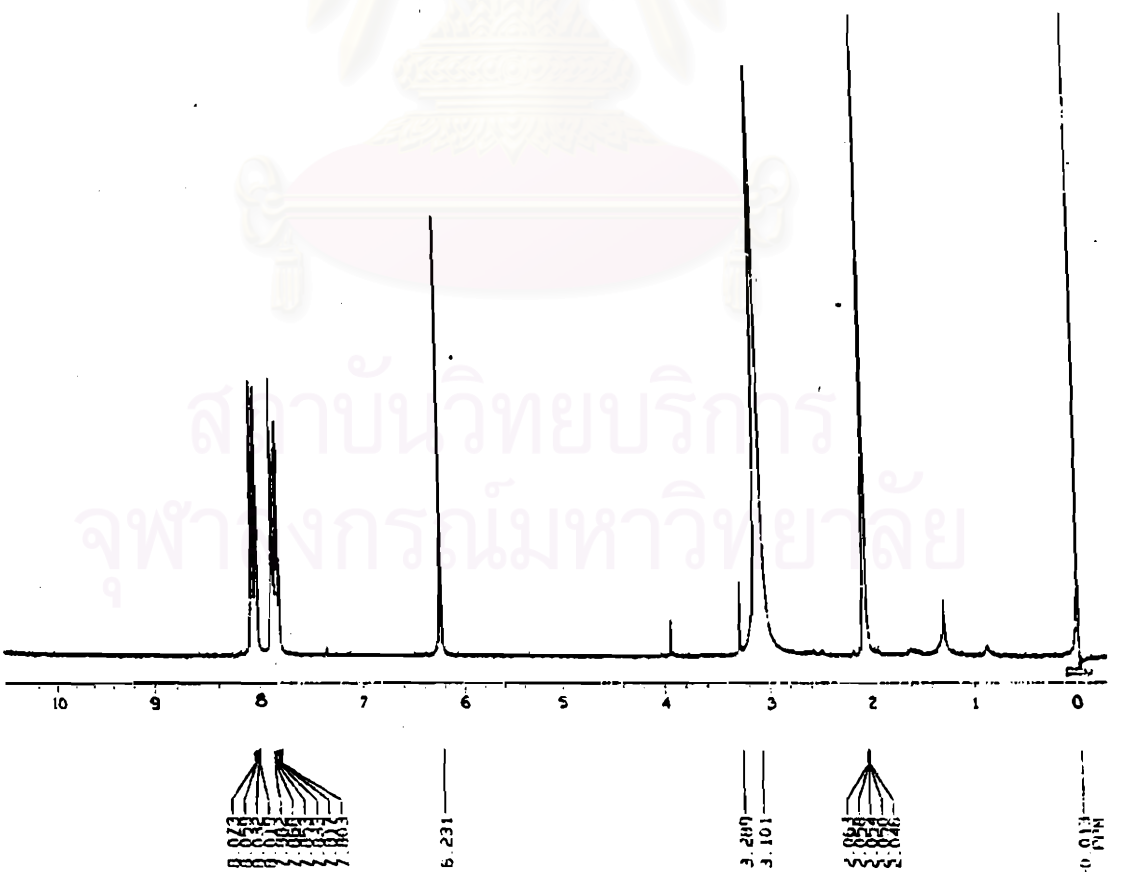

Fig. 24 ^1H NMR (500 MHz) spectrum of **ET-2**, with added D_2O (in CD_3OD)

1.3 Identification of ET-3

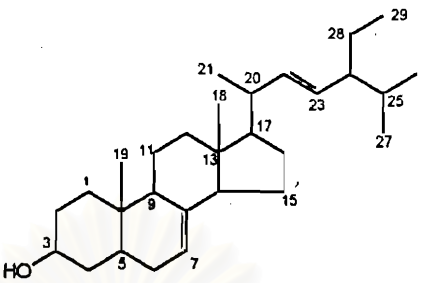

Fig. 25 Structure of **ET-3**

ET-3 was obtained as colorless needles (8.5 mg, 0.005% dry weight) crystallized from a mixture of chloroform and methanol. This compound was found to be a plant sterol, namely spinasterol (Fig. 25). The spot of **ET-3** was not visible on the silica gel 60 F254 plate (benzene/acetone, 9:1) under UV light at 254 or 365 nm, suggesting this compound as having no conjugated double bond system. When the TLC plate was sprayed with 10% sulfuric acid and heated, a purple spot appeared. This spot showed its Rf value (0.45) very closed to that of β-sitosterol, but its color after being sprayed with 10% sulfuric acid and heated was quite different. According to the literature, the seeds of this plant have been reported to contain spinasterol (Mukherjee and Roy, 1956; Dikshit, 1973). Since **ET-3** also has the same melting point (169-170°C) as spinasterol (Windholz, 1983), it was speculated that this compound might be spinasterol.

Based on its mass spectrum (Fig. 26), **ET-3** showed the molecular ion peak [M^+] at *m/z* 412, corresponding to its molecular formula of $C_{29}H_{48}O$. The fragment at *m/z* 300 is a characteristic retro Diels Alder fragmentation of spinasterol (Fig. 27). Its IR spectrum (Fig. 28) showed the characteristic absorption bands of O-H stretching at 3,420 cm^{-1}, C=C stretching at 1,625 cm^{-1} and C-H bending at 1,450 and 1,380 cm^{-1}. In addition, its ^1H (Fig. 29) and ^{13}C (Fig. 30) NMR spectra were also very closed to that reported for spinasterol (Table 9) (Henry and Chantalat-Dublanche, 1985; Toshihiro *et al.*, 1986). These spectoscopic data firmly supported the identification of **ET-3**.

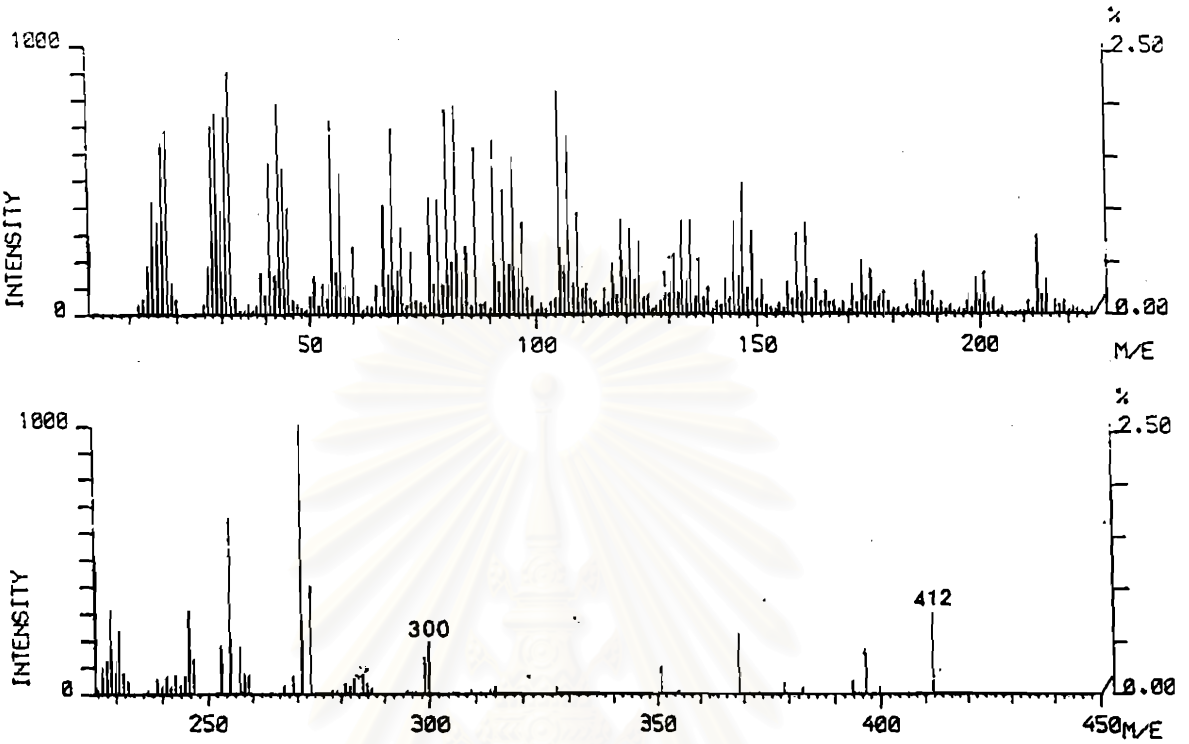

Fig. 26 Mass spectrum of **ET-3**

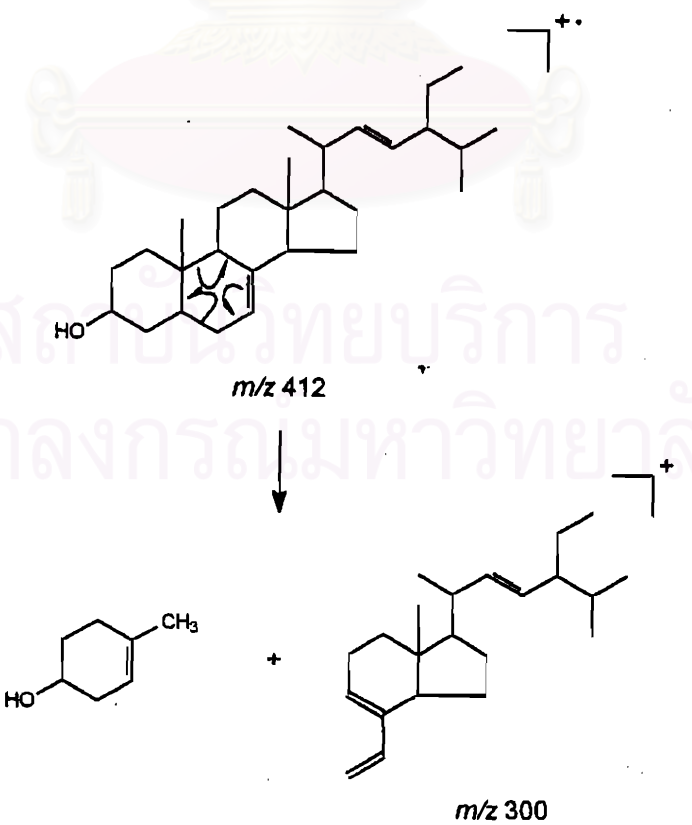

Fig. 27 Characteristic mass fragmentation of **ET-3**

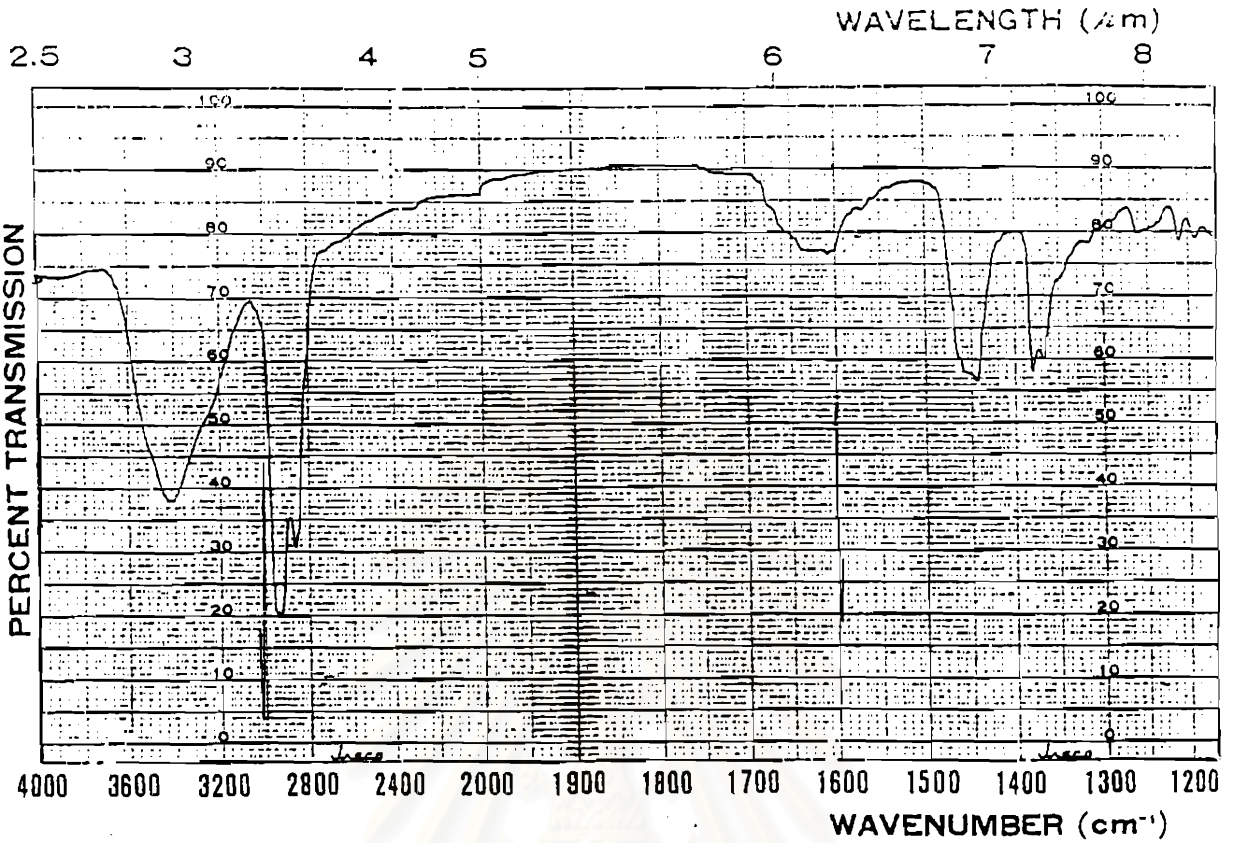

Fig. 28 IR spectrum of ET-3 (KBr disc)

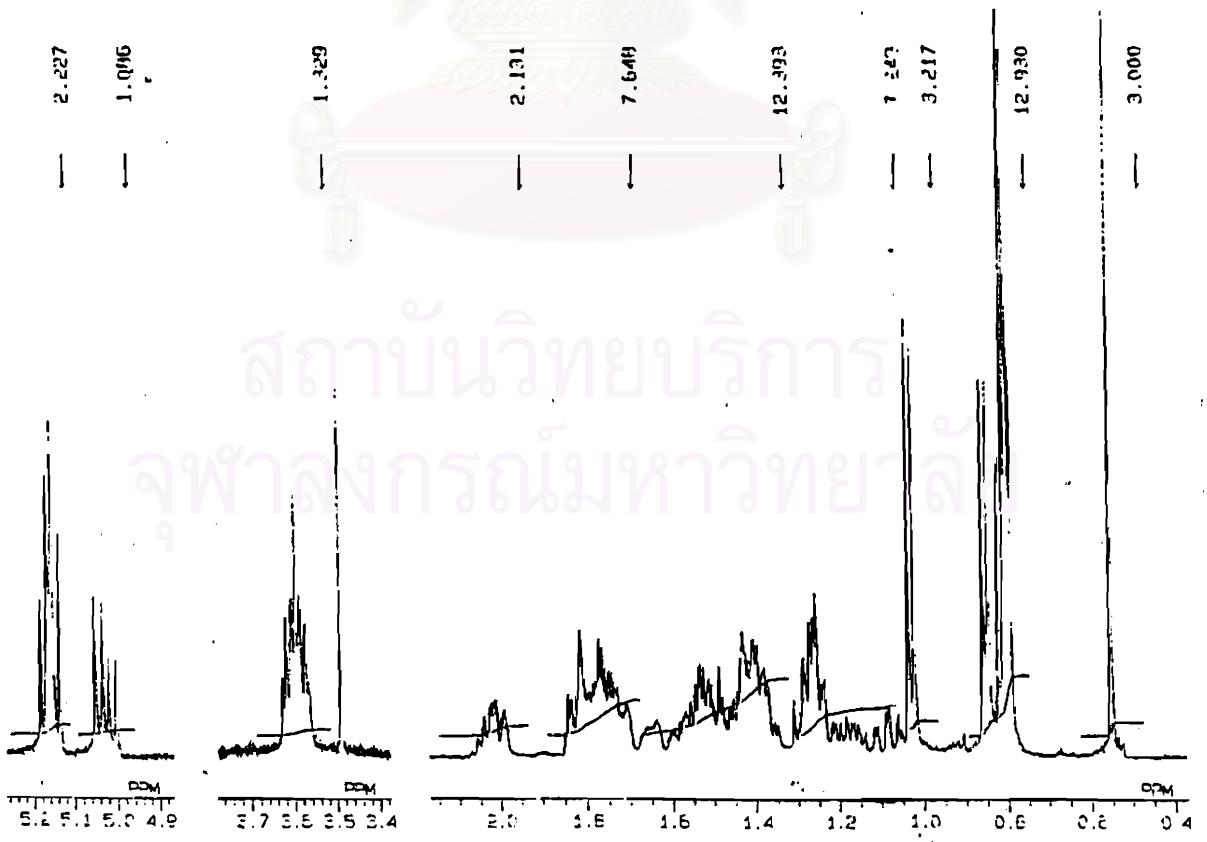

Fig. 29 ^{1}H NMR (500 MHz) spectrum of **ET-3** (in $CDCl_3$)

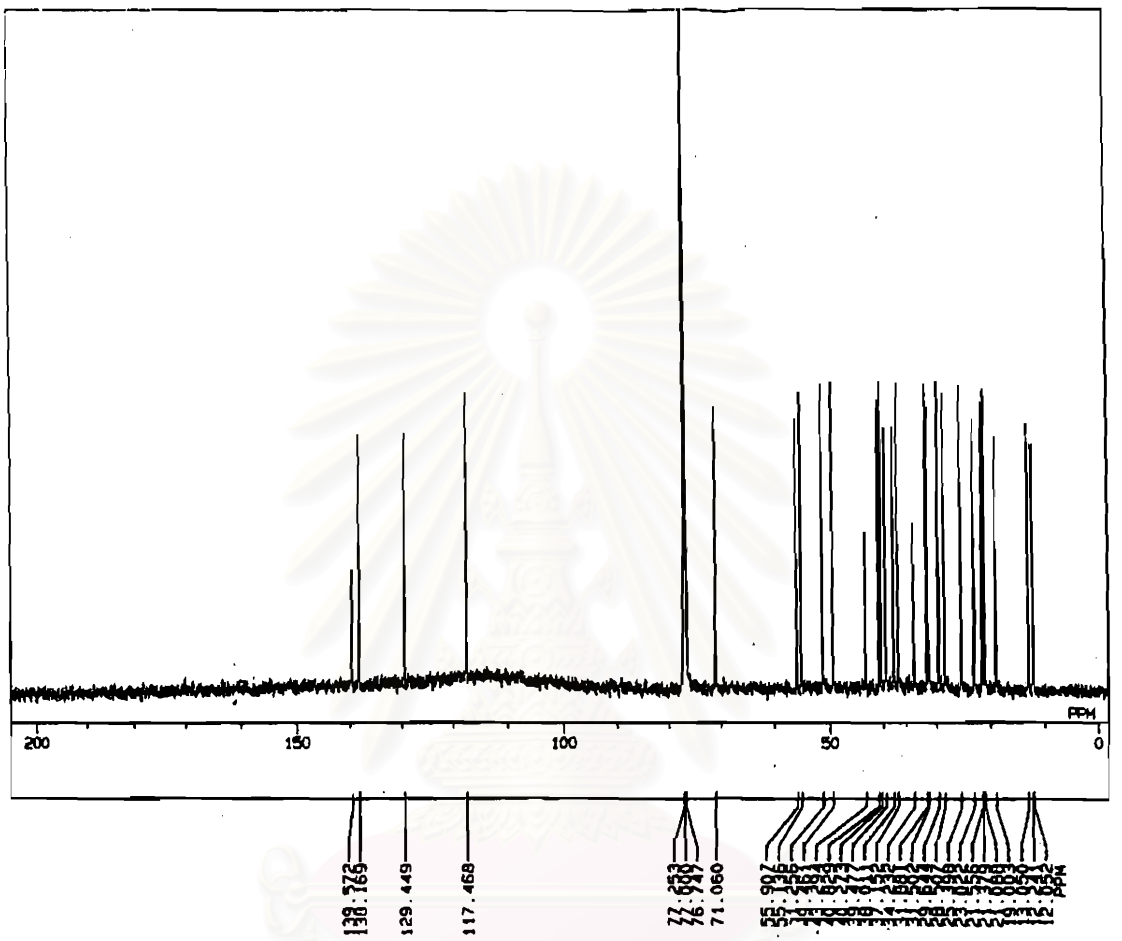

Fig. 30 ^{13}C NMR (125 MHz) spectrum of **ET-3**

Table 9 ^{13}C NMR data of ET-3 (125 MHz, $CDCl_3$)

C	ET-3 δ_C (ppm)	Spinasterol δ_C (ppm)
1	37.2 (t)	37.2 (t)
2	31.5 (t)	31.6 (t)
3	71.1 (d)	71.1 (d)
4	38.0 (t)	38.1 (t)
5	40.3 (d)	40.4 (d)
6	29.6 (t)	29.7 (t)
7	117.5 (d)	117.5 (d)
8	139.6 (s)	139.6 (s)
9	49.5 (d)	49.6 (d)
10	34.2 (s)	34.3 (s)
11	21.6 (t)	21.6 (t)
12	39.5 (t)	39.6 (t)
13	43.3 (s)	43.3 (s)
14	55.1 (d)	55.2 (d)
15	23.0 (t)	23.1 (t)
16	28.5 (t)	28.5 (t)
17	55.9 (d)	56.0 (d)
18	12.1 (q)	12.1 (q)
19	13.1 (q)	13.1 (q)
20	40.8 (d)	40.8 (d)
21	21.1 (q)	21.1 (q)
22	138.2 (d)	138.2 (d)
23	129.4 (d)	129.5 (d)
24	51.3 (d)	51.3 (d)
25	31.9 (d)	32.0 (d)
26	21.4 (q)	21.3 (q)
27	19.0 (q)	19.0 (q)
28	25.4 (t)	25.5 (t)
29	12.2 (q)	12.3 (q)

Splitting patterns are given in parentheses

1.4 Structure elucidation of ME-1

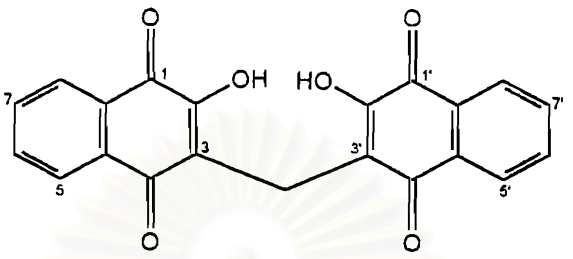

Fig. 31 The structure of ME-1

ME-1 was obtained as yellowish crystals (25.7 mg, 0.015% dry weight) crystallized from methanol. This compound was identified as methylene-3,3'-bilawsone (diphthicol) (Fig. 31) by various spectroscopic data as described below:

ME-1 exhibited UV absorption maxima at 271.5 nm (Fig. 32), suggesting the presence of the same chromophore as the other naphthoquinones. Its EI mass spectrum (Fig. 33) showed a molecular ion peak [M^+] at *m/z* 360, and gave fragmentation of *m/z* 342 for [$M - H_2O$]$^+$, 314 for [$M - H_2O - CO$]$^+$, 188 for [$C_{11}H_8O_3$]$^+$ and 173 for [$C_{10}H_5O_3$]$^+$ (Fig. 34). The high resolution mass spectrum gave a molecular formula of $C_{21}H_{12}O_6$ (*m/z* 360.0631 [M^+]; calc. for $C_{21}H_{12}O_6$: 360.0628) and the fragments of 342 showed as *m/z* 342.0497 [M^+]; calc. for $C_{21}H_{10}O_5$: 342.0494, 314 as *m/z* 314.0584 [M^+]; calc. for $C_{20}H_{10}O_4$: 314.0583. The fragments of *m/z* 188 and 173 can be assigned as those of phthicol and deprotonated lawsone.

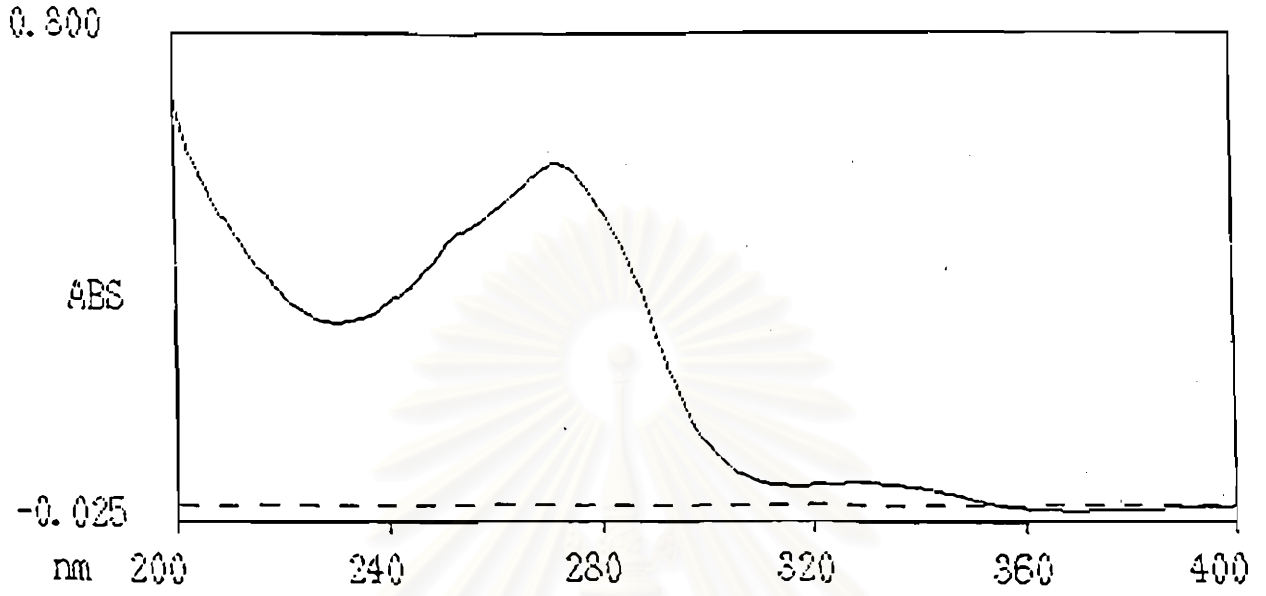

Fig. 32 UV spectrum of ME-1 (in ethanol)

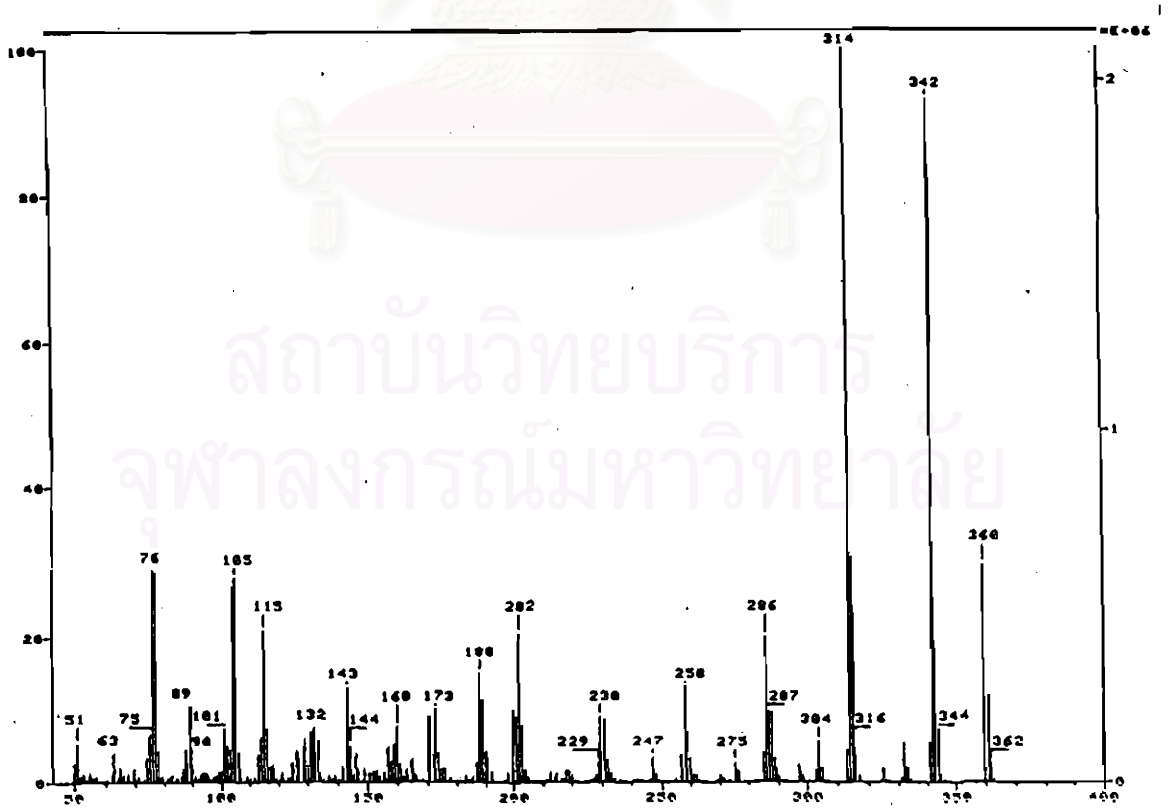

Fig. 33 Mass spectrum of ME-1

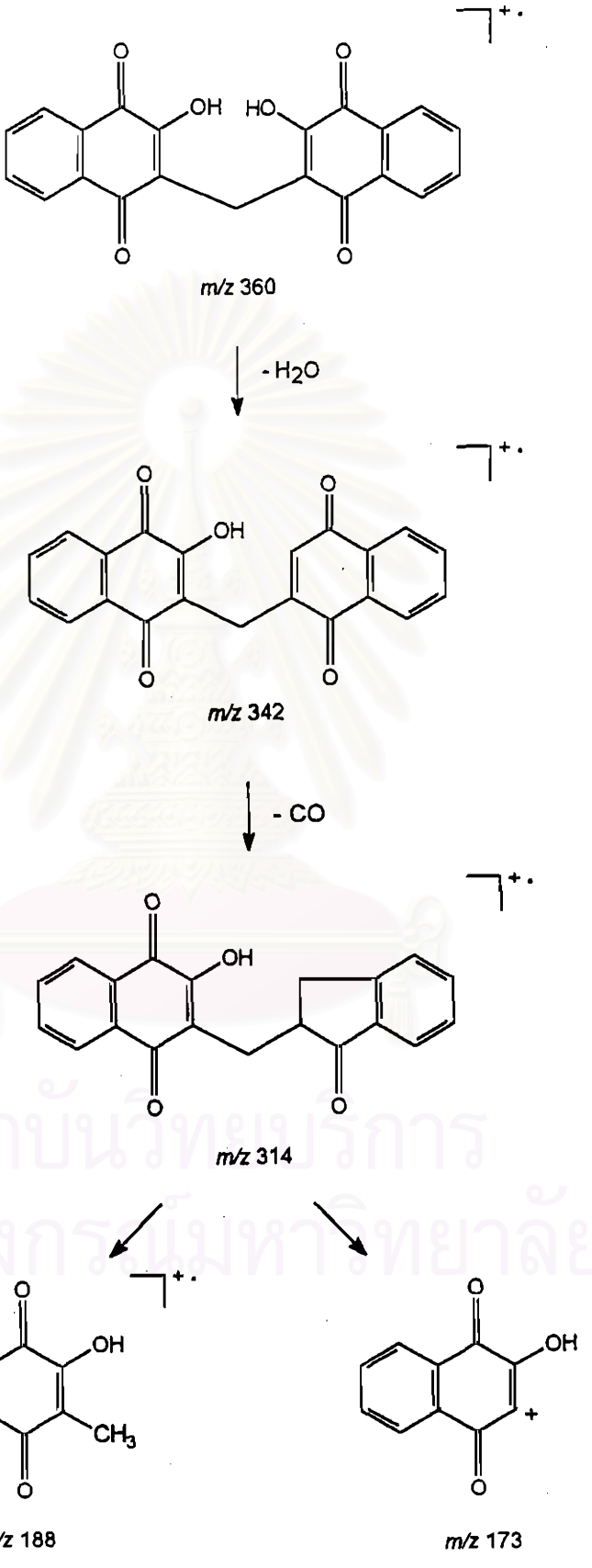

Fig. 34 Fragmentation of **ME-1**

Its IR spectrum (Fig. 35) exhibited the characteristic bands of O-H stretching at 3,420 cm^{-1}, C=O stretching at 1,674 cm^{-1}, C=C stretching of aromatic ring at 1,605 and 1,570 cm^{-1} , C=C stretching at 1,455 cm^{-1} and C-O stretching at 1,260 and 1,210 cm^{-1}.

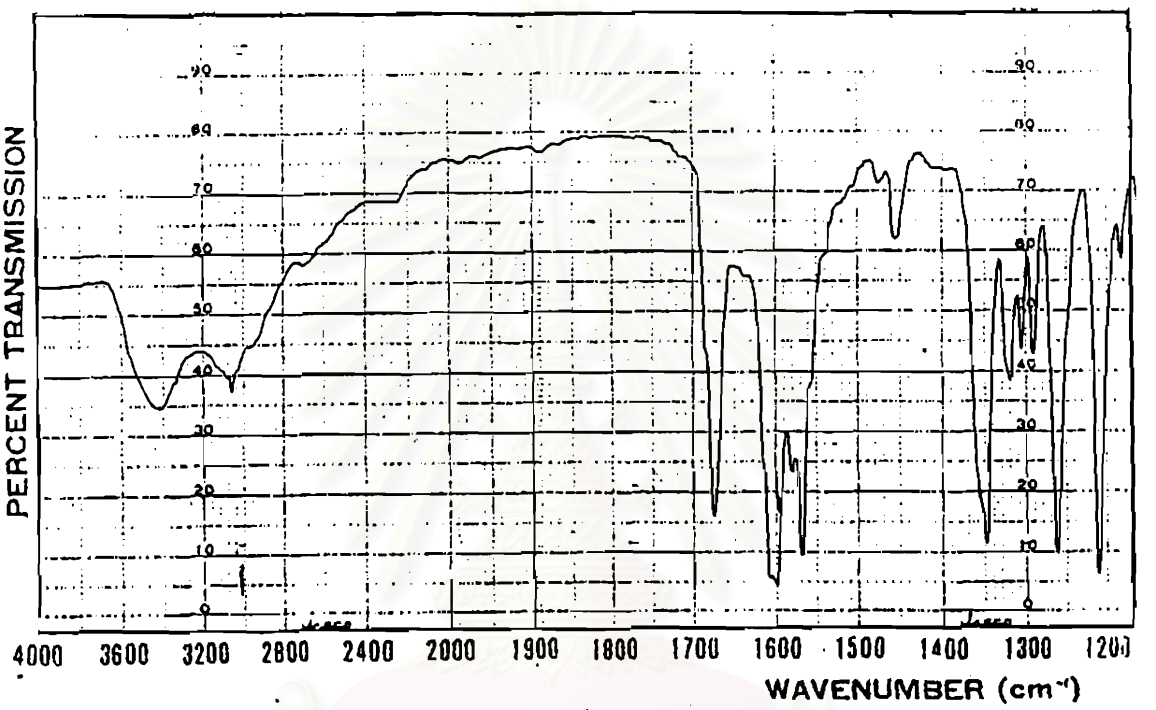

Fig. 35 IR spectrum of **ME-1** (KBr disc)

The results from the proton decoupled ^{13}C NMR spectrum (Fig. 36) suggested that the molecule contained eleven carbons, yet the results of the high resolution mass spectrum gave a molecular formula of $C_{21}H_{12}O_6$. This inconsistency suggested that ten signals were doubled (Table 10). The pattern of ^{13}C signals was similar to that of **ET-2**, except for the absence of the signal at δ 111.3 (C-3 of **ET-2**), and the appearance of a quaternary signal at δ 121.9 (C-3 of **ME-1**) and also a signal at 17.9 ($-CH_2$ of **ME-1**). This suggests the presence of a new quaternary carbon instead of one sp^2 carbon bearing proton.

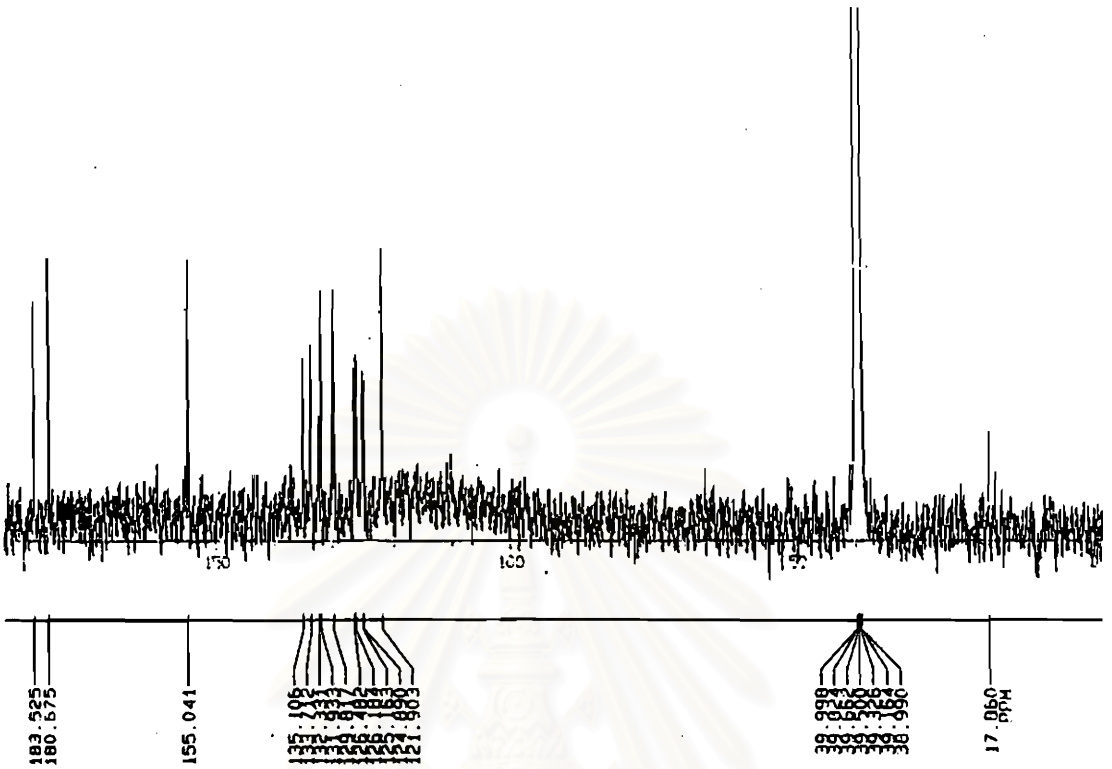

Fig. 36 ^{13}C NMR (125 MHz) spectrum of **ME-1** (in DMSO-*d*)

Table 10 ^{13}C NMR data of **ME-1** (125 MHz, DMSO-*d*)

C	δ_C (ppm)
1, 1'	180.7
2, 2'	155.0
3, 3'	121.9
4, 4'	183.5
4a, 4a'	131.9
5, 5'	125.5
6, 6'	134.4
7, 7'	133.0
8, 8'	125.8
8a, 8a'	129.8
3-CH_2	17.9

A DEPT 135° pulse sequence gave only five signals (Fig. 37). Among these five ^{13}C signals, the most upfield signal at 17.9 ppm was first considered to be a methyl carbon signal. However, its signal intensity was fairly small, when compared with the down field signals (The odinary methyl signal appears in high intensity in both ^{13}C and ^{1}H spectra). For the single frequency off resonanced (OFR) spectrum (Fig. 38), it gave a triplet signal of this chemical shift value, indicating that this signal should be methylene. Other four signals were all assigned as sp^2 carbons. Thus, there should be at least four sp^2 carbons and one methylene carbon in this molecule as well as six quaternary carbons.

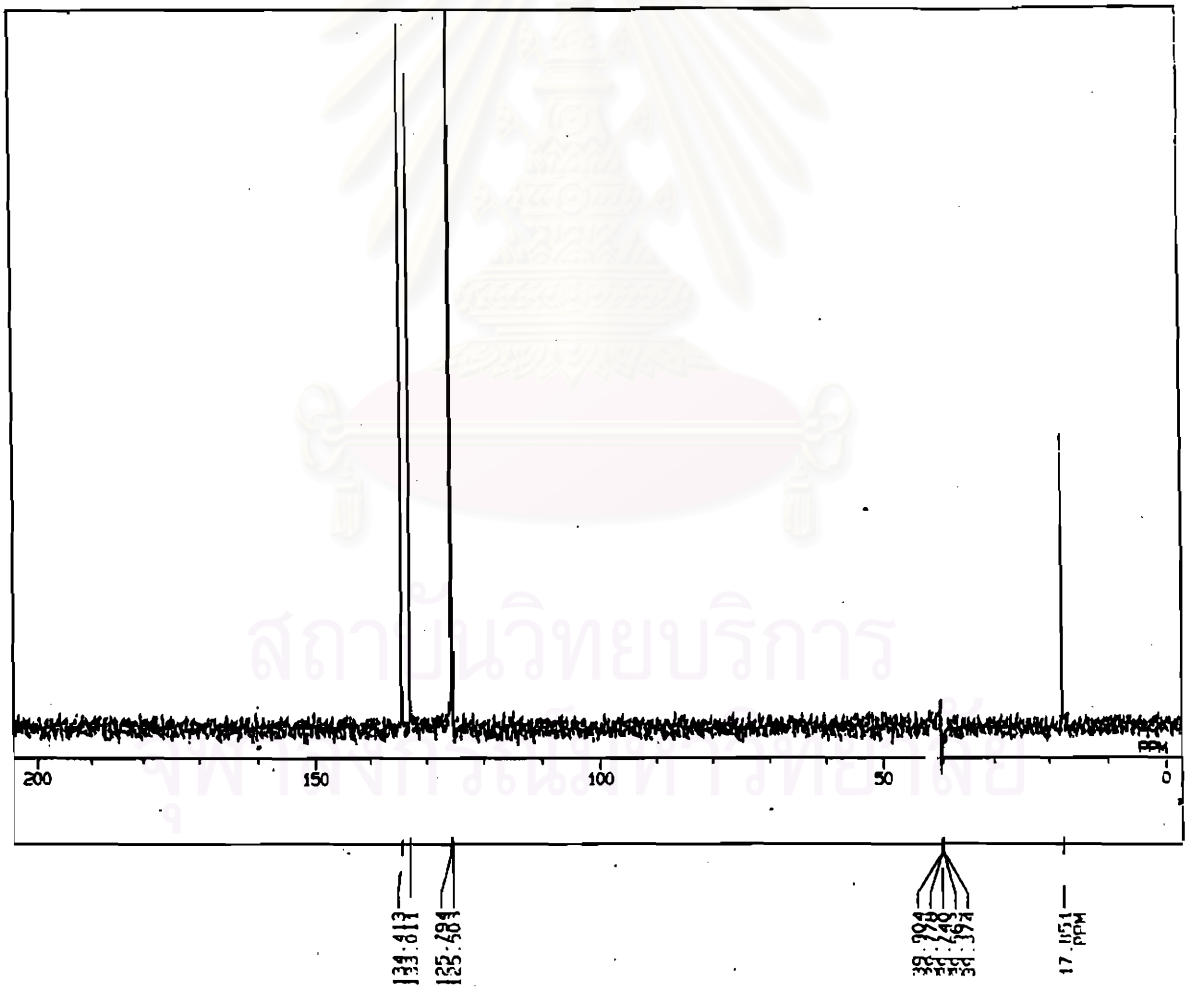

Fig. 37 DEPT 135° NMR (125 MHz) spectrum of **ME-1** (in DMSO-*d*)

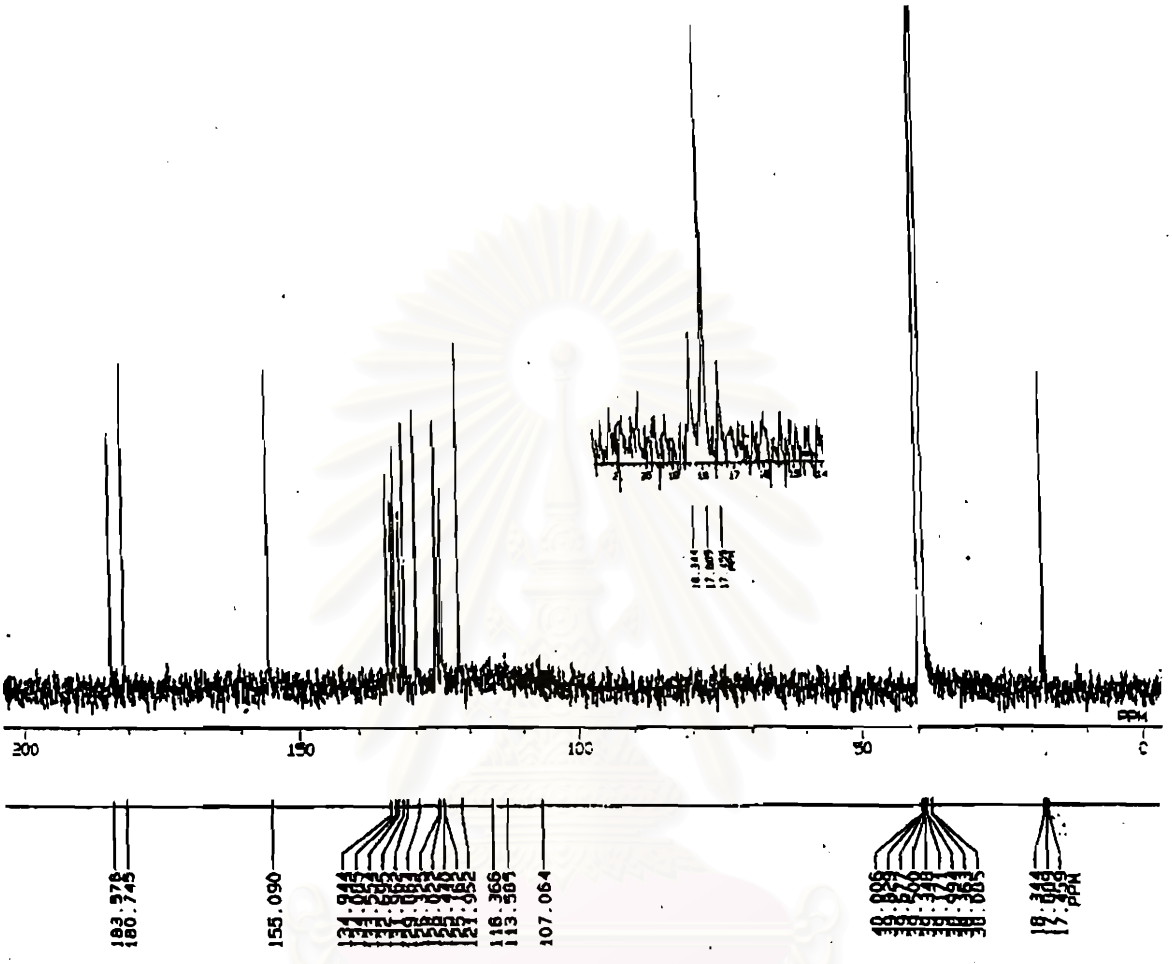

Fig. 38 Single frequency off resonance ^{13}C NMR (125 MHz) spectrum of **ME-1** (in DMSO-d)

The ^{1}H NMR of **ME-1** (Fig. 39) also showed closed similarity to that of **ET-2**. The fine splitting in the aromatic region was also the same as **ET-2**, indicating that this molecule was composed of the same naphthoquinone moiety. Another one broad proton singlet appearing at δ 10.86, seemed to be a hydrogen-bonded proton signal. There was a two-proton singlet signal at δ 3.76 which could be considered to be methylene protons (Table 11). Hetero COSY clearly exhibited this signal as correlating to the carbon signal at δ 17.9 and also long range correlated to the signals at δ 121.9 (C-3 and C-3'), 155.0 (C-2 and 2') and 183.5 (C-4 and 4') in HMBC (Fig. 40 and 41). Following the additive rule in chemical shift assignment, bis-

benzylmethylene gives reasonable chemical shift values of 3.9-4.0 ppm. It is plausible that the methylene carbon bonded to two aromatic rings or similar systems can afford the same electronic atmosphere as benzene ring. This consideration was supported by the result of the mass measurement. Therefore, the structure of **ME-1** was clearly identified as methylene-3,3'-bilawsone. This is the first report on the occurrence of methylene-3,3'-bilawsone in the natural source.

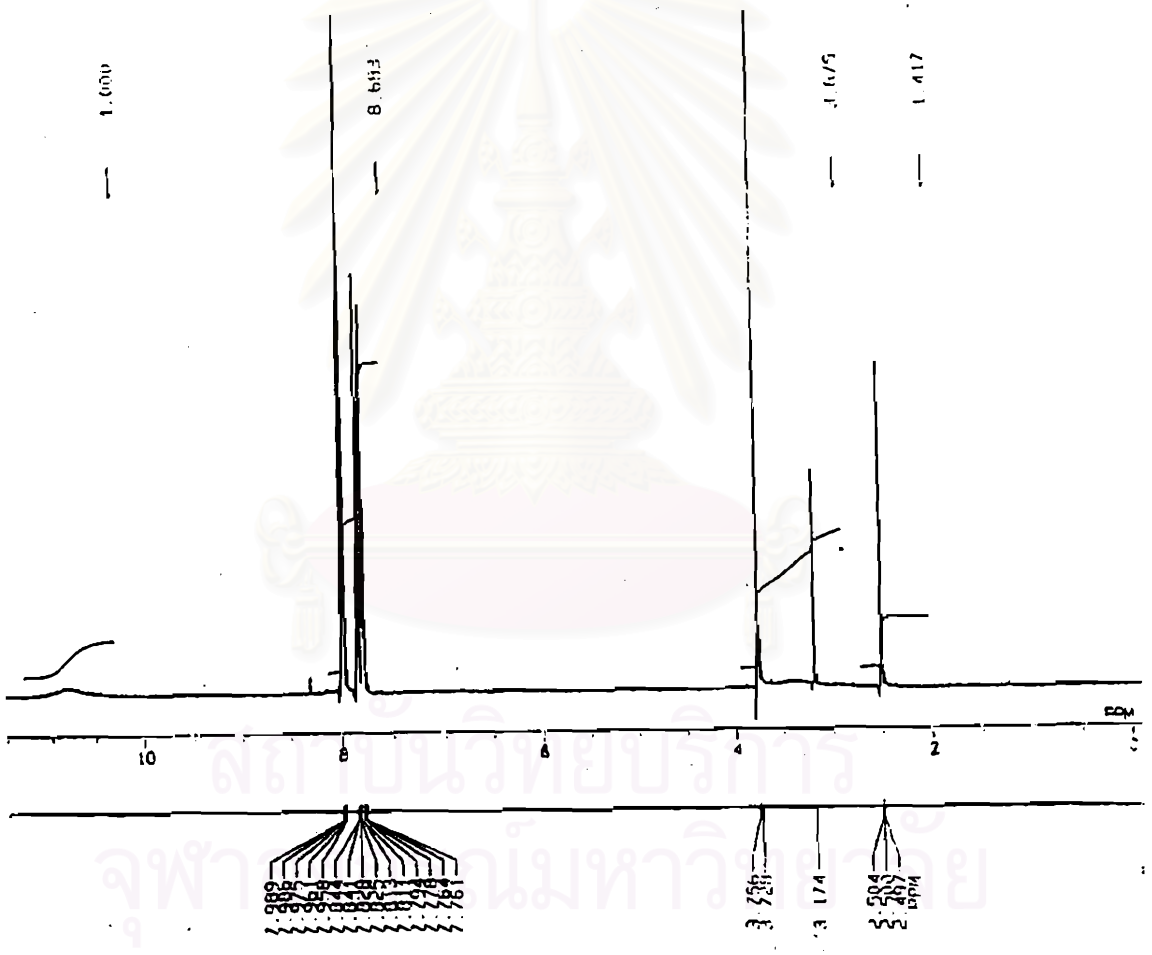

Fig. 39 ^{1}H NMR (500 MHz) spectrum of **ME-1** (in DMSO-*d*)

Table 11 ^{1}H NMR data of **ME-1** (500 MHz, DMSO-*d*)

H	δ_H (ppm)	Splitting pattern and coupling constant
5, 5'	7.98	2H, dd, *J* = 7.0, 1.5 Hz
6, 6'	7.78	2H, ddd, *J* = 7.5, 7.5, 1.5 Hz
7, 7'	7.83	2H, ddd, *J* = 7.5, 7.5, 1.5 Hz
8, 8'	7.97	2H, dd, *J* = 7.5, 1.5 Hz
3-CH_2	3.76	2H, s
2, 2'-OH	10.86	2H, s

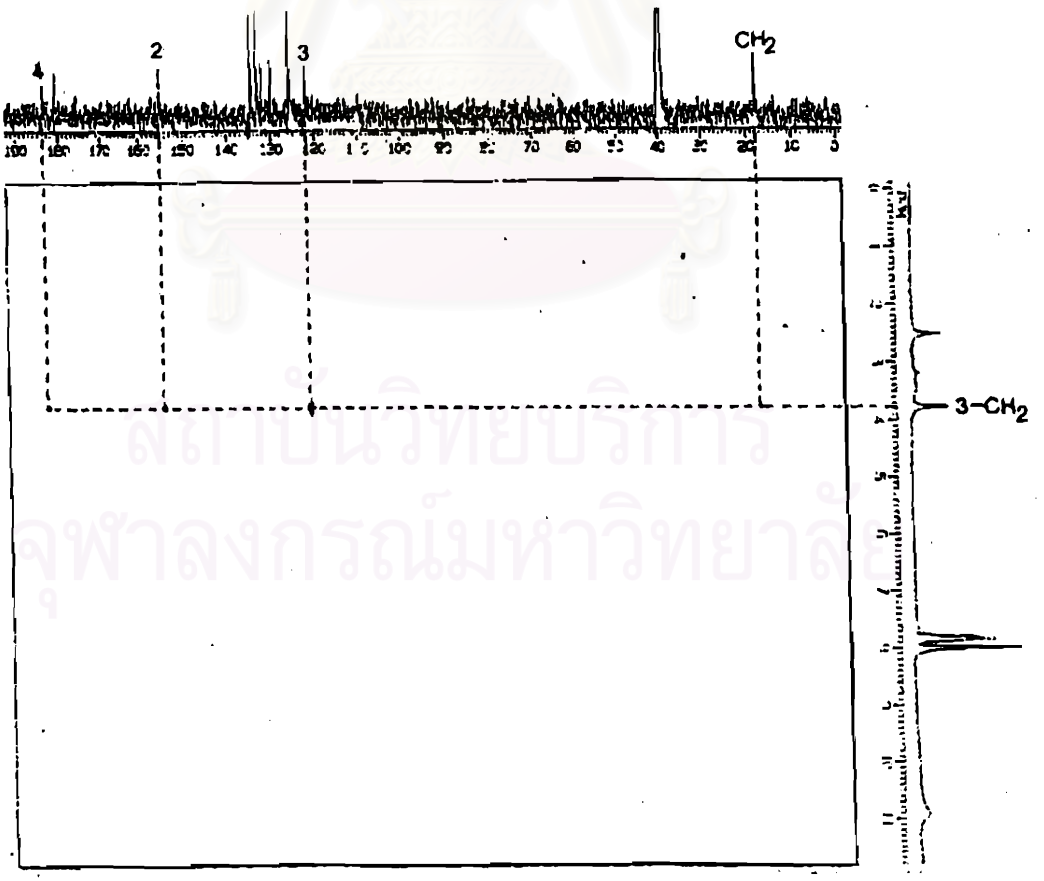

Fig. 40 HMBC spectrum (125 MHz) spectrum of **ME-1** (in DMSO-*d*)

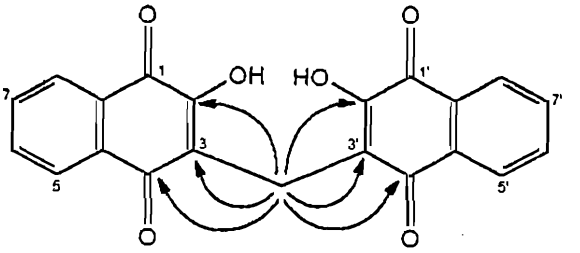

Fig. 41 Important ^{13}C-^{1}H long range correlations observed by heteronuclear COSY of **ME-1**

1.5 Identification of ME-2

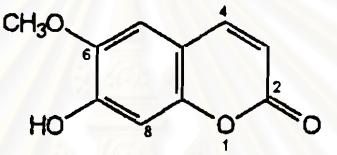

Fig. 42 Structure of **ME-2**

ME-2 was obtained as white crystals (3.4 mg, 0.002% dry weight) from a mixture of chloroform and hexane. **ME-2** was identified as the known compound, scopoletin (Fig. 42). This compound showed a characteristic blue fluorescent spot on the TLC plate under UV light (365 nm) was similar to that of scopoletin (Pharkphoom Panichayupakaranant and Wanchai De-Eknamkul, 1992). Its mass spectrum (Fig. 43) revealed the presence of the molecular ion peak [M^{+}] at *m/z* 192 and also major fragment peaks at *m/z* 177, 164, 149 and 121. The fragment at *m/z* 177 corresponds to the emission of a methyl radical to provide a conjugated oxonium ion. The peak at *m/z* 164 arose from the expulsion of -CO group from the molecule. The fragment peak at *m/z* 149 was due to the loss of a methyl and -CO groups. The fragment peak at *m/z* 121 corresponds to the loss of another -CO group from the carbonyl group of oxonium ion (Fig. 44).

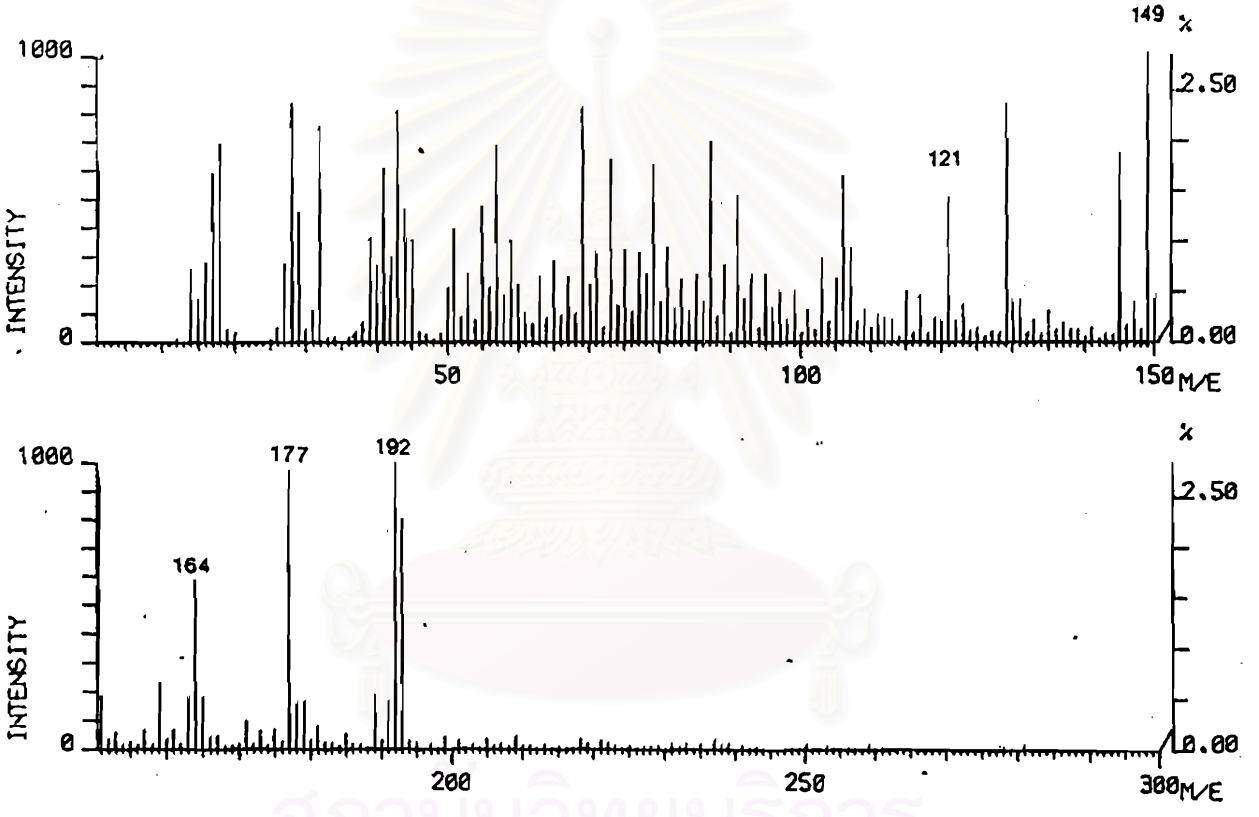

Fig. 43 Mass spectrum of ME-2

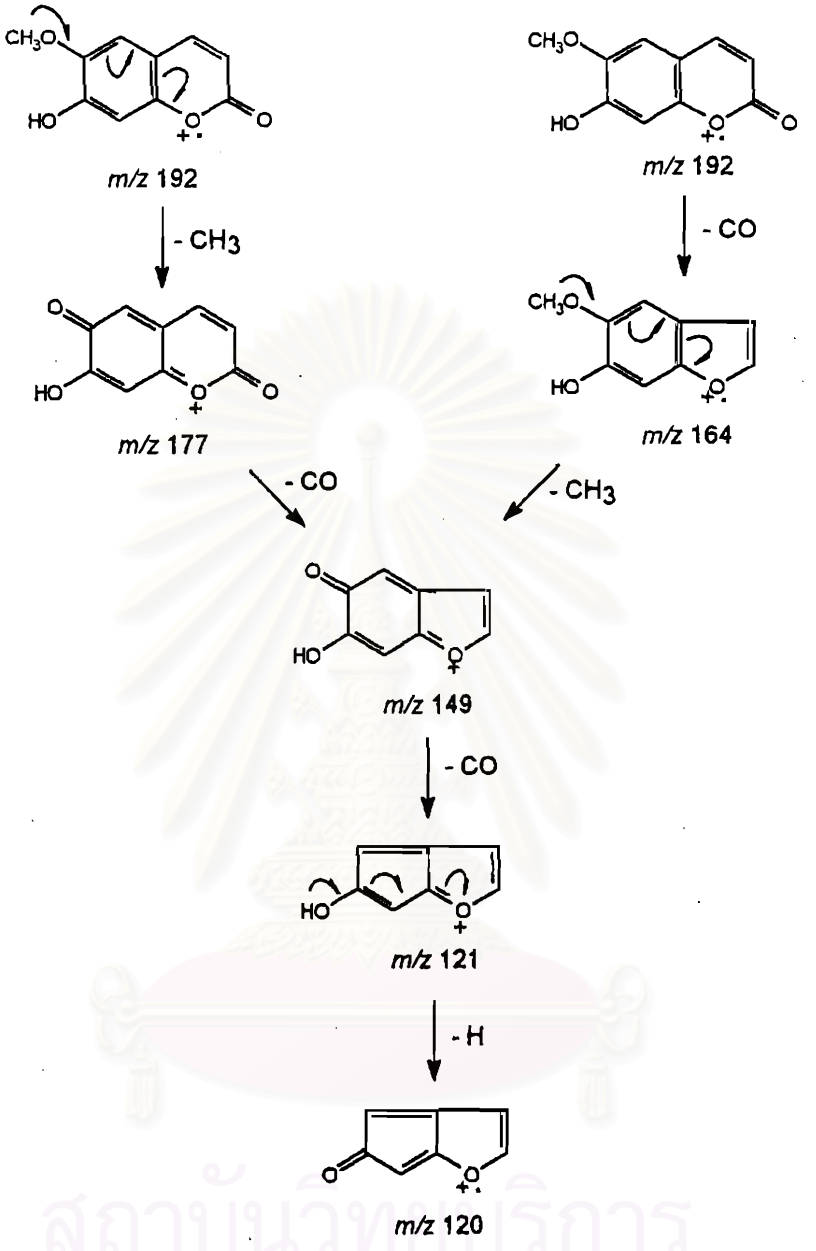

Fig. 44 Fragmentation of ME-2

Its IR spectrum (Fig. 45) exhibited characteristic bands of O-H stretching at 3,325 cm^{-1}, C=O stretching at 1,720 cm^{-1}, C=C stretching of aromatic ring at 1,610, 1,560 and 1,510 cm^{-1} and C(O)-O stretching at 1,330 and 1,130 cm^{-1}. Based on these data and the comparison of IR (Fig. 45) and UV absorption (Fig. 46) spectra with the authentic compound firmly indicated that this compound is scopoletin.

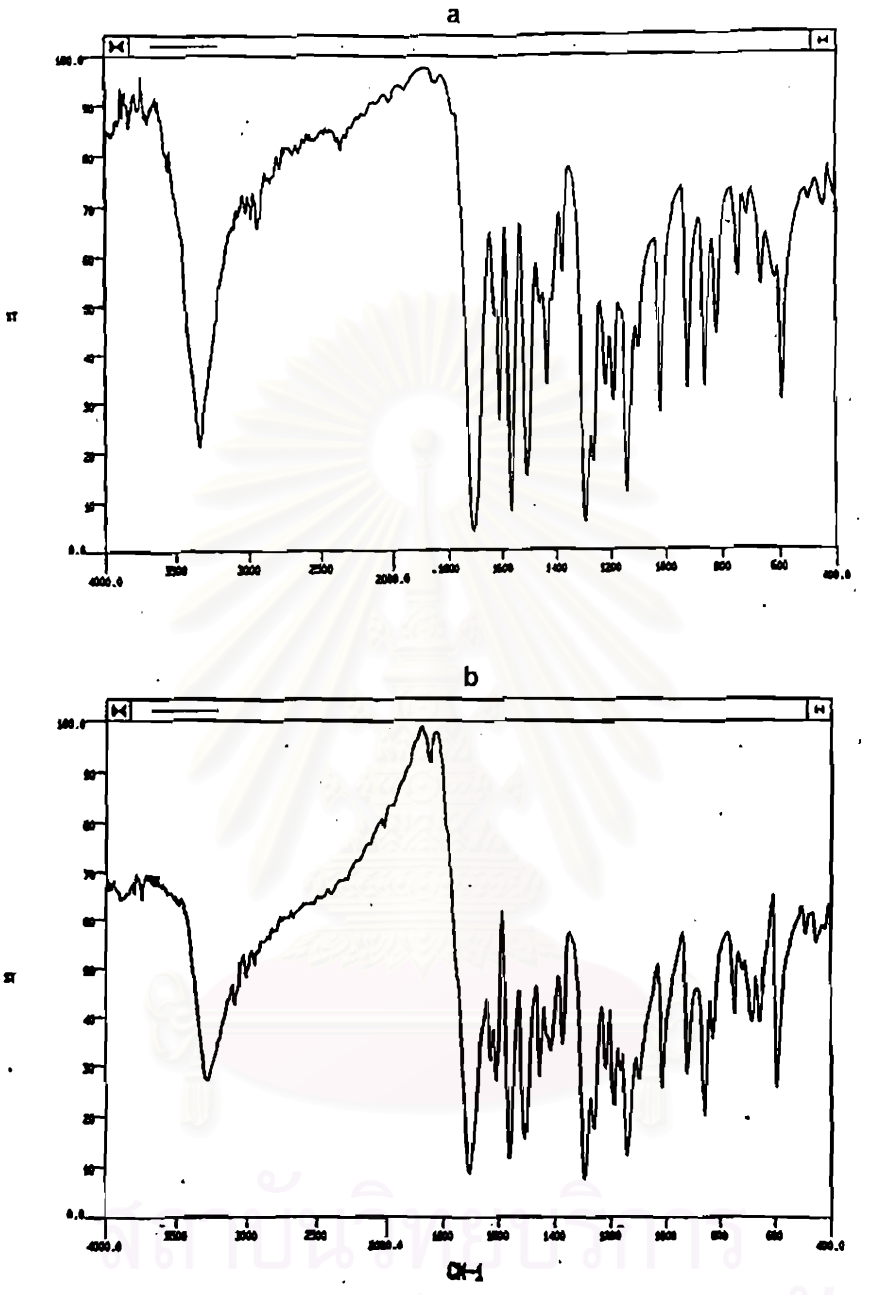

Fig. 45 IR spectra of ME-2 (a) and authentic scopoletin (b) (KBr disc)

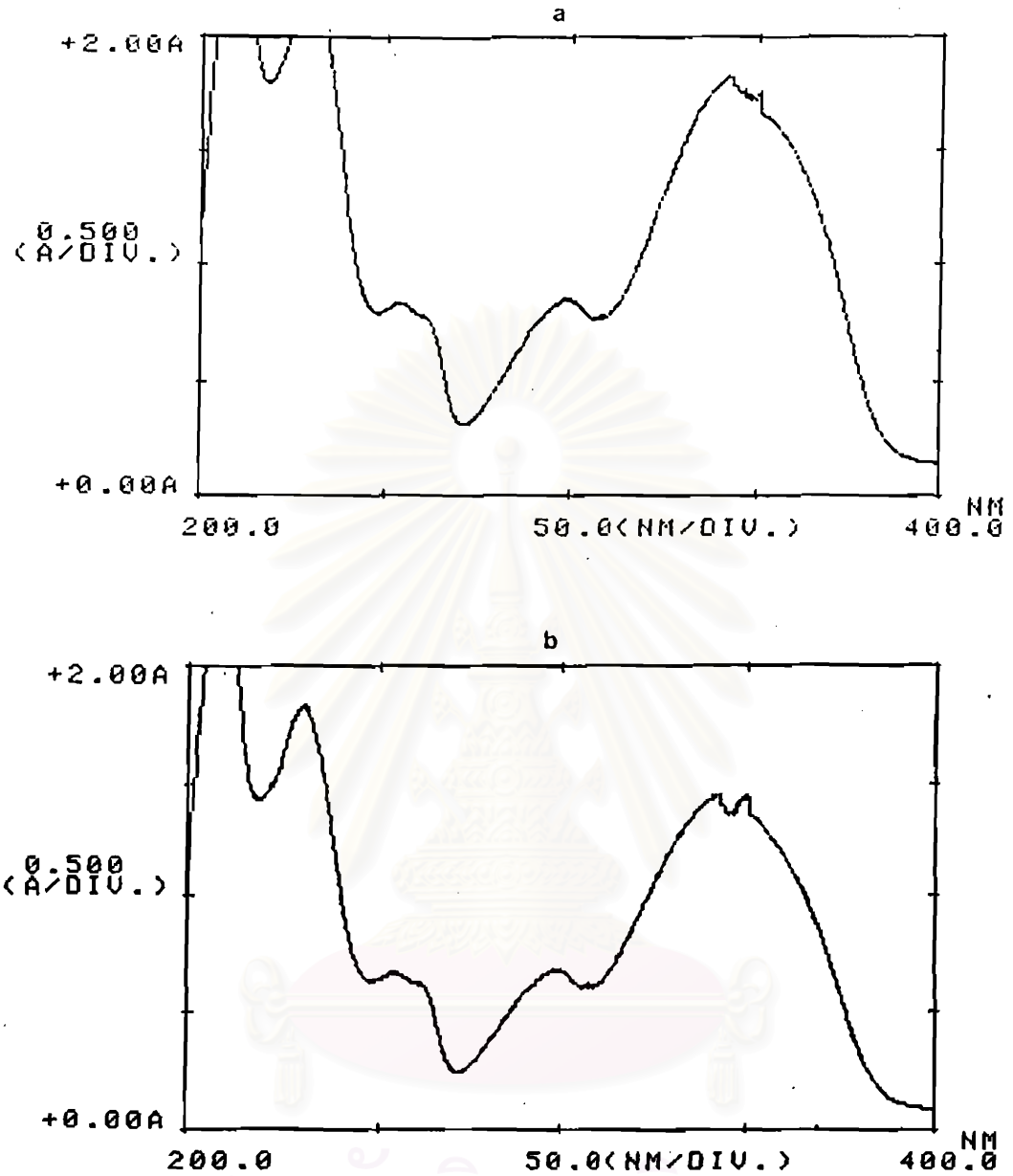

Fig. 46 UV spectra of ME-2 (a) and authentic scopoletin (b) (in ethanol)

1.6 Identification of ME-3

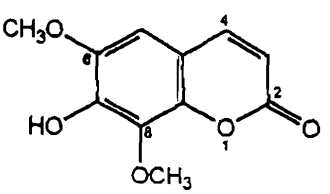

Fig. 47 Structure of ME-3

ME-3 was obtained as red rosette aggregates (9 mg, 0.005% dry weight) obtained from a mixture of chloroform and hexane. **ME-3** was identified as the known compound isofraxidin (Fig. 47). This compound exhibited a characteristic yellowish fluorescent spot on TLC plate under UV light (365 nm). Its Rf value was a little lower than **ME-2** in several TLC solvent systems, such as chloroform/ethyl acetate (19:1). Its mass spectrum (Fig. 48) showed a molecular ion peak [M^+] at *m/z* 222 and major fragment peaks at 207, 194 and 179. The fragment at *m/z* 207 corresponds to the loss of methyl radical to provide the conjugated oxonium ion.

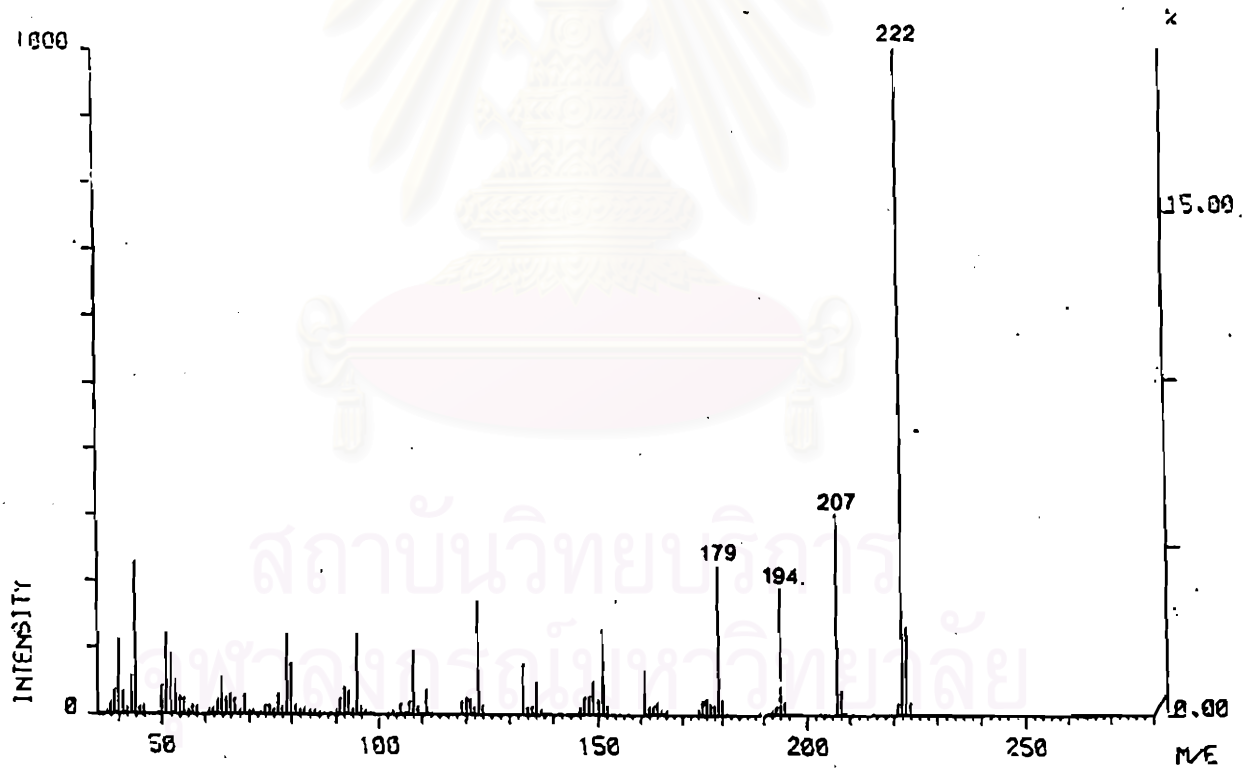

Fig. 48 Mass spectrum of **ME-3**

The peak at *m/z* 194 occurred by the expulsion of -CO group from the lactone carbonyl group. The fragment peak at *m/z* 179 could come from the expulsion of -CO

together with the loss of methyl radical to form another conjugated oxonium ion (Fig. 49). From its molecular ion peak, which was 30 amu higher than that of **ME-2,** and the pattern of fragmentation which was similar to that of **ME-2**, it could be inferred that this compound might be a methoxy derivative of **ME-2.**

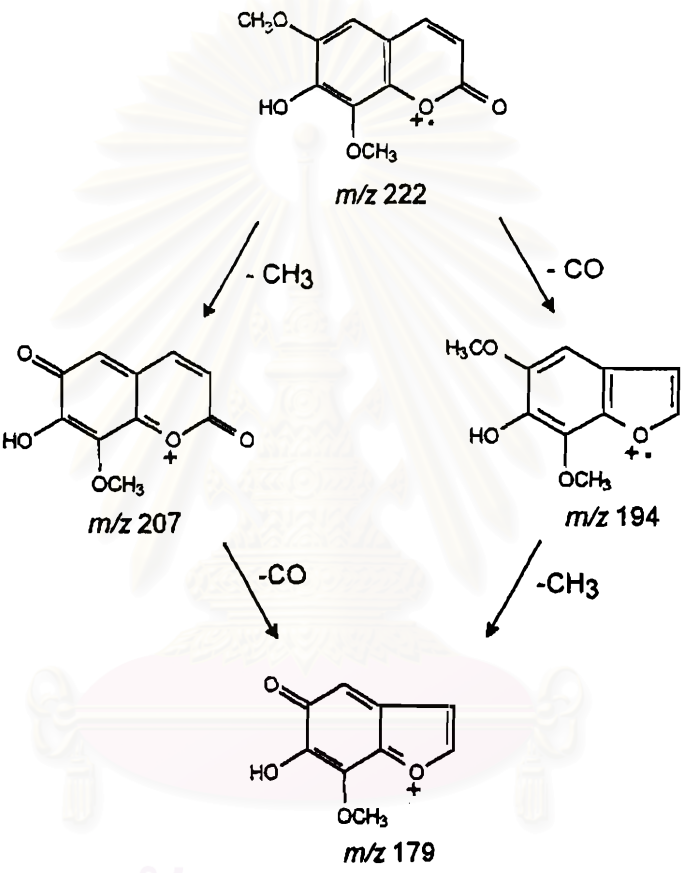

Fig. 49 Fragmenttation of **ME-3**

To confirm this assumption, its ^{1}H (Fig. 50) and ^{13}C (Fig. 51) NMR spectra were measured and compared with those of the known isofraxidin (Borris, Cordell and Farnsworth, 1980). In addition, NOE difference experiment showed that irradiation of the methoxyl protons at δ 3.94 enhanced the H-5 signal at δ 6.66 by 12.83% (Fig. 52). All these results, therefore, suggests that this compound is isofraxidin (8-methoxyscopoletin). The complete assignment of its structure are given in Table 12 and 13.

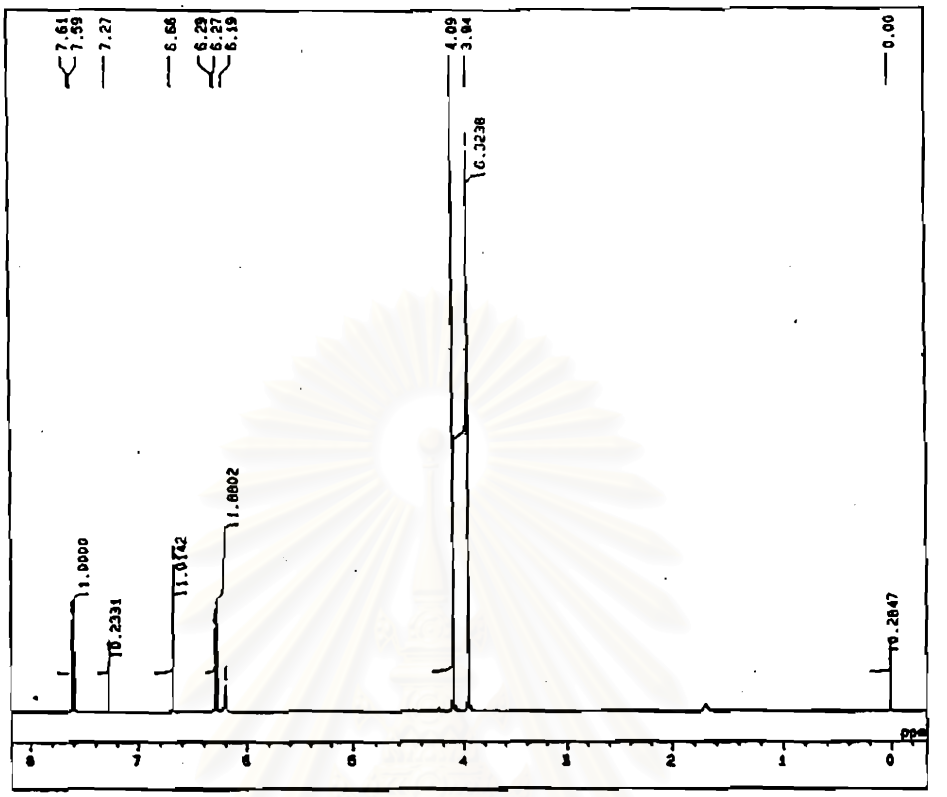

Fig. 50 ^{1}H NMR (500 MHz) spectrum of **ME-3** (in $CDCl_3$)

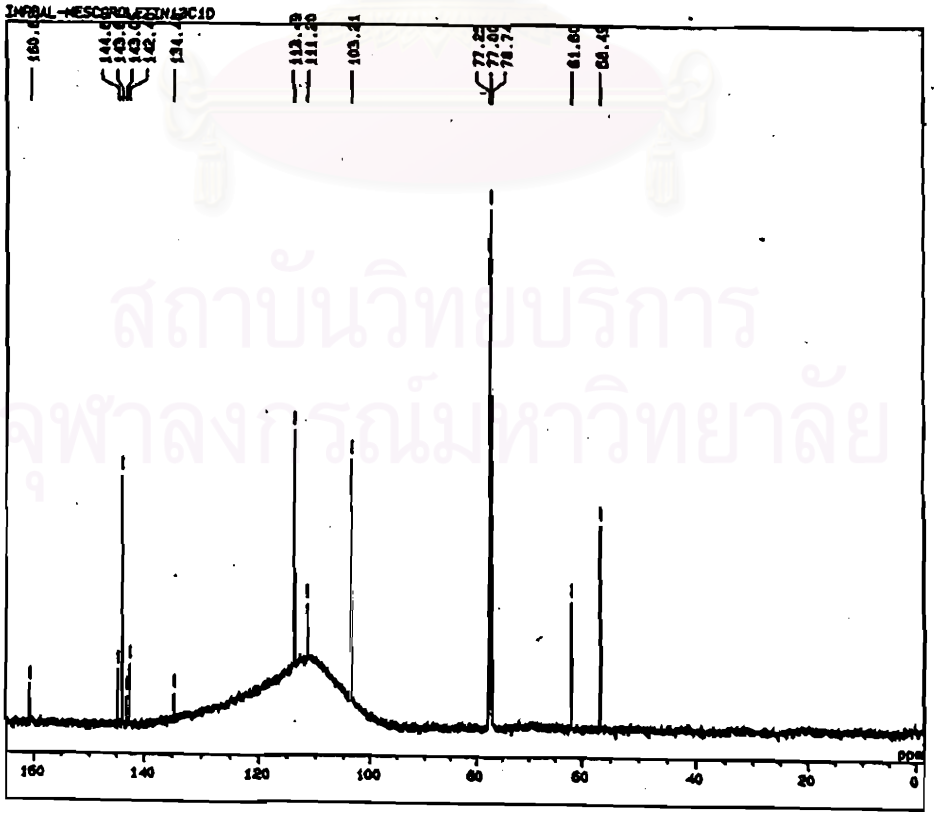

Fig. 51 ^{13}C NMR (125 MHz) spectrum of **ME-3** (in $CDCl_3$)

Fig. 52 NOE difference spectrum (500 MHz) of **ME-3**

Table 12 ^{13}C NMR data of **ME-3** (125 MHz, $CDCl_3$)

C	δ_C (ppm)
2	160.6
3	103.2
4	143.8
5	113.5
4a	111.2
6	144.6
7	134.5
8	143.1
8a	142.5
6-OMe	56.5
8-OMe	61.6

Table 13 ^{1}H NMR data of **ME-3** (500 MHz, $CDCl_3$)

H	δ_H (ppm)	Splittig pattern and coupling constant
3	6.28	1H, d, *J* = 10 Hz
4	7.60	1H, d, *J* = 10 Hz
5	6.66	1H, s
6-OMe	3.94	3H, s
8-OMe	4.09	3H, s

1.7 Structure elucidation of ME-4

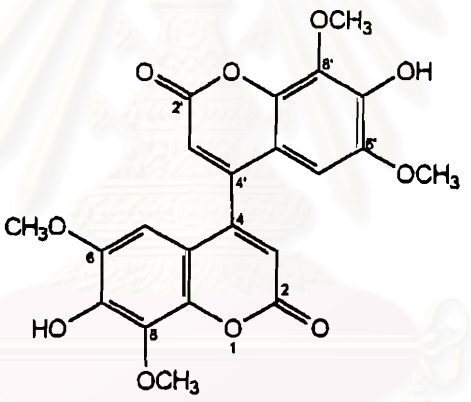

Fig. 53 Structure of **ME-4**

ME-4 was obtained as yellow crystals (6 mg, 0.004% dry weight) crystallized from a mixture of chloroform and methanol. Examination of the spectroscopic data of **ME-4** clearly established that this compound is a new biscoumarin, 4,4'-biisofraxidin (Fig. 53). This compound gave a characteristic green-yellowish fluorescent spot on the TLC plate under UV light (365 nm), and exhibited UV absorption maxima at 390 nm (Fig. 54). Its EI mass spectrum (Fig. 55) showed a molecular ion peak [M^+] at *m/z* 442, and gave fragmentation of *m/z* 414 and *m/z* 399 which arise, as in **ME-3**, by the expulsion of -CO from the lactone carbonyl group and subsequent loss of methyl radical (Fig. 49).

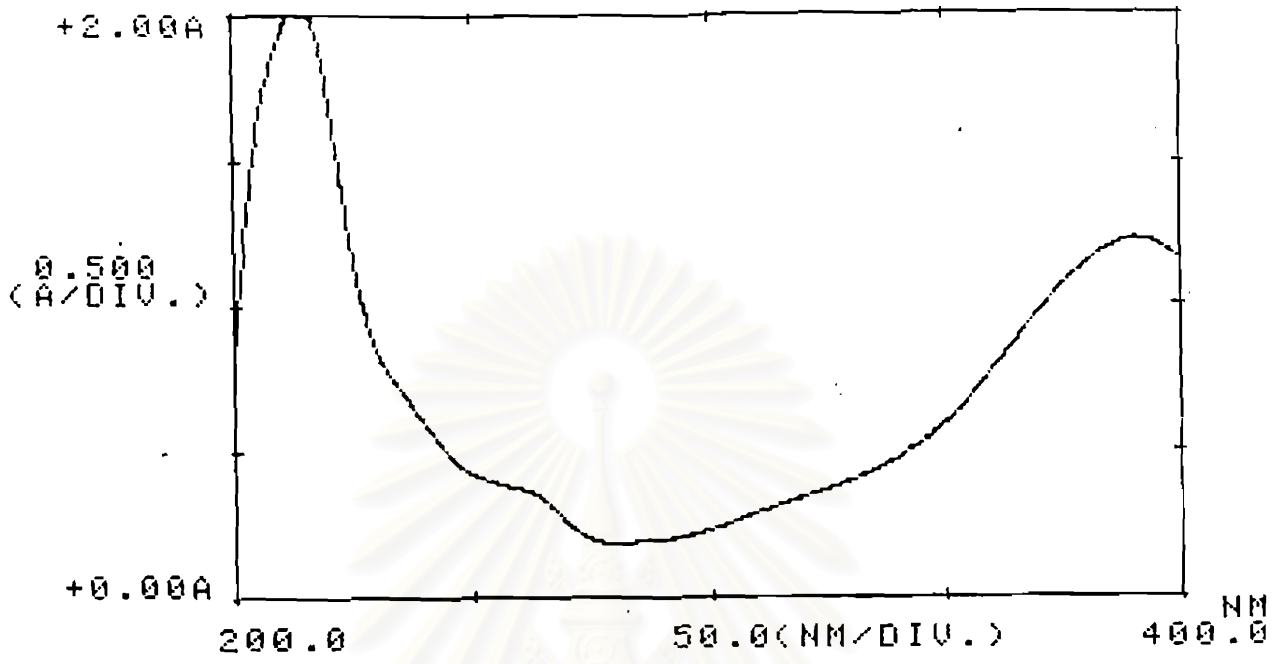

Fig. 54 UV spectrum of ME-4 (in ethanol)

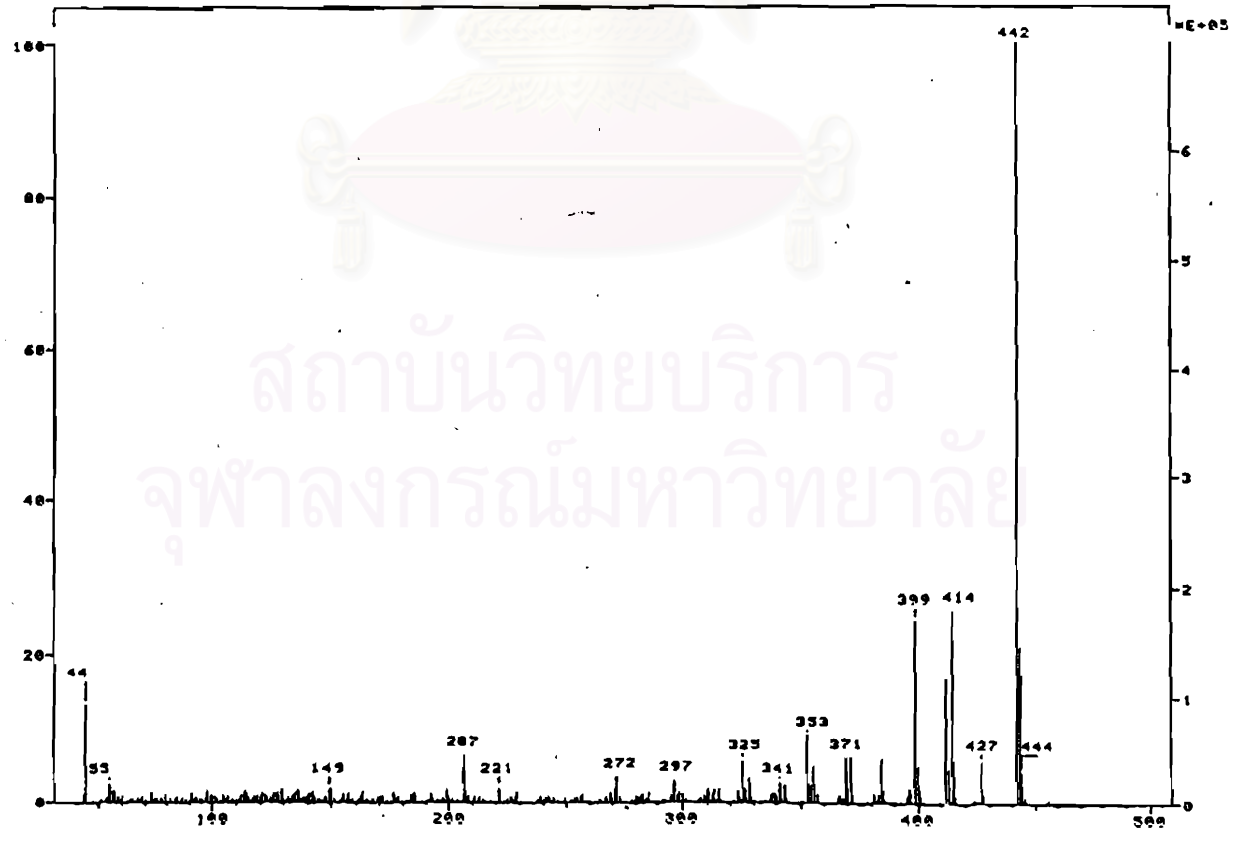

Fig. 55 Mass spectrum of ME-4

High resolution mass spectrum gave a molecular formula of $C_{22}H_{18}O_{10}$ (*m/z* 442.0900 [M^+] ; calc. for $C_{22}H_{18}O_{10}$:442.0891). Its IR spectrum (Fig. 56) exhibited the characteristic bands of O-H stretching at 3,410 cm^{-1}, C=O stretching at 1,706 cm^{-1}, C=C stretching of aromatic ring at 1,608, 1,576 and 1,500 cm^{-1}, C=C stretching at 1460 cm^{-1} and C (O)-O stretching at 1,232 and 1,106 cm^{-1}.

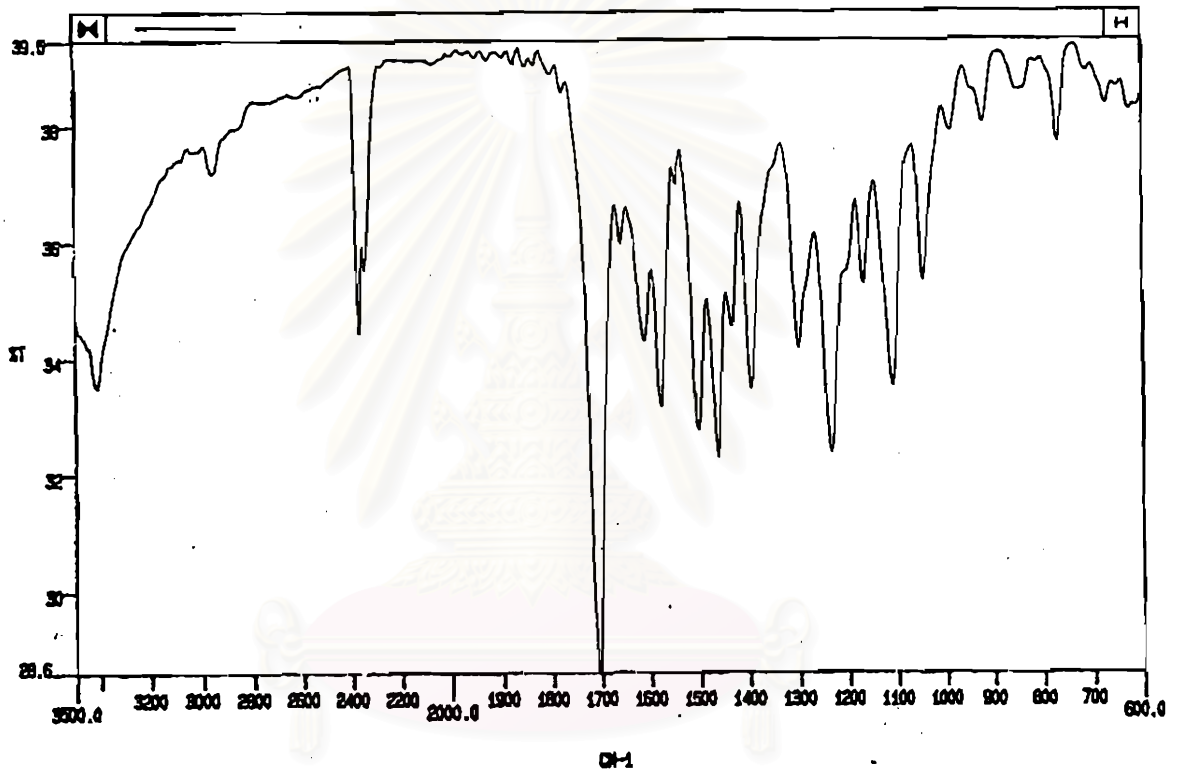

Fig. 56 IR spectrum of **ME-4** (KBr disc)

The proton noise decoupled ^{13}C NMR (Fig. 57) showed eleven carbon signals, coresponded to only half of the carbon atoms in the molecular formula of $C_{22}H_{18}O_{10}$. These results suggested that this compound should be composed of two symmetric C_{11}-molecules. The pattern of ^{13}C signals showed very close similarity to that of **ME-3**. **ME-4** might therefore be a dimer of **ME-3**. A DEPT 135° (Fig. 58) exhibited only two methine (sp^2) carbon signals at δ 104.7 and 143.4, indicating that one of the methine carbons of **ME-3** was substituted. According to its ^{13}C NMR data and **ME-3** assignment, the ^{13}C-chemical shifts of **ME-4** were assigned as shown in Table 14.

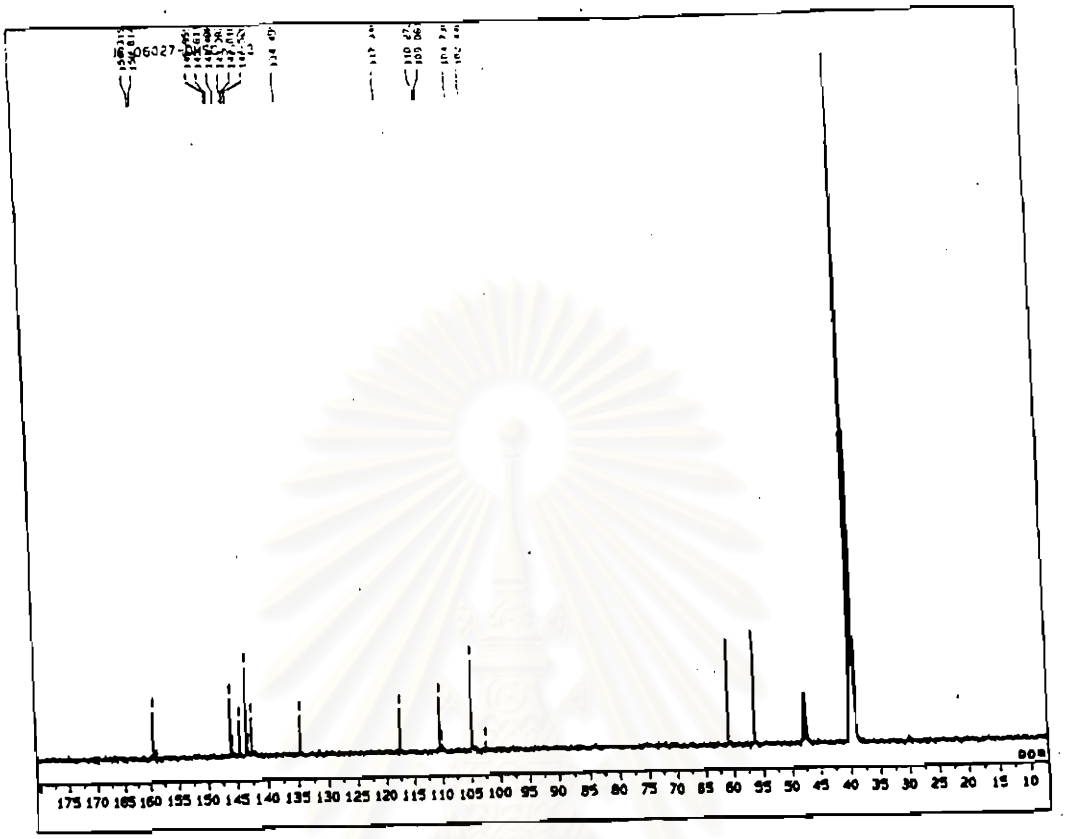

Fig. 57 Proton decoupled ^{13}C NMR (100 MHz) spectrum of ME-4 (in DMSO-*d*)

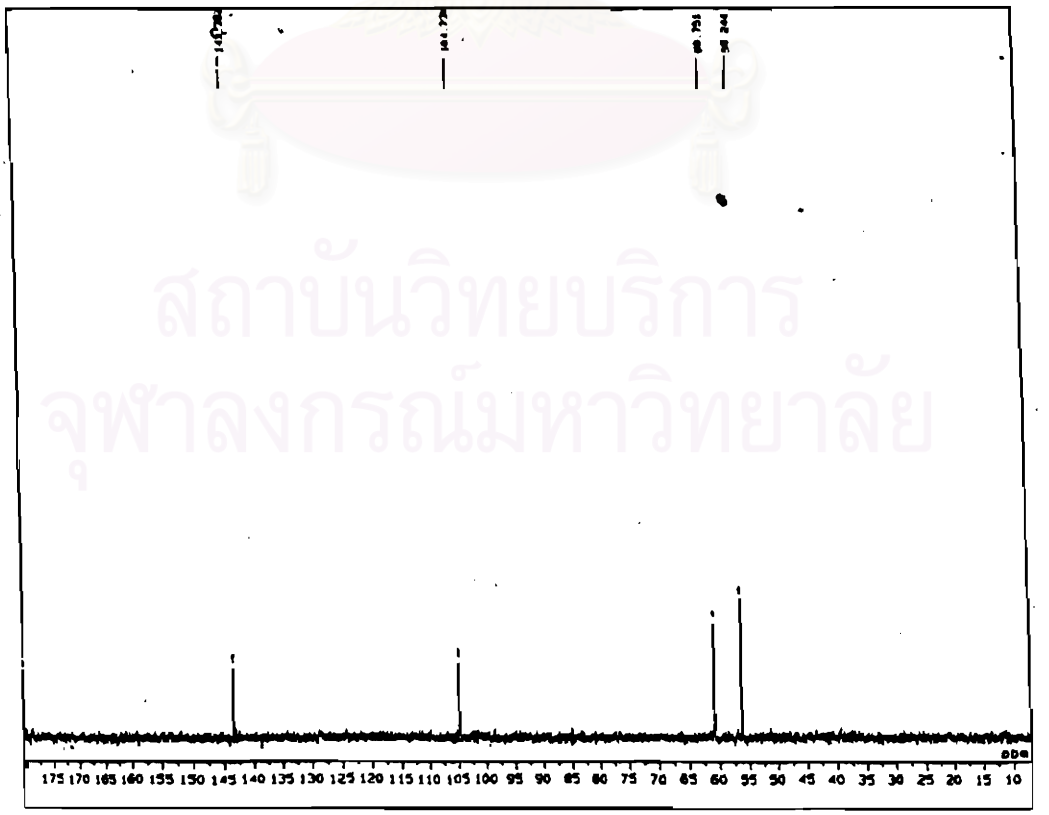

Fig. 58 DEPT135° NMR (100 MHz) spectrum of ME-4 (in DMSO-*d*)

Table 14 ^{13}C NMR data of ME-4 (100 MHz, DMSO-*d*)

C	δ_C (ppm)
2, 2'	159.3
3, 3'	104.7
4, 4'	117.3
5, 5'	143.4
4a, 4a'	110.3
6, 6'	146.0
7, 7'	134.5
8, 8'	144.5
8a, 8a'	142.5
6, 6'-OMe	56.2
8, 8'-OMe	60.8

The ^1H NMR spectrum(Fig. 59 and Table 15) of ME-4 was very simple and also similar to that of ME-3. Both signals at δ 7.08 and 8.27 were singlets, indicating that neither of them had any adjacent proton. The results of the HMBC experiment (Fig. 60) of ME-4 demonstrated that the ^1H signal at δ 7.08 gave correlations to the ^{13}C signals at δ 134.5, 142.5, 144.5 and 146.0, while the ^1H signal at δ 8.3 gave the correlation to the ^{13}C signals at 104.7, 117.3, 142.5 and 159.3 (Fig. 61). Moreover, there was no correlation between the methine carbons and protons of the other positions. These results suggested that the proton at δ 7.08 should be assigned as H-5 and the other as H-3. In addition, irradiation of H-5 gave NOE of about 1.0% to the methoxyl protons at δ 3.84 (Fig. 62) and no NOE was observed when the proton at δ 8.27 was irradiated. These results confirm that two molecules of ME-3 should be connected to each other at C-4 forming ME-4. Therefore, the structure of ME-4 was clearly established as 4,4'-biisofraxidin.

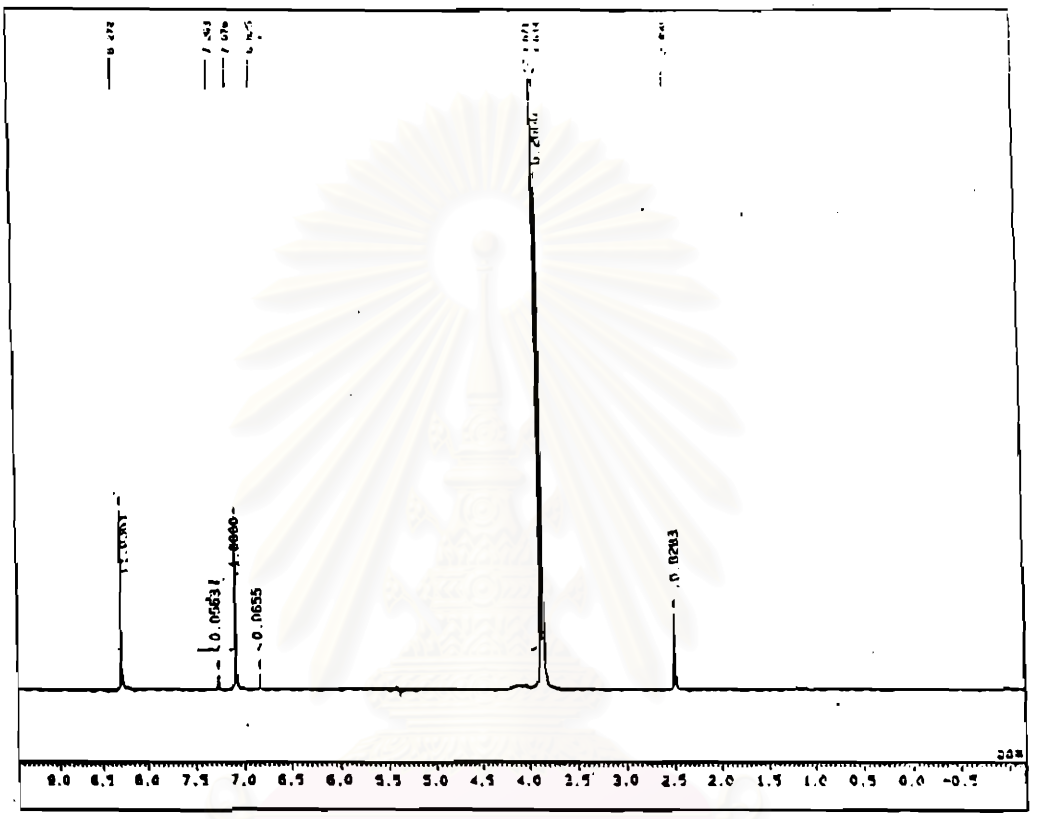

Fig. 59 ^{1}H NMR (400 MHz) spectrum of ME-4 (in DMSO-*d*)

Table 15 ^{1}H NMR data of ME-4 (400 MHz, DMSO-*d*)

H	δ_H (ppm)	Splitting pattern and coupling constant
3	8.27	1H, s
5	7.08	1H, s
3'	8.27	1H, s
5'	7.08	1H, s
6, 6'-OMe	3.84	6H, s
8, 8'-OMe	3.87	6H, s

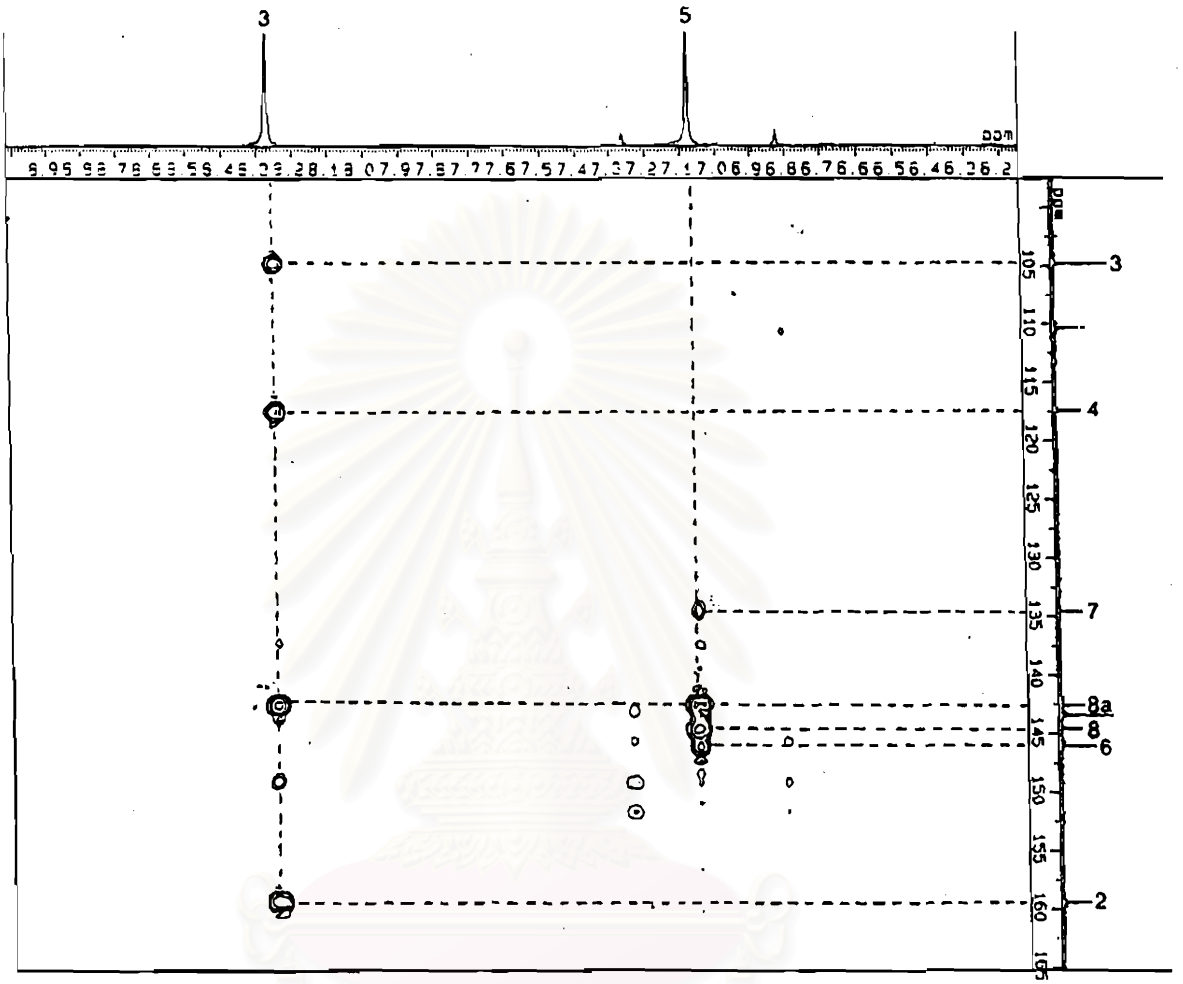

Fig. 60 HMBC spectrum (100 MHz) of **ME-4** (in DMSO-*d*)

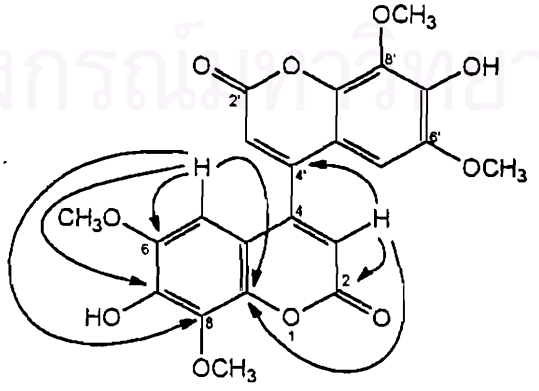

Fig. 61 Important ^{13}C-^{1}H long-range correlations observed by heteronuclear COSY of **ME-4**

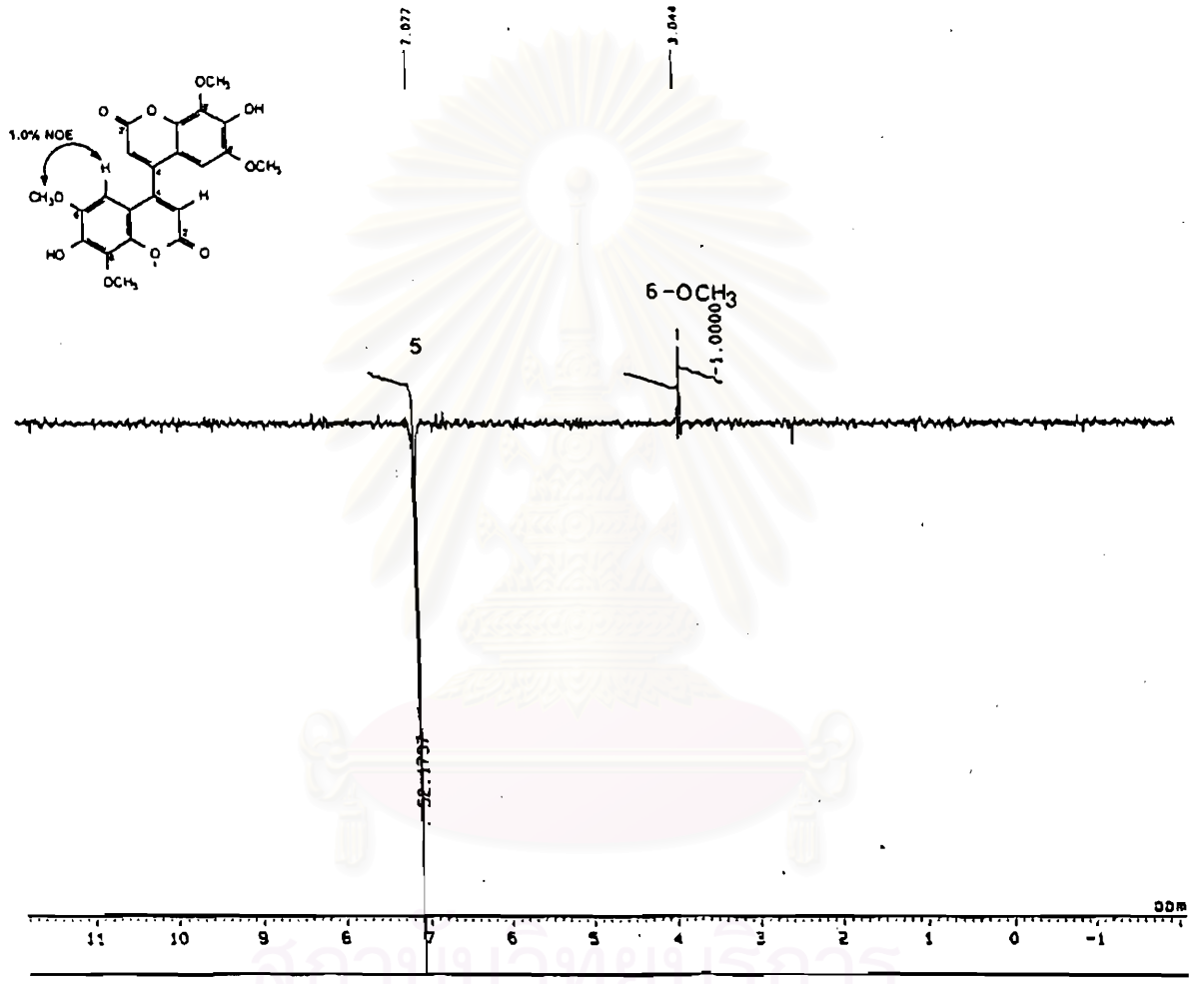

Fig. 62 NOE difference spectrum (400 MHz) of **ME-4** (in DMSO-*d*)

2. SECONDARY PRODUCT COMPOSITION OF THE CULTURED ROOTS AND INTACT PLANTS

2.1 Chemical patterns of secondary products

Based on the results of the isolation and structure elucidation of the secondary products produced by the cultured roots of *I. balsamina*, it appeared that the root cultures contained essentially two main groups, namely naphthoquinones and coumarins. The naphthoquinones include lawsone, 2-methoxy-1,4naphthoquinone and methylene-3,3'-bilawsone, and the coumarins include scopoletin, isofraxidin and 4,4'-biisofraxidin. Among these, methylene-3,3'-bilawsone (**ME-1**) was found to be the novel natural products found in this plant whereas 4,4'-biisofraxidin (**ME-4**) was found to be the new compound that has not been found before. To study in more detail about the nature of secondary products produced by the root culture, their chemical pattern were compared with those in the intact plants. In doing this, the methanolic extracts of the cultured roots, leaves and the whole roots of *I. balsamina* were prepared and analyzed by high performance liquid chromatography (HPLC) equipped with a photodiode array detector.

It appeared that all the secondary compounds, including lawsone (**ET-2**), 2-methoxy-1,4-naphthoquinone (**ET-1**), methylene-3,3'-bilawsone (**ME-1**), scopoletin (**ME-2**), isofraxidin (**ME-3**) and biisofraxidin (**ME-4**) could be effectively separated from one another (Fig. 63) by the solvent system of methanol/water, containing 0.15 M H_3PO_4 (gradient system) using RP-18 column. The acidity of the solvent system could overcome the problem of broad tailing peaks by suppressing the ionization effect of these compounds. According to their UV absorption maxima, both the napthoquinones and coumarins were detected at UV 275 nm, whereas, only the coumarin derivatives were detected at 365 nm. The identification of each peak was performed by comparison with the retention times (R_t) and UV absorption spectra of authentic compounds. The results showed that the naphthoquinones lawsone, 2-methoxy-1,4-naphthoquinone and methylene-3,3'-bilawsone exhibited the R_t values of 38.17, 40.98 and 59.58 min while the coumarin derivatives, scopoletin, isofraxidin and biisofraxidin showed the R_t values of 31.00, 31.90 and 48.58 min, respectively.

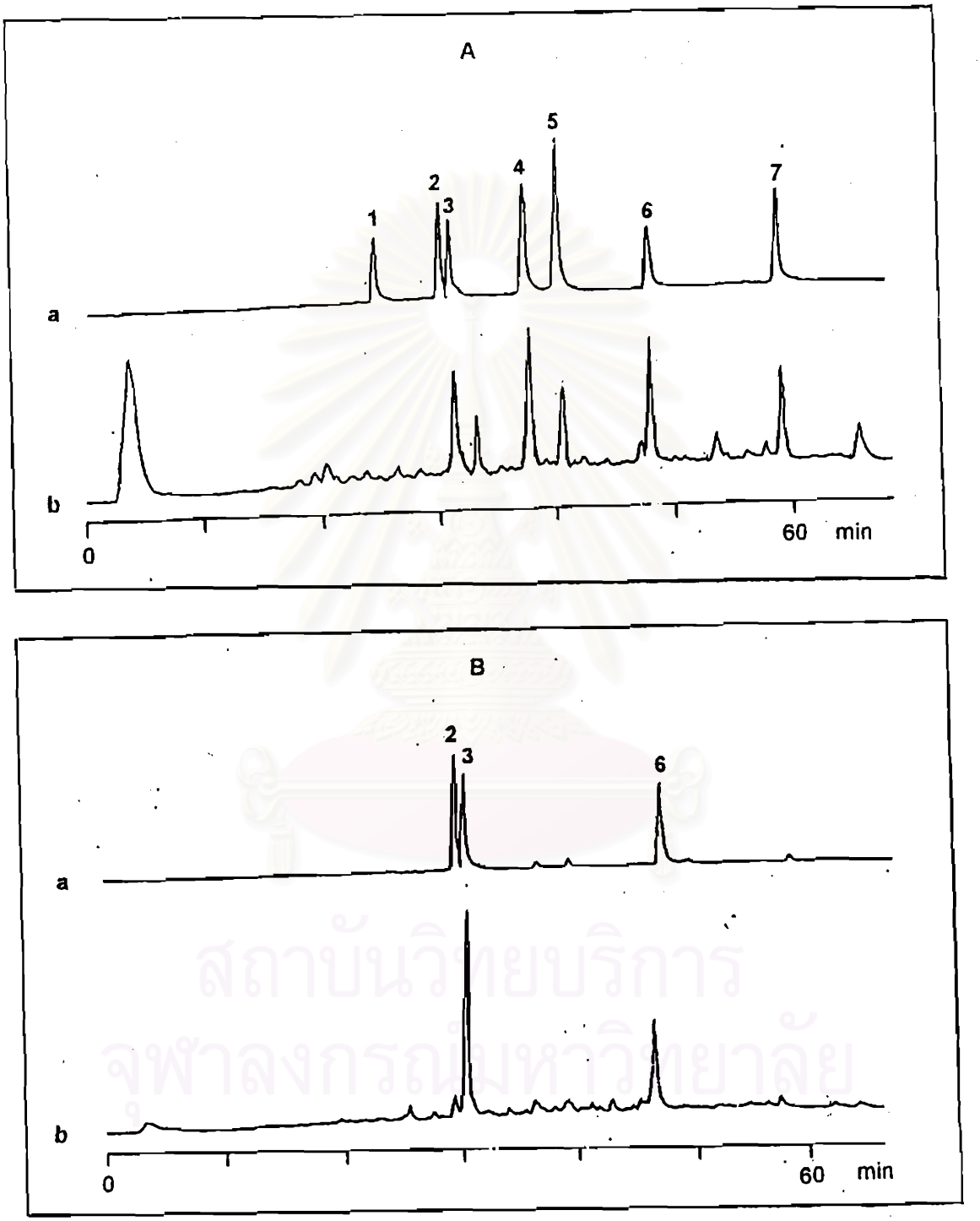

Fig. 63 HPLC chromatograms detected with UV 275 nm (A) and 350 nm (B) of the authentic compounds (a) and the extract of cultured roots (b). 1 : O-succinylbenzoic acid; 2 : scopoletin; 3 : isofraxidin; 4: lawsone; 5 : 2-methoxy-1,4-naphthoquinone; 6 : 4,4'-biisofraxidin; 7 : methyl-3,3'-bilawsone

HPLC chromatograms of the methanolic extracts confirmed that the naphthoquinone and coumarin derivatives are the two major groups of secondary products of the root culture. However, its chemical composition was found to be considerably different from those of the leaves and the whole roots of the plant. (Fig. 64 and 65). With respect to the naphthoquinones (Fig. 64), the root cultures appeared to contain lawsone as the major constituent, while 2-methoxy-1,4-naphthoquinone seemed to be the major naphthoquinone in the leaves and the roots. Furthermore, the root cultures showed higher content of lawsone but lesser content of 2-methoxy-1,4-naphthoquinone than the leaves and the roots of the intact plant. Interestingly, it was found that the root cultures could produce a certain amount of methylene-3,3'-bilawsone which could not be detected in the leaves and the roots.

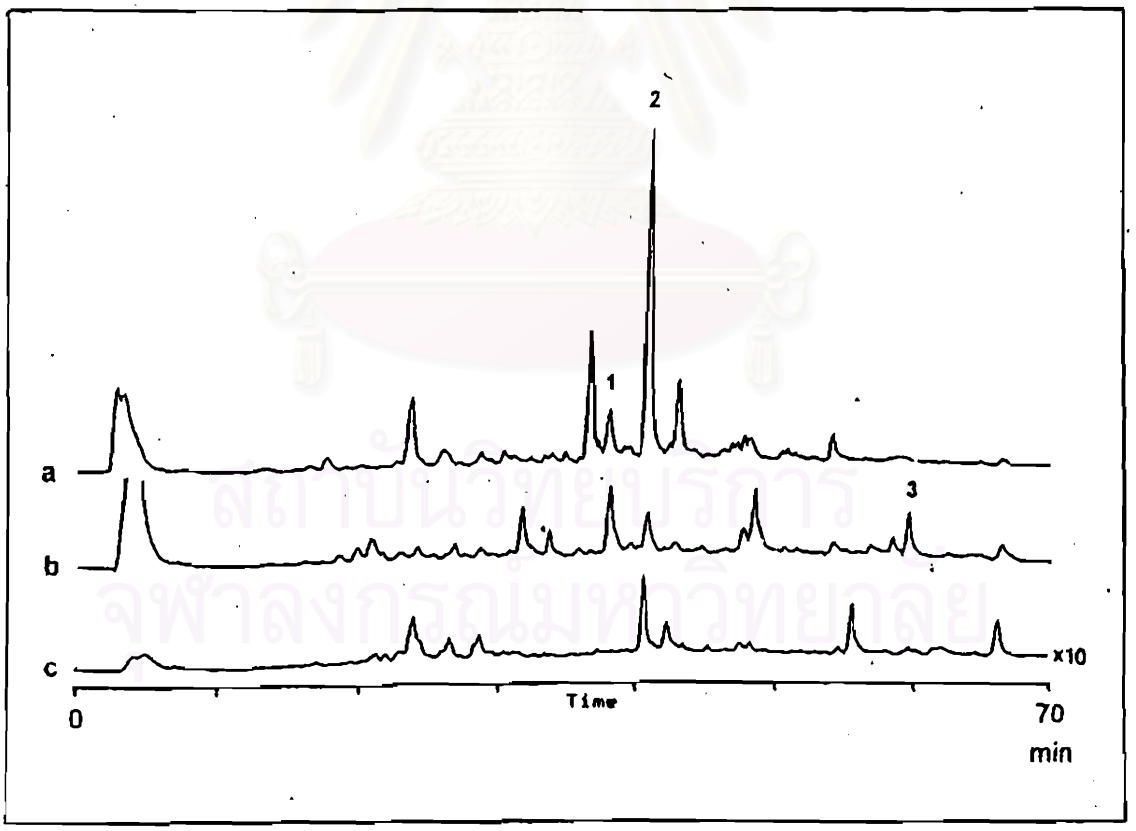

Fig. 64 HPLC chromatograms, detected with UV 275 nm, of the methanolic extracts of leaves (a), the cultured roots (b) and the whole roots (c) of *I. balsamina* ; 1 : lawsone, 2 : 2-methoxy-1,4-naphthoquinone, 3 : methylene-3,3'-bilawsone

For the coumarin derivatives, the HPLC chromatograms (Fig. 65) showed that the root cultures could accumulate much higher amount of the coumarin derivatives than the leaves and the roots. Isofraxidin appeared to be the major coumarin derivative accumulated in the root cultures whereas it was detected only in trace amount in the leaves and the roots. Although scopoletin was detected in both root cultures and the intact plants (leaves and roots), it was found also in small amount. As was found for the bisnapthoquinone, 4,4'-biisofraxidin could be detected only in the root cultures not in the intact plant. These results indicate that the secondary metabolism in the root cultures is different from that in the intact plants.

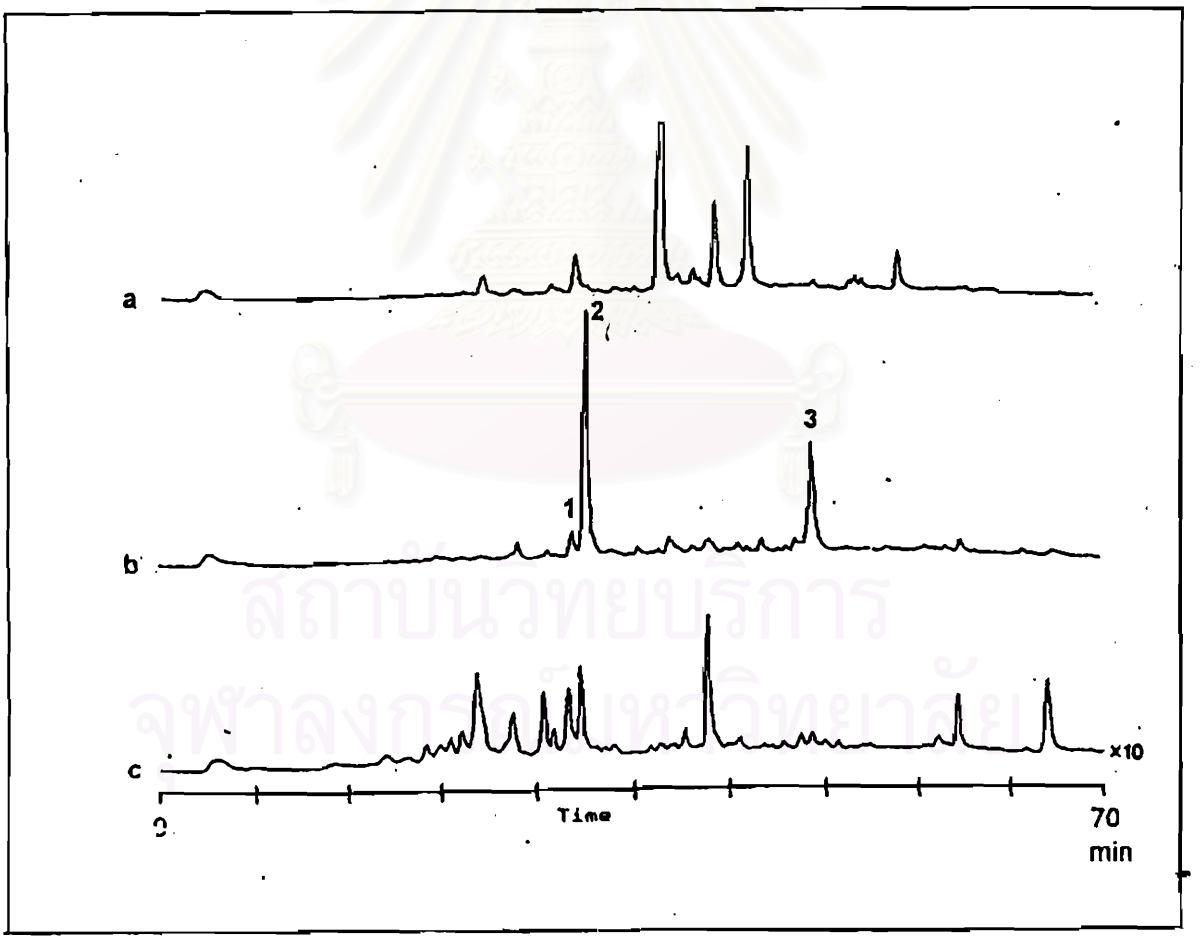

Fig. 65 HPLC chromatograms, detected with UV 350 nm, of the methanolic extracts of the leaves (a), the cultured roots (b) and the whole roots (c) of *I. balsamina* ; 1 : scopoletin, 2 : isofraxidin, 3 : 4,4'-biisofraxidin

Therefore, the root cultures of *I. balsamina* have a potential to produce the secondary metabolites with structures similar to or even more complex than those original found in the intact plants. In this case, the step of dimerization to form methylene-3,3'-bilawsone and 4,4'-biisofraxidin hardly found in the intact plants, appears to take place in the root cultures of *I. balsamina*. The reason for this difference in secondary metabolism is still unknown.

This HPLC conditions are also effective for the analysis of *o*-succinylbenzoic acid (OSB), a key intermediate in lawsone biosynthesis. This study, therefore, also put an attempt for the detection of OSB in the extracts of cultured root and the intact plants. Although, it has been reported that OSB is a key intermediate in lawsone biosynthesis (Dansette and Azerad, 1970; Grotzinger and Campbell, 1974), it could not be detected in all these extracts. These results suggested that the cellular pool of OSB is extremely small, thus it could not be detected in all these extracts.

2.2 Quantitative analysis of naphthoquinone and coumarin derivatives

The complete separation of each naphthoquinone and coumarin derivative by the HPLC method, allowed the compounds be quantitated by using the calibration curves of the authentic compounds. Although the amount authentic methylene-3,3'-bilawsone, isofraxidin and 4,4'-biisofraxidin were not sufficient to make their own calibration curves, their quantitative determinations were performed by using calibration curves of lawsone for methylene-3,3'-bilawsone, and of scopoletin for isofraxidin and biisofraxidin because of their similar chromophores. A linear relationship between the amount of lawsone (Fig. 66), 2-methoxy-1,4-naphthoquinone (Fig. 67) and scopoletin (Fig. 68) and their corresponding peak integrated areas were obtained in the range between 0.03 and 0.50 μg in each case. The correlation coefficients were found to be 0.9987, 0.9990 and 0.9995 for lawsone, 2-methoxy-1,4-naphthoquinone and scopoletin, respectively.

Amount (μg)	Peak area ($x10^6$)
0.031	0.26
0.062	0.42
0.125	0.87
0.25	1.75
0.5	3.27

Regression Output:	
Constant	0.058946904
Std Err of Y Est	0.050140494
R Squared	0.998768281
No. of Observations	5
Degrees of Freedom	3
X Coefficient(s)	6.482712273
Std Err of Coef.	0.131437566

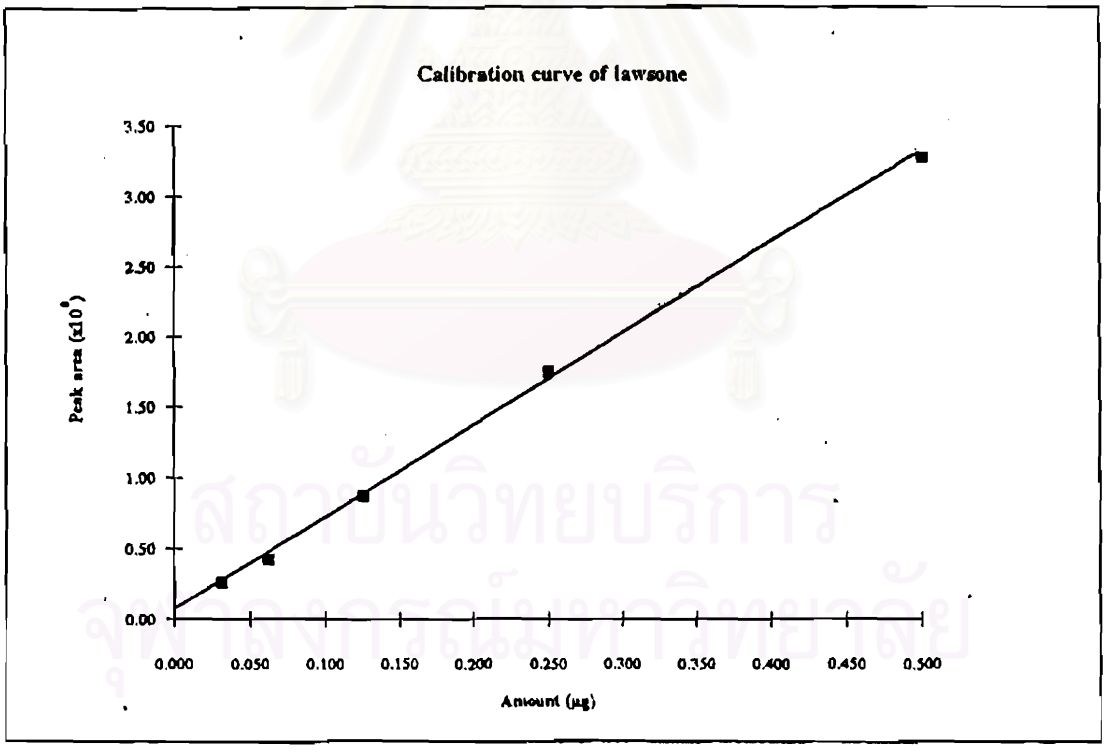

Fig. 66 Calibration curve of lawsone

Amount (µg)	Peak area ($x10^6$)
0.032	0.32
0.064	0.51
0.128	1.05
0.255	2.03
0.51	3.82

Regression Output:	
Constant	0.066602015
Std Err of Y Est	0.049859643
R Squared	0.999093558
No. of Observations	5
Degrees of Freedom	3
X Coefficient(s)	7.378149569
Std Err of Coef.	0.128308016

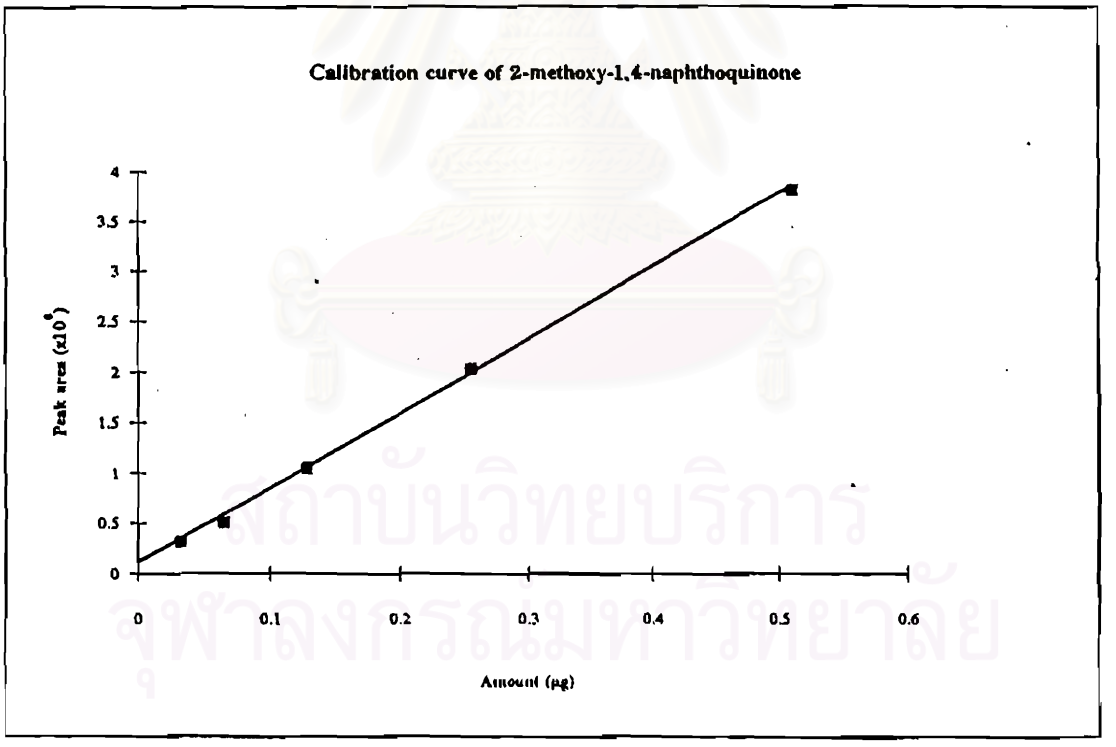

Fig. 67 Calibration curve of 2-methoxy-1,4-naphthoquinone

Amount (μg)	Peak area ($x10^6$)
0.033	0.22
0.066	0.35
0.132	0.72
0.265	1.36
0.53	2.61

Regression Output:	
Constant	0.060580207
Std Err of Y Est	0.024684415
R Squared	0.99952116
No. of Observations	5
Degrees of Freedom	3
X Coefficient(s)	4.831480471
Std Err of Coef.	0.061054642

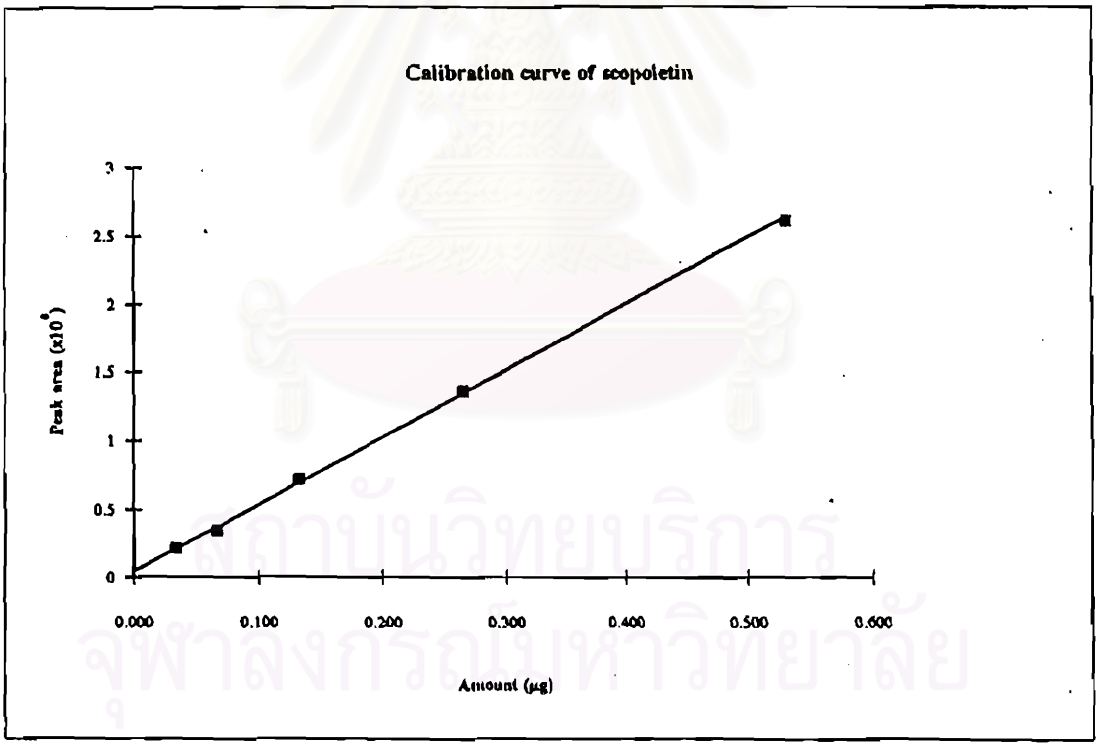

Fig. 68 Calibration curve of scopoletin

Based on this HPLC quantitative analysis, the content of lawsone, 2-methoxy-1,4-naphthoquinone, methylene-3,3'-bilawsone, scopoletin, isofraxidin and 4,4'-biisofraxidin, accumulated in the root cultures, the leaves and the roots of intact plants, were determined (Table 16). With respect to naphthoquinones, it was found that the root cultures accumulated higher content of lawsone (0.032 %) than the leaves (0.025 %) and the roots (less than 0.001%). The content of 2-methoxy-1,4-naphthoquinone accumulated in the root cultures (0.019 %), however, was less than that in the leaves (0.107 %) and the roots (0.028 %). These results suggested that the enzyme lawsone-O-methyltransferase better operate in the intact plants than in the root cultures. In contrast, methylene-3,3'-bilawsone was found to be accumulated in the root cultures (0.020 % base on lawsone) nearly the same amount as 2-methoxy-1,4-naphthoquinone, but not in the leaves and the whole roots. These results suggested that in the root cultures the enzyme system functioning on the formation of methylene 3,3'-bilawsone is as active as lawsone-O-methyltransferase while this enzyme system is not operated in the intact plants.

Table 16 The content of naphthoquinones and coumarin derivatives in *I. balsamina* root cultures (4-week old), the leaves and whole roots of the intact plants

Compound	Root culture (% dry weight)	Leaves (% dry weight)	Roots (% dry weight)
Lawsone	0.032	0.025	< 0.001
2-methoxy-1,4-naphthoquinone	0.019	0.107	0.028
Methylene-3,3'-bilawsone	0.020[a]	-	-
Scopoletin	0.005	0.07	0.01
Isofraxidin	0.032[b]	< 0.001[b]	0.02[b]
Biisofraxidin	0.010[b]	-	-

[a] Calculated from the calibration curve of lawsone, [b] calculated from the calibration curve of scopoletin.

For coumarin derivatives, the root cultures were found to accumulate scopoletin (0.005 %) in a rather smaller amount than the leaves (0.007%), though higher than the roots (0.001 %). On the other hand, the root cultures were found to contain in the highest amount of isofraxidin (0.035 % base on scopoletin) compared with the leaves (less than 0.001% base on scopoletin) and the roots (0.002 % base on scopoletin). These results suggested that the enzyme systems (oxidase and O-methyltransferase) functioning on the formation of isofraxidin are better operated in the root cultures than in the intact plants. As methylene-3,3' bilawsone, 4,4'-biisofraxidin was also accumulated only in the root cultures (0.010 % base on scopoletin) though in the higher amount than scopoletin. These results also suggested that the enzyme systems after scopoletin formation are well operated.

The ability of *I. balsamina* root cultures to produce the naphthoquinones and coumarin derivatives indicate that they can be a material of choice for biosynthetic studies of these naphthoquinones and coumarin derivatives. Such ability implies that various enzymes involved in these biosynthetic pathways are operating under these control conditions.

3. KINETIC STUDIES OF GROWTH AND THE FORMATION OF NAPHTHOQUINONE AND COUMARIN DERIVATIVES

In a batch culture system, the biosynthetic activity of cultured cells usually varies with the stage of cell growth. Clarification of the relationship between cell growth and product formation is, therefore, an essential step in developing a better understanding of the controls operating in secondary metabolite production. Thus, in this study, the relationship between growth and the formation of naphthoquinones and coumarins of *I. balsamina* root cultures was examined. The dry weight , in gram per flask, of the harvested root was used as a parameter for expressing the culture growth. Fig. 69A shows the growth cycle of the root cultures during a period of 30 days. It can be seen that there was a short period of the lag phase followed by a rapid growth of the exponential and linear phases. This resulted in a continuous increase in the biomass throughout the period of 19 days. The most active period of the increase in dry weight was observed from days 5 to 15. The growth rate was then slowing down to a zero-increase rate, which made the root culture reach a stationary growth phase at day 22. Thereafter, the dry weight of the biomass began to be constant and then declined, presumably due to the nutrient depletion of the medium. The root cultures attained their highest dry biomass weight of 1.02 g at day 22, equivalent to approximately 6 times of the inoculated root culture mass.

During this 30-day period of the culture growth, the formation of naphthoquinone and coumarin derivatives was also monitored and the results were expressed in the unit of milligram per gram dry weight. For the naphthoquinones (Fig. 69B), it was found that lawsone was initially accumulated in the early linear phase and actively biosynthesized throughout the linear phase, whereas methylene-3,3'-bilawsone was initially formed in the middle of the linear phase and actively biosynthesized until reaching the stationary phase. In contrast, 2-methoxy-1,4-naphthoquinone began to form in the late linear phase and was actively biosynthesized throughout the stationary phase. The highest level of lawsone was observed at day 15 and then the content slowly declined until the end of the growth cycle, while the formation of methylene-3,3'-bilawsone and 2-methoxy-1,4-naphthoquinone reached the

maximum at days 22 and 28, respectively. These results suggested that the biosynthesis of lawsone is well operated in the early stage of growth, resulting in its accumulation in the middle growth stage. Subsequently, when the enzymes utilizing lawsone (e.g. methyl-transferase or condensing enzyme) were induced to be active, the cellular lawsone was used for the formation of 2-methoxy-1,4-naphthoquinone and methylene-3,3'-bilawsone in the middle or late stage growth phase.

As for the kinetic formation of coumarin derivatives (Fig. 69C), it was found that scopoletin began to be accumulated in the lag phase and still actively biosynthesized until the early linear phase, whereas isofraxidin and biisofraxidin were initially biosynthesized in the early linear phase and actively biosynthesized through the late linear phase until the stationary phase. The formation of scopoletin reached the maximum at day 7, while those of isofraxidin and biisofraxidin were at days 26 and 22, respectively. These production patterns also suggest that the biosynthesis of scopoletin is very active in the very early stage of growth, whereas the formations of isofraxidin and its dimer are actively operated in the late stage of growth. These are, again, probably due to the expression of the enzymes involved in the utilization of scopoletin at the middle growth phase.

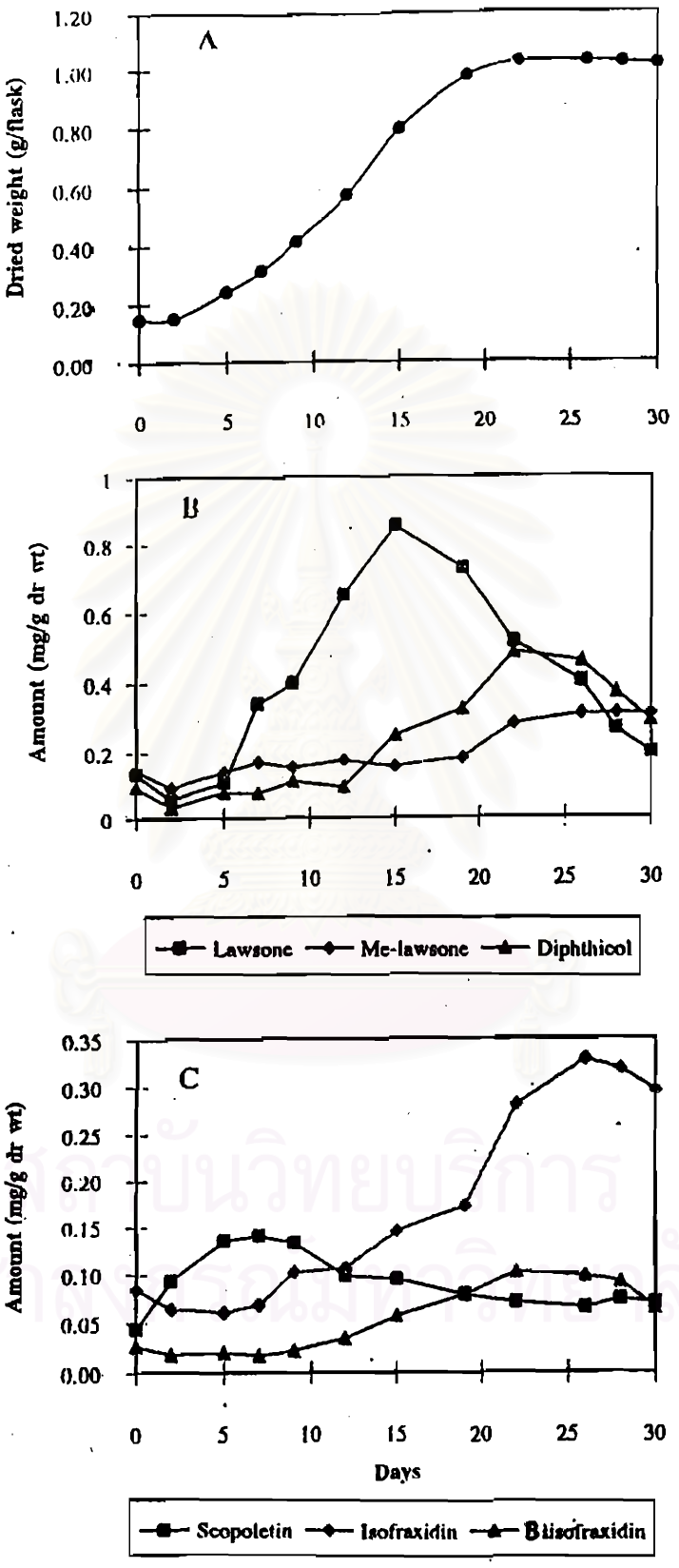

Fig. 69 Time-course of growth (A) and the formation of naphthoquinone (B) and coumarin (C) derivatives in *I. balsamina* root cultures

4. STUDIES ON THE BIOSYNTHESIS OF LAWSONE AND 2-METHOXY-1,4-NAPHTHOQUINONE

4.1 Detection of OSB-CoA ligase activity

A study on the biosynthetic enzyme of lawsone and 2-methoxy-1,4-naphthoquinone in *I. balsamina* was first emphasized on the detection of the enzyme activity of *o*-succinylbenzoyl-CoA ligase activity which converts *o*-succinylbenzoic acid (OSB) to be its activated form, OSB-CoA ester (Fig. 70). This enzyme has been found previously in microorganisms and anthraquinone producing plants (Sieweke and Leistner, 1991; Sieweke and Leistner, 1992).

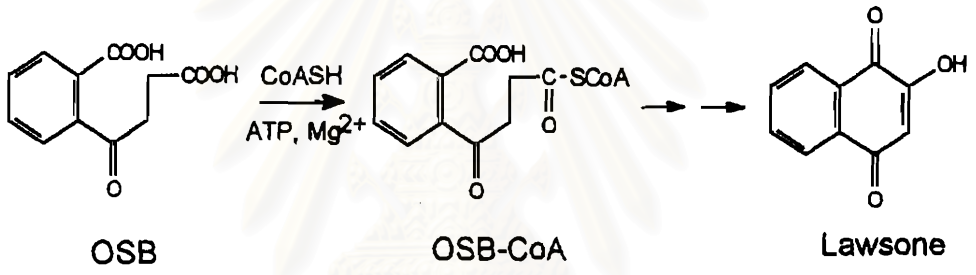

Fig. 70 Biogenesis of lawsone from OSB *via* its activated form, OSB-CoA ester.

In this study both [2,3-^{14}C]-OSB and nonlabelled OSB were used for the detection of OSB-CoA ligase activity in cell-free extract of *I. balsamina* root cultures. The routine assay mixture contained 0.7 mM OSB or 23,000 cpm [2,3-^{14}C]-OSB, 7.1 mM ATP, 1.8 mM CoASH, 7.1 mM $MgCl_2$ and 100 µl cell-free extract in a total volume of 140 µl. The incubation mixture was incubated at 30°C, for 30 minutes. Thereafter, the reaction was stopped by adding 20 µl formic acid and then analyzed for OSB-CoA ester. The techniques of both HPLC and TLC-radioscanning were used for the detection of this enzymatic product. No activity of the OSB-CoA ligase, however, was detected in the cell-free extract of *I. balsamina* root cultures with both techniques (Fig. 71). Furthermore, detection of the endogeneous OSB by HPLC revealed that no cellular OSB was presented in the root cultures (Fig. 63). These results suggested two possibilities. First, the biosynthetic pathway of lawsone in *I. balsamina* might not involve OSB as the intermediate. Second, the enzymes involved in

the biosynthetic pathway of lawsone might be organized in such a way that they were closely associated to each other as a tight multienzyme complex and, thus, the added OSB could not reach the enzyme OSB-CoA ligase in the pathway.

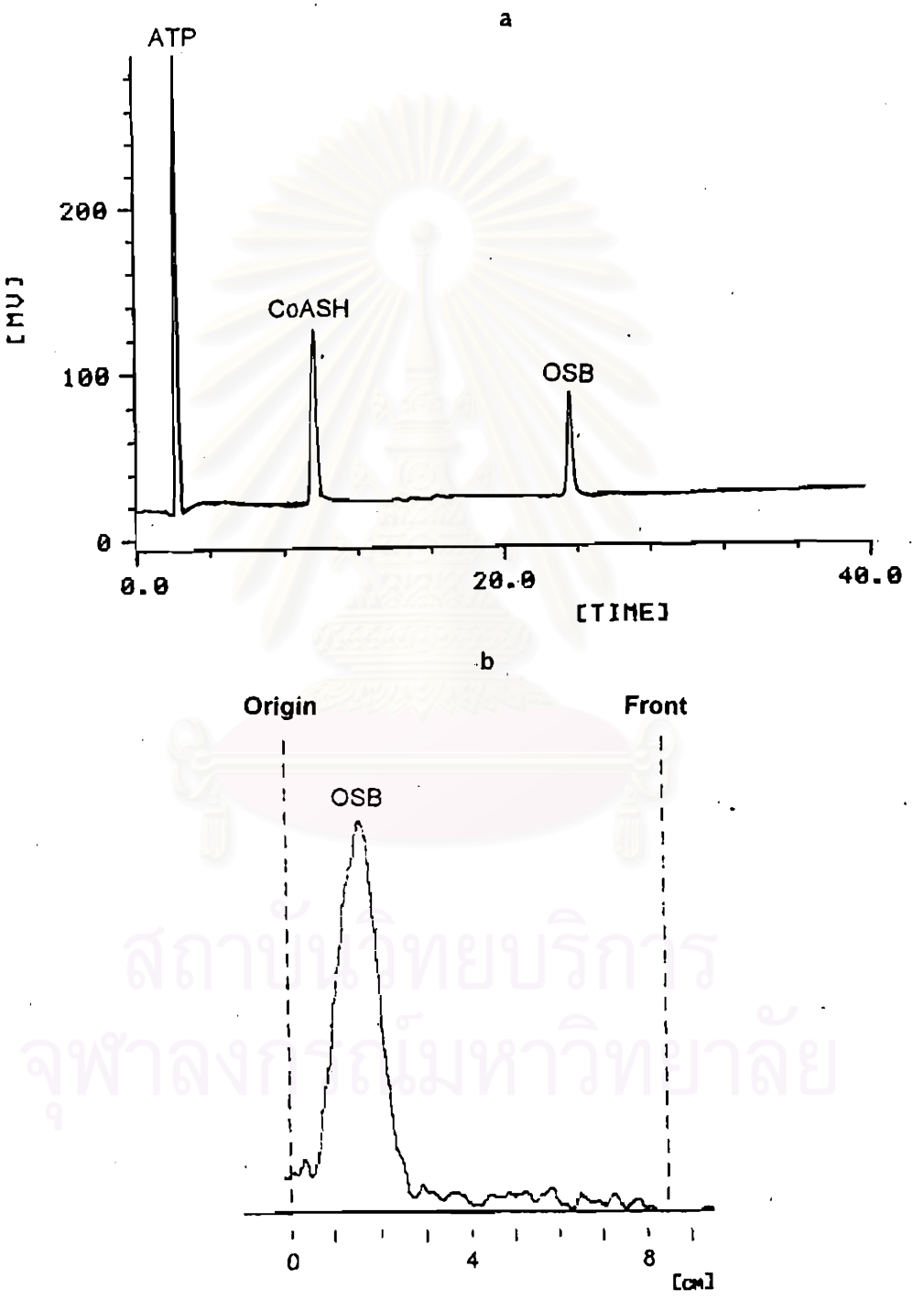

Fig. 71 HPLC chromatogram (a) and TLC-radiochromatogram showing no OSB-CoA ester was detected in the incubation mixtures of the OSB-CoA ligase assay.

4.2 *In vivo* feeding experiments with [^{14}C-U]α-ketoglutarate

In order to examine the possibilities mentioned above, *in vivo* feeding experiments were carried out using radiolabelled α-ketoglutarate as a precursor. In doing this, [^{14}C-U]α-ketoglutarate was feeded to the one-week and four-week-old root cultures and they were incubated for 3 days. After the incubation, an aliquot of the medium was taken and counted for the remaining radioactivity. It was found that 40 % and 76% of the radiolabelled α-ketoglutarate disappeared in the media of the one-week and four-week-old root cultures, respectively. This suggested that α-ketoglutarate was taken up by the old cultured roots (four weeks old) more effectively than the young roots (one week old). Both cultured roots were then harvested, extracted and the crude extracts were analyzed for their radioactive patterns. The results with the young root cultures showed that the radiolabelled substrate, [^{14}C-U]α-ketoglutarate, taken up by the root culture was incorporated directly into lawsone (Fig. 72). In contrast, feeding of [^{14}C-U]α-ketoglutarate to the old root cultures revealed that the labelled precursor was incorporated into 2-methoxy-1,4-naphthoquinone, interestingly, without significant detection of radiolabelled lawsone (Fig. 73). These results suggested that the enzymes involved in the biosynthesis of lawsone might be active in both the young and old root cultures, but the enzyme O-methyltransferase which methylates lawsone to form 2-methoxy-1,4-naphthoquinone might be active only in the old root cultures. This assumption was confirmed by the kinetic studies of lawsone and 2-methoxy-1,4-naphthoquinone formation in *I. balsamina* root cultures (Fig. 69) which showed that lawsone was initially formed in the early linear phase and biosynthesized throughout the linear phase, whereas 2-methoxy-1,4-naphthoquinone began to form in the late linear phase and actively biosynthesized throughout the stationary phase. Furthermore, it was also found that the incorporation of radioactive α-ketoglutarate into lawsone was smaller than in 2-methoxy-1,4-naphthoquinone. This might be explained by the uptake radiolabelled precursor was diluted by the primary metabolism which more active in young roots.

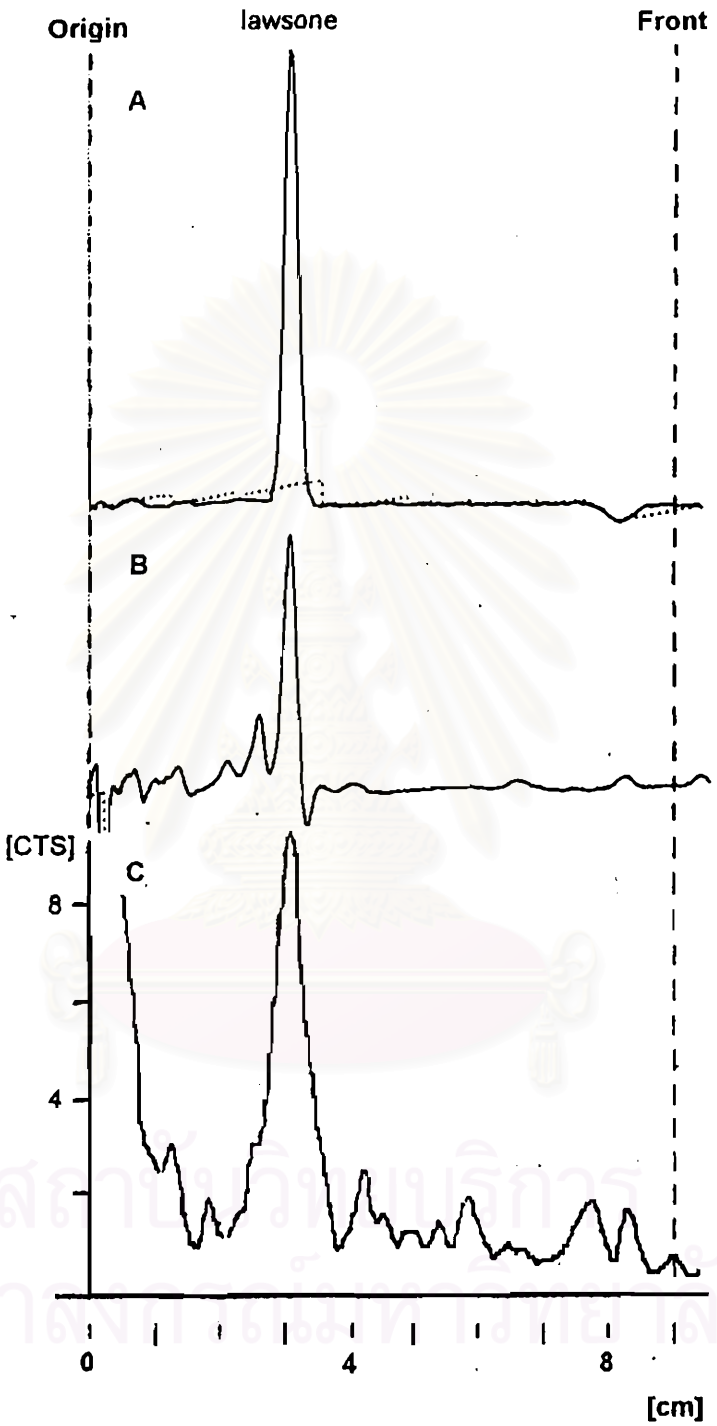

Fig. 72 TLC chromatograms of the authentic lawsone (A) and the cultured root extract (B) and the radiochromatogram of the cultured root extract (C)

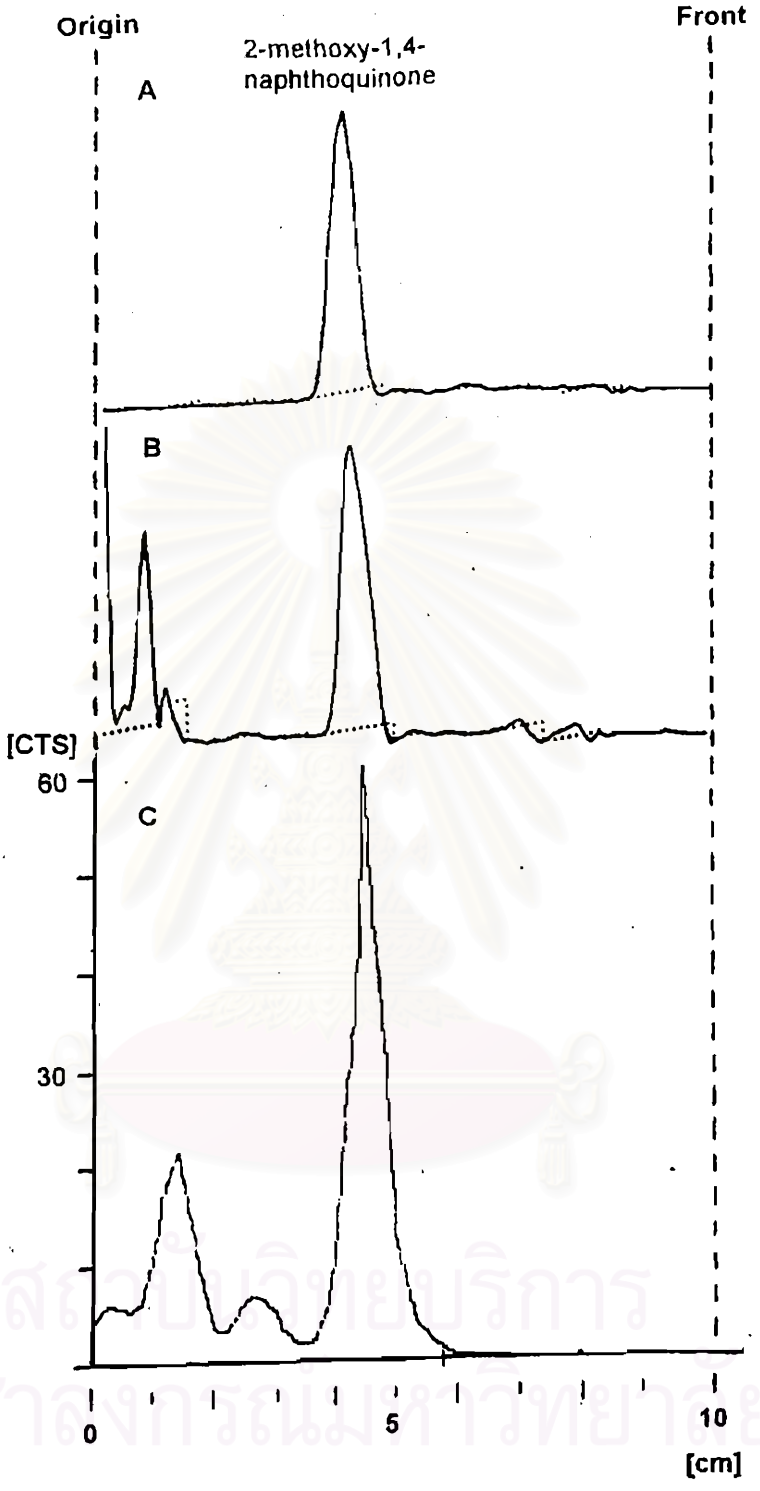

Fig. 73 TLC chromatograms of the authentic 2-methoxy-1,4-naphthoquinone (A) and the cultured root extract (B) and the radiochromatogram of the cultured root extract (C)

It should also be noted that the incorporation of [^{14}C-U]α-ketoglutarated into both naphthoquinones were taking place without any significant appearance of radiolabelled intermediates of the proposed biosynthetic pathway. These results suggested that the cellular pools of various intermediates in the biosynthetic pathway of lawsone and 2-methoxy-1,4-naphthoquinone are extremely small and those enzymes involved in the pathway should be organized in a complex form.

4.3 *In vivo* feeding experiments with [^{13}C]-methionine

To search for the chemical source of the methyl group of 2-methoxy-1,4-naphthoquinone and the methylene bridge of methylene-3,3'-bilawsone, another feeding experiment using [^{13}C]-methionine was carried out. Methionine is an amino acid in which its activated form, S-adenosylmethionine (SAM) acts as a general methyl group donor to methylate specific acceptors to form corresponding methylated products. The feeding experiment was performed as described in section 7.6, Chapter 3. After the feeding, 2-methoxy-1,4-naphthoquinone and methylene-3,3'-bilawsone were isolated. The identity of 2-methoxy-1,4-naphthoquinone and methylene-3,3'-bilawsone were confirmed with their Rf values (0.72 and 0.55, respectively) and UV absorption spectra compared with those of the authentic compounds. The results showed that the ^{13}C NMR spectrum of 2-methoxy-1,4-naphthoquinone exhibited a ^{13}C-enriched signal at δ 56.4 (Fig 74), indicating that [^{13}C]-methionine was incorporated into the methoxy group of 2-methoxy-1,4-naphthoquinone. In contrast, ^{13}C NMR spectrum of methylene-3,3'-bilawsone gave no ^{13}C-enriched signal of the methylene carbon at δ 18.4 (Fig. 75), indicating that [^{13}C]-methionine was not incorporated into the methylene bridge of methylene-3,3'-bilawsone. These results suggest that S-adenosylmethionine is served as the methyl source in the O-methylation of 2-methoxy-1,4-naphthoquinone biosynthesis, but not in C-methylation of methylene-3,3'-bilawsone biosynthesis.

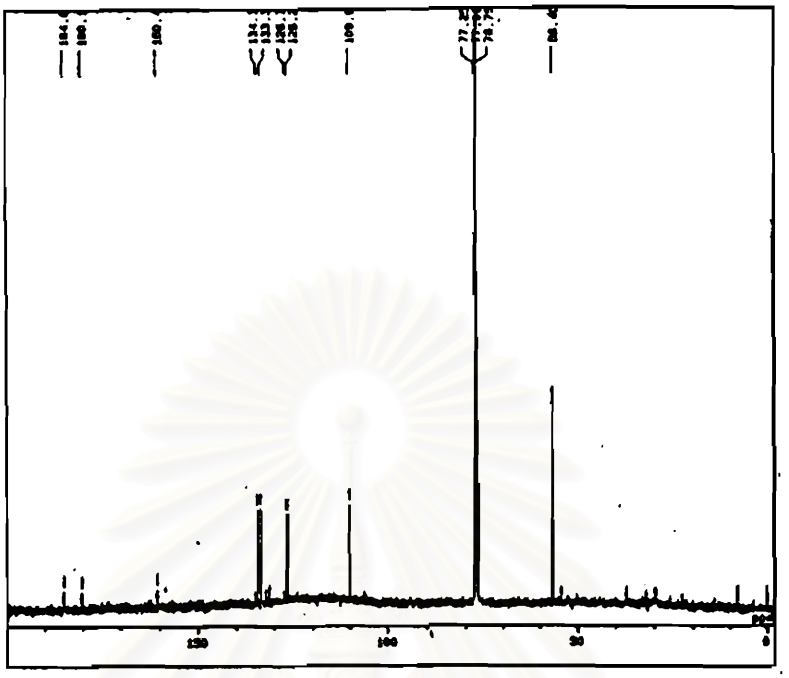

Fig. 74 ^{13}C NMR (125 MHz) spectrum of 2-methoxy-1,4-naphthoquinone showing the ^{13}C-enriched signal at δ 56.4

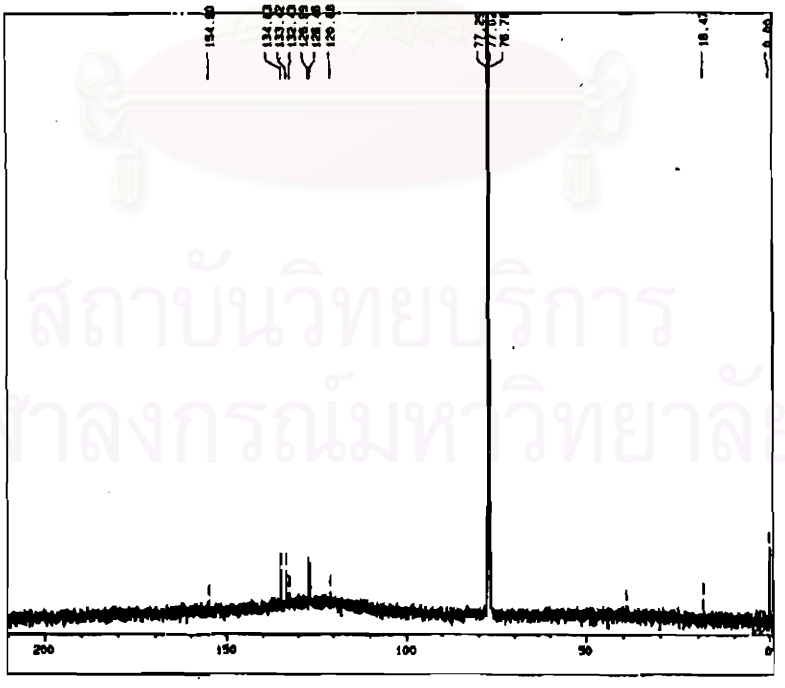

Fig. 75 ^{13}C NMR (125 MHz) spectrum of methylene-3,3'-bilawsone showing no ^{13}C-enriched signal at δ 17.9

4.4 Enzymatic formation of 2-methoxy-1,4-naphthoquinone by cell-free extracts of root cultures

To search for the enzyme activity involved in the biosynthetic pathway of lawsone and 2-methoxy-1,4-naphthoquinone, the cell-free extraction of four-week-old *I. balsamina* root cultures was prepared and examined for the enzyme activity using a radioactive substrate. The results showed that incubation of a crude cell-free extract of *I. balsamina* root cultures with [^{14}C-U]α-ketoglutarate in the presence of coenzyme A, ATP and Mg^{2+} led to rapid formation of the radioactive labelled 2-methoxy-1,4-naphthoquinone. This radioactive product was detected by TLC-radiochromatography (Fig. 76).

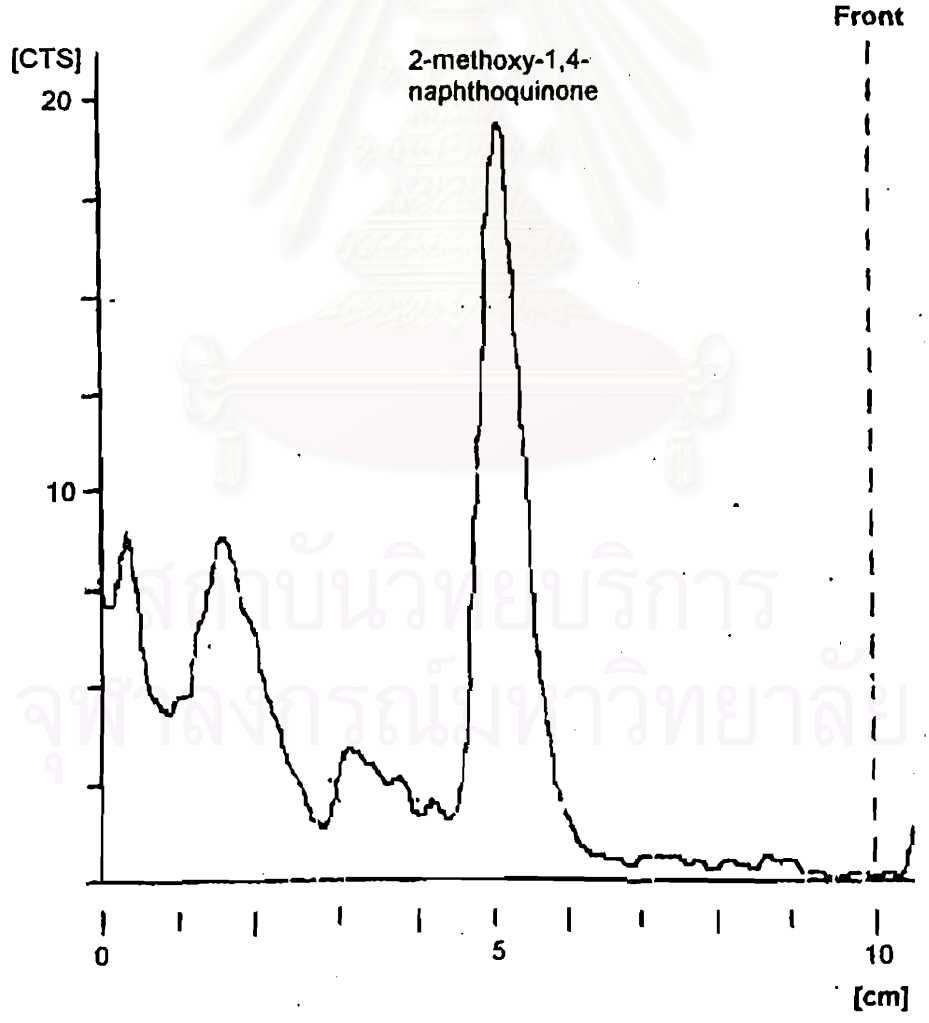

Fig. 76 TLC-Radiochromatogram showing the conversion of [^{14}C-U]α-ketoglutarate into 2-methoxy-1,4-naphthoquinone by cell-free extract of *I. balsamina* root cultures

In contrast, the boiled control reaction mixture did not show any reaction product of the labelled α-ketoglutarate. These results indicate that there is an enzyme activity involved in the biosynthesis of 2-methoxy-1,4-naphthoquinone in the cell-free extract of root cultures. It was also observed that no significant intermediate was detected in TLC-radiochromatogram. This confirms our assumption that the enzymes of lawsone and 2-methoxy-1,4-naphthoquinone are organized as an enzyme complex.

4.5 Identification of the enzymatic product

Identification of the enzymatic product was, first, carried out by TLC. The Rf values of the reaction product, 0.52 and 0.38, are the same as those of the authentic 2-methoxy-1,4-naphthoquinone in two solvent systems, (I) petroleum ether/chloroform (2:8) and then benzene/acetic acid (98:2); and (II) chloroform, respectively. Its UV absorption spectrum, measured by TLC densitometric method, was also similar to that of the authentic 2-methoxy-1,4-naphthoquinone (Fig. 77).

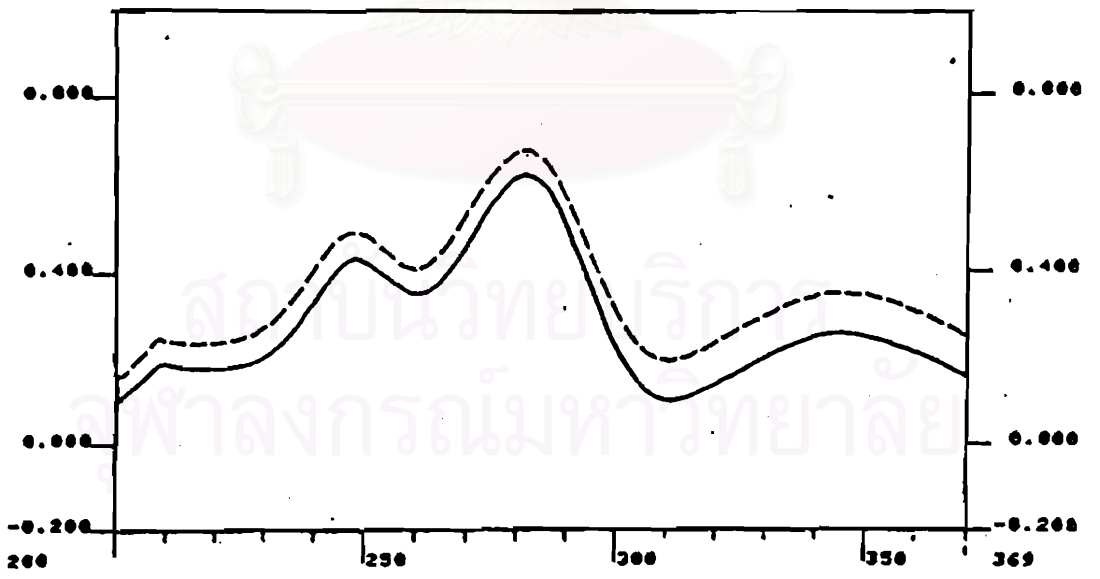

Fig. 77 UV spectra of the enzymatic product (———) and the authentic 2-methoxy-1,4-naphthoquinone (- - - -) measured by TLC-densitometric method

Moreover, the enzymatic product was further identified by recrystallization method. The spots of the enzymatic product on TLC were cut off and eluted with chloroform. This enzymatic product was then diluted with unlabelled 2-methoxy-1,4-naphthoquinone (10 mg) and recrystallized (62.50 cpm x μmol^{-1}). Additional recrystallization from chloroform-methanol (x3) showed a constant specific activity of 62.23 cpm x μmol^{-1}. These results confirm that the enzymatic product is 2-methoxy-1,4-naphthoquinone.

4.6 Partial purification of the enzyme system producing 2-methoxy-1,4-naphthoquinone

In order to confirm that the enzymes responsible for lawsone biosynthesis are organized as an enzyme complex system, the technique of gel filtration was introduced. This technique allows different protein molecules to be separated from one another based on their molecular sizes. The very big protein sizes would be eluted with void volume whereas the ones with smaller sizes would be eluted later. The purpose of this experiment was to observe whether the activity of lawsone biosynthesis disappeared or still remained after the crude extract was subjected to the step of gel filtration. The disappearance of the enzyme activity would oppose our suggestion on the multienzyme complex while the retaining of enzyme activity would support this proposal. In this experiment, the crude cell-free preparation was first subjected to the ultracentrifugation (100,000g, for 30 min). Both the supernatant and pellet fractions obtained by 100,000g ultracentrifugation were assayed for the enzyme activity. It was found that when the labelled α-ketoglutarate was incubated with 100,000g supernatant fraction, it was converted rapidly into 2-methoxy-1,4-naphthoquinone (Fig. 78). No enzyme activity was observed with the pellet fraction. Therefore, the 100,000g supernatant part was used for further experimentation. By desalting the supernatant fraction using a Sephadex PD-10 column, however, the enzyme activity could not be detected anymore. The possible reason might be due to the deficiency of some cofactors needed in the biosynthetic pathway. Various cofactors which potentially required in the biosynthetic pathway, including NADPH, NADP and thiamine were therefore added into the incubation mixture. The enzyme activity, however, still could not be detected in the desalted enzyme

solution. This suggested that there are other undefined cofactors in the crude enzyme extracts that are essential for the biosynthesis of 2-methoxy-1,4-naphthoquinone. The crude salt fraction eluted lately from PD-10 column was therefore saved for checking whether this small molecule fraction could restore the enzyme activity of the desalted extract. This was done by adding the small molecule fraction into the incubation mixture during the enzyme assay. Indeed, the desalted crude extract appeared to gain the enzyme activity back after the reconstitution. This suggested that the small molecular fraction from PD-10 contains some unknown cofactors which are required for the biosynthesis of 2-methoxy-1,4-naphthoquinone. These findings were useful for the further purification of the enzyme complex.

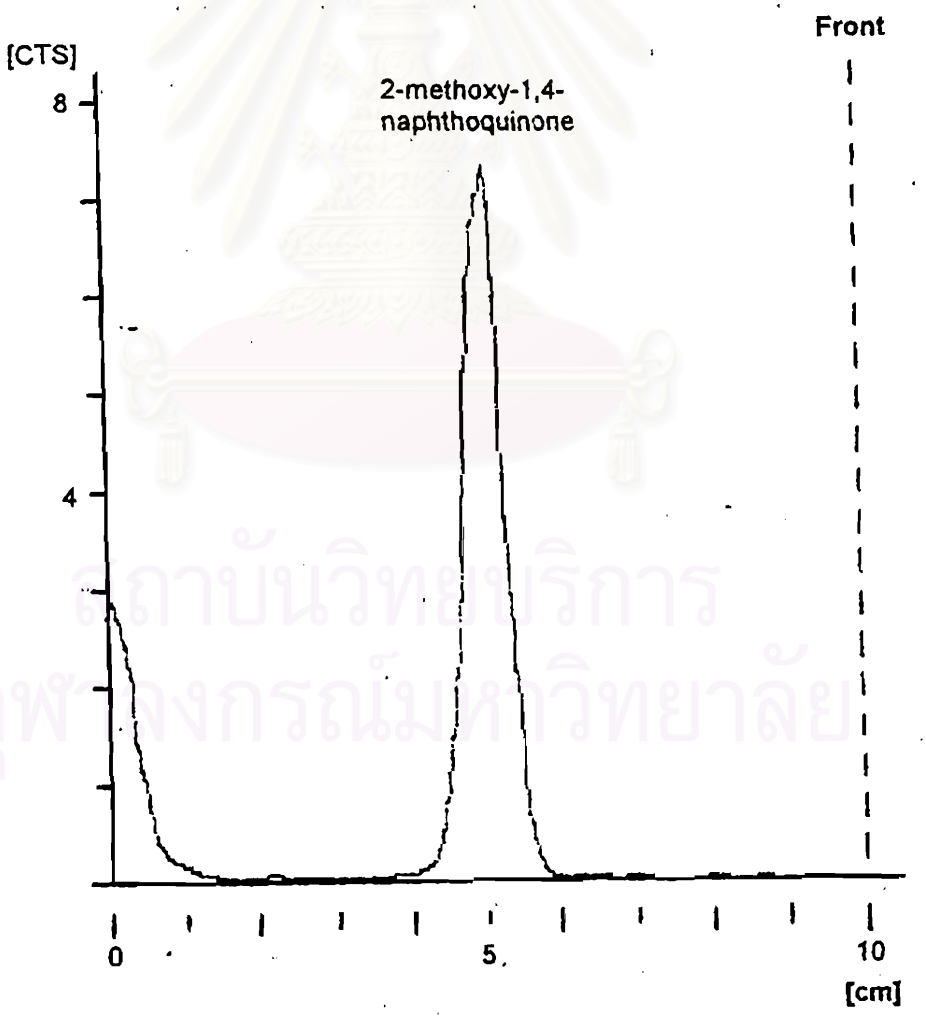

Fig. 78 TLC-radiochromatogram showing the conversion of [^{14}C-U]α-ketoglutarate into 2-methoxy-1,4-naphthoquinone by 100,000g supernatant part of the cell-free extract

In the step of gel filtration, the desalted 100,000g supernatant fraction was first concentrated by Centricon-30, and then fractionated on a Superose 12 HR column. The column was eluted with 0.1 M potassium phosphate buffer (pH 7.0) containing 0.2 mM DTT. The amount of protein in each collected fraction was determined by Bradford's method (Bradford, 1976). The eluted profile (Fig. 79) of protein showed a major single peak eluted with the void volume which covered the fractions 30-32. Enzyme assay of all the fractions also showed that the enzyme activity was present only in the fractions of the same major protein peak (fractions 31 and 32). The void volume of Superose 12 HR 16/50 column was determined as 30 ml, suggesting that the enzyme fractions 31 and 32 contained high molecular weight proteins These results confirm our proposal that the enzymes involved in lawsone biosynthesis are organized as a high-molecular-weight enzyme complex.

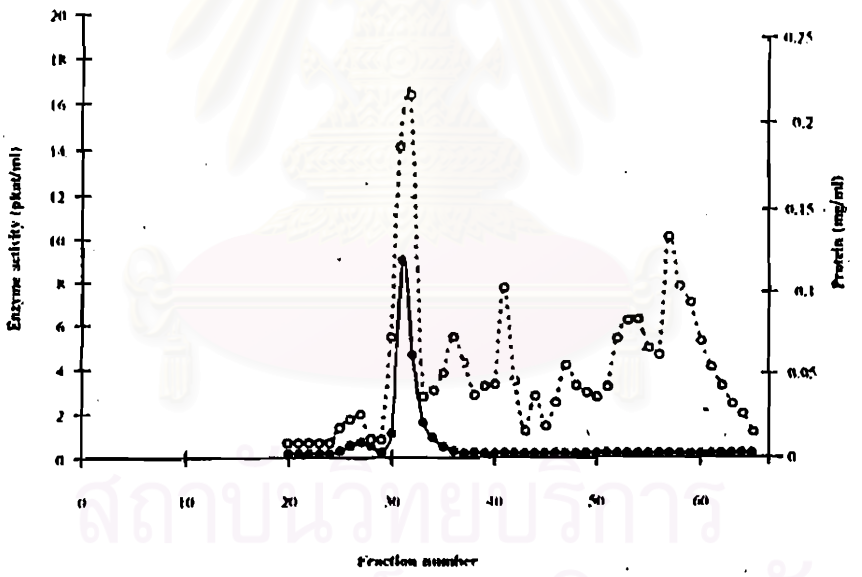

Fig. 79 The elution profile of enzyme activity (— ● —) and protein (- - o - -) on Superose 12 gel filtration column

4.7 Some characteristics of the enzyme complex

With the partially purified enzyme preparation, the involvement of some cosubstrates or cofactors in the functioning of enzyme complex was examined. In this experiment, the relative enzyme activity was calculated based on the incorporation of the labelled α-

ketoglutarate into 2-methoxy-1,4-naphthoquinone in the complete incubation (100 %). As shown in Table 17 it was found that the conversion of the labelled α-ketoglutarate to 2-methoxy-1,4-naphthoquinone was accelerated by the addition of chorismic acid, but not affected by the addition of OSB or benzoic acid into the incubation mixture. The relative enzyme activity could be increased to 122.6 % by chorismic acid, suggesting that chorismic acid, but not OSB or benzoic acid, could be channeled by the enzyme complex, as a cosubstrate, into 2-methoxy-1,4-naphthoquinone. In addition, the decrease in the radioactivity of 2-methoxy-1,4-naphthoquinone was observed by the addition of unlabelled lawsone into the incubation mixture. This suggested that the labelled lawsone could be diluted by the added unlabelled lawsone prior to the step of methylation by the enzyme O-methyltransferase. Therefore, the enzyme O-methyltransferases seem to be loosely bound to the enzyme complex due to the ability of the unlabelled lawsone in interfering the formation of 2-methoxy-1,4-naphthoquinone in the methylation step.

Table 17 Relative incorporation of [^{14}C]α-ketoglutarate into 2-methoxy-1,4-naphthoquinone by cell-free preparation of *I. balsamina* root cultures

Condition	Relative enzyme activity (%)
Complete incubation	100.0
boiled enzyme	0.2
+ OSB	105.2
+ chorismic acid	122.6
+ benzoic acid	100.1
+ lawsone	53.4
Incomplete incubation	
- CoASH	60.6
- ATP	36.0
- $MgCl_2$	43.7

In the absence of CoASH or ATP, or Mg^{2+}, the radioactivity of 2-methoxy-1,4-naphthoquinone, compared with the complete incubation , was also decreased. The relative enzyme activity decreased to 60.6 %, 36.0 % and 43.7 %, when coenzyme A or ATP or Mg^{2+} were omitted, respectively. This suggested that CoASH, ATP and Mg^{2+} were also required as cosubstrate or cofactor in the biosynthesis of lawsone and 2-methoxy-1,4-naphthoquinone.

CONCLUSION

From this research work of "Biosynthetic Studies of Naphthoquinones in *Impatiens balsamina* Root Cultures", the following conclusion can be drawn:

1. A novel natural bisnaphthoquinone, methylene-3,3'-bilawsone and a novel biscoumarin, 4,4'-biisofraxidin were isolated from the root cultures of *Impatiens balsamina*, along with two naphthoquinones (lawsone and 2-methoxy-1,4-naphthoquinone), two coumarin derivatives (scopoletin and isofraxidin) and a sterol (spinasterol).

2. The secondary products produced by the cultured roots are different from those of the intact plants (leaves and roots) both qualitatively and quantitatively.

2.1 The novel compounds, methylene-3,3'-bilawsone and 4,4'-biisofraxidin can be produced only by the root cultures.

2.2 The major naphthoquinone produced by the root cultures is lawsone, while that of the intact plants (leaves) is 2-methoxy-1,4-naphthoquinone.

2.3 The major coumarin derivative produced by the root cultures is isofraxidin, while that of the intact plants (leaves) is scopoletin.

3. The formation of lawsone is actively operated during the middle linear phase, whereas those of 2-methoxy-1,4-naphthoquinone and methylene-3,3'-bilawsone are during the late linear phase of the growth cycle.

4. The formation of scopoletin is actively operated during the early linear phase, whereas those of isofraxidin and biisofraxidin are during the late linear phase of the growth cycle.

5. [^{14}C]α-ketoglutarate is incorporated into lawsone and 2-methoxy-1,4-naphthoquinone, both *in vivo* feeding experiments and *in vitro* cell-free system, without detection of any radiolabelled intermediate.

6. The enzyme involved in the biosynthesis of lawsone or 2-methoxy-1,4-naphthoquinone are organized as a multienzyme complex.

7. α-Ketoglutarate and chorismic acid are used as the precursors of the enzyme complex.

8. Coenzyme A, ATP and Mg^{2+} are essential for the enzyme complex activity.

9. Methionine is a source of methyl group for the biosynthesis of 2-methoxy-1,4-naphthoquinone, but not for methylene-3,3'-bilawsone.